AN ABSTRACT OF THE THESIS OF

ROBERT EDWARD HOLMES for the Ph. D. in Chemistry
(Name) (Degree) (Major)

Date thesis is presented September 3, 1965

Title ELECTRICAL AND OPTICAL PROPERTIES OF POTASSIUM CHLORIDE SINGLE CRYSTALS CONTAINING LEAD ION

Abstract approved Redacted for Privacy
(Major professor)

A survey of the methods of purification of KCl, for use in preparing single crystals by growth from the melt, was made. Two methods, fractional recrystallization and ion exchange, were used. The purity of the salt and crystals grown from the same salt were compared with the findings of other authors. The ion exchange method of purification produced a salt with < 0.01 ppm lead ion and the material was suitable as a "pure" host matrix for the study of the properties of lead ion in KCl single crystals.

Two crystal-growing apparatus were designed and built to produce pure and lead ion-containing KCl single crystals in an atmosphere of air or other gases. A novel method of producing a "dual" crystal, one section pure, the other containing lead ion, in a continuous host crystal, was introduced.

The incorporation of lead ion into these crystals was studied

by means of spectrophotometry and evidence for the incorporation of the ion at more than one site was noted. The homogeneity of doping was considered a function of the crystal growth method and the manner of incorporation of the lead ion into the crystal. A scanning absorption cell was designed and built to observe the uniformity of lead ion distribution in the crystal.

The dithizone method of trace analysis of lead was adapted to the analysis of KCl single crystals containing lead. The oscillator strength of the 273 mμ band, called the A band, of lead ion in KCl was found to be 0.11. A preliminary investigation of the thermal sensitivity of the A band and some other bands due to lead ion, observed in the 250-270 mμ region, was made. It was found that quenching from 600° C maximized the A band.

The diffusion and electrolytic transport of lead ion were studied to evaluate the effective charge on the lead ion species migrating under the influence of an electric field. Migration was studied from both plane and extended sources and the mobility of the species at 560° C was found to be no greater than 8×10^{-9} cm^2/volt sec. The effective charge on the species was determined to be no greater than 0.6 of an electronic charge. This value is smaller than the charge on the free lead ion, and it is suggested that the lead ion migrates as a complex. The possible complexes involve the association of positive ion vacancies or chloride ions with the lead ion. The

reduction of lead ion to elemental lead near the junction between the pure and lead-containing regions partially explained the apparent migration of lead ion, in a field, toward the anode as observed by other authors.

The conductivity of pure and lead ion-containing crystals was observed. The association energy of a positive ion vacancy with the lead ion was found to be about 0.1 eV or greater. An anomaly in the experimental conductivity curves is explained by the loss of lead ion from crystals.

ELECTRICAL AND OPTICAL PROPERTIES OF POTASSIUM CHLORIDE SINGLE CRYSTALS CONTAINING LEAD ION

by

ROBERT EDWARD HOLMES

A THESIS

submitted to

OREGON STATE UNIVERSITY

in partial fulfillment of
the requirements for the
degree of

DOCTOR OF PHILOSOPHY

June 1966

APPROVED:

Redacted for Privacy

Professor of Chemistry
In Charge of Major

Redacted for Privacy

Chairman of Department of Chemistry

Redacted for Privacy

Dean of Graduate School

Date thesis is presented September 3, 1965

Typed by Opal Grossnicklaus

DEDICATION

To my wife Marilyn, whose untiring support, encouragement, and understanding made this possible.

ACKNOWLEDGMENTS

The author is indebted to Dr. Allen B. Scott for numerous suggestions, valuable criticisms and discussions, and to the Office of Naval Research for material support.

Dr. Donald Conant was a collaborator in the design of some sections of the controlled-atmosphere crystal-growing apparatus. His assistance is gratefully acknowledged.

The use of the ion exchange columns for KCl purification, furnished by Dr. W. J. Fredericks, and the conductivity cell furnished by Dr. Allen B. Scott is sincerely appreciated.

To my friends who helped with the proof reading of the manuscript, D. Hinks, L. Lewis, B. Newton, and L. Scheurman, many thanks.

Especial thanks to C. D. Woods whose assistance in converting theoretical design to functional practicality was invaluable.

TABLE OF CONTENTS

TABLE OF CONTENTS (Continued)

LIST OF FIGURES

LIST OF FIGURES (Continued)

LIST OF TABLES

ELECTRICAL AND OPTICAL PROPERTIES OF POTASSIUM CHLORIDE SINGLE CRYSTALS CONTAINING LEAD ION

I GENERAL INTRODUCTION

Over 2000 years ago Lucretius (9, p. 59-63) wrote some of the early hypotheses on the atomistic nature of the universe:

> We see how quickly through a colander
> The wines will flow; how, on the other hand,
> The sluggish olive-oil delays: no doubt,
> Because 'tis wrought of elements more large,
> Or else more crooked and intertangled...
>
> And note, besides, that liquor of honey or milk
> Yields in the mouth agreeable taste to tongue,
> Whilst nauseous wormwood, pungent centaury,
> With their foul flavour set the lips awry;
> Thus simple 'tis to see that whatsoever
> Can touch the senses pleasingly are made
> Of smooth and rounded elements, whilst those
> Which seem the bitter and the sharp, are held
> Entwined by elements more crook'd, and so
> Are wont to tear their ways into our senses,
> And rend our body as they enter in...
>
> Some too, there are which justly are supposed
> To be nor smooth nor altogether hooked,
> With bended barbs, but slightly angled-out,
> To tickle rather than to wound the sense--
> And of which sort is the salt tartar of wine
> And flavours of the gummed elecampane...
>
> And, again,
> What seems to us the hardened and condensed
> Must be of atoms among themselves more hooked,
> Be held compacted deep within, as 'twere
> By branch-like atoms--of which sort the chief
> Are diamond stones, despisers of all blows,
> And stalwart flint and strength of solid iron,
> And brazen bars, which, budging hard in locks,
> Do grate and scream...

> But that thou seest among the things that flow
> Some bitter, as the brine of ocean is,
> Is not the least a marvel . . .
> For since 'tis fluid, smooth its atoms are
> And round, with painful rough ones mixed therein;
> Yet need not these be held together hooked:
> In fact, though rough, they're globular besides,
> Able at once to roll, and rasp the sense.
> And that the more thou mayst believe me here,
> That with smooth elements are mixed the rough
> (Whence Neptune's salt astringent body comes),
> There is a means to separate the twain,
> And thereupon dividedly to see
> How the sweet water, after filtering through
> So often underground, flows freshened forth
> Into some hollow; for it leaves above
> The primal germs of nauseating brine,
> Since cling the rough more readily in earth.

From this and the writings of other authors, a pattern of understanding and order evolves. Man in his need to understand the world about him classifies and notes order in all that is related and attempts to relate those things which have no apparent or obvious order. Both philosopher and scientist utilize this method to formulate ideas, theories, and hypotheses about nature. Although some theories may change or even be found in error, the net result is a gradual increase in the understanding of nature and the development of a formal knowledge of our surroundings. So too does this author hope to define and order a small aspect of the overall field of science.

The order present in alkali halides is that of structure, for they are, in concept, a perfect three dimensional array of alkali

and halogen ions linked with forces of attraction and stabilized with forces of repulsion. This concept of an ideally perfect crystal, as suggested by the x-ray diffraction of crystals, does not explain all the intrinsic properties of the alkali halides. Some of these properties are based on the periodic arrangement of the ions while others are a function of the disorder in this perfect array. When this order is disturbed or perturbed, changes take place in the properties expected of a perfect array and additional "extrinsic" properties are introduced. These extrinsic properties are of particular interest in the study of alkali halides for it is by them that we can learn more about the nature of the host material. A whole new field of investigation is afoot on this second order perfection, that of the order about a perturbed lattice site or region in the crystal.

Imperfections, a general term used for deviations from the order of the lattice, whether inherent or externally caused, have been postulated to account for crystal growth (105, p. 28-30), color centers (82), electrolytic conductivity (95), and diffusion (71, p. 33-35), to name but a few. These imperfections are classified as line, point, and plane defects. Even pure crystals were found best described as relatively imperfect structures.

Although structurally imperfect to some degree, pure alkali halides are transparent over a broad wave length region, extending from the ultraviolet to the infrared. The transparency of potassium

chloride is limited by electronic transitions in the ultraviolet at 160 mμ and by fundamental lattice vibrations in the infrared at 70.9μ. With the introduction of point defects such as "foreign" ions, extrinsic absorptions can appear in various regions of the spectrum. F centers in KCl, a model for which is an electron in a negative ion vacancy, absorb in the visible region at 560 mμ, lead ion in KCl absorbs at 273 mμ and thallium absorbs at 247 mμ.

Atomic migration through solids, as considered in diffusion phenomena and electrolytic migration, requires the presence of imperfections in the crystal lattice. The motion of atoms through a solid is dependent on the structure of the crystal and is realized by the action of an atom leaving its normal lattice site and taking up a position at another site. Movement can take place on an atomic scale by various mechanisms. These can be described by motion at point defects or motion in conjunction with larger scale defects such as dislocations and grain boundaries. On the whole, the presence of defects is required to explain these phenomena.

The role and effect of lead in some of these phenomena have been the object of this study. In the ensuing sections, the ultraviolet absorbance due to lead ion in KCl, the migration of lead ion in KCl, and the conductivity of KCl containing lead ion will be considered. The necessary preparative techniques, such as purification of KCl or single-crystal growth, are included in the body of the presentation.

II SALT PURIFICATION

Introduction

The basic matrix for this entire study was potassium chloride and considerable attention was given to the quality of the material used for single-crystal growth. The common starting material was either J. T. Baker Co. or Matheson-Coleman-Bell Co. reagent-grade potassium chloride. The manufacturer's specifications for their product were equivalent.

The standard method of commercial purification of KCl has been recrystallization. Many authors have used this on a small scale to produce material with a lower impurity content. However, purification can be attained by various means. Vacuum distillation, ion exchange, extraction, and fractional recrystallization have been employed.

Preliminary investigations in all phases of this study were made using reagent-grade KCl. The heavy-metal ion content (83) and the hydroxide ion content (88) of this salt has been previously described. From the common base of reagent-grade material, further steps of purification were undertaken. The processes finally adopted to improve purity were fractional recrystallization and ion exchange. These are described in detail in the next two sections

while other methods surveyed are discussed briefly in the following paragraphs.

Recent studies by Kobayashi and Tomiki (46) have suggested that commercial KCl contains a considerable amount of bromide ion. They found that this type of contamination could be estimated by studying the position of the ultraviolet absorption edge. One method used by these authors to produce purer salt was the vacuum distillation of the reaction product between the respective alkali bicarbonate and HCl. The bicarbonate was treated with dithizone for heavy-metal ion removal before reaction with the HCl. This method introduced sodium into the KCl. Kanzaki and Kido (42) found that fractional, vacuum distillation in quartz at 10^{-6} mm Hg decreased the cation and anion impurities by a factor of 10. The resultant material was free of OH^- or $O^=$ absorption bands and did not react with the quartz container when used for crystal growth.

Quincy and La Valle (84, p. 2-3) extracted a solution of recrystallized KCl with thenoyltrifluoroacetone in 4-methyl-2-pentanone to remove transition metals, alkaline earth metals and other trivalent cations. Fusion and filtration of the KCl, carried out in quartz, was followed by treatment with chlorine and HCl. The resultant ingots obtained contained less than 25 ppm total cation and 15 ppm total anion impurities.

Investigation of two additional methods of purification were

undertaken in this laboratory. These were recrystallization using HCl in a common-ion-effect precipitation of KCl, and freeze drying. The freeze drying method proved to be too slow and the recrystallization using HCl precipitated chlorides other than potassium. Both these methods were discarded.

Purification by Fractional Recrystallization

Potassium chloride or "salt", as it will often be referred to in this text, crystallizes in a f. c. c. cubic lattice. Its nonreactivity and solubility in water enable the salt to be readily recrystallized and purified from water. Based on the differences in solubility of KCl and other compounds as a function of temperature, a separation and purification can be made on a purely physico-chemical basis. In addition, this method of purification is based on the fact that insoluble matter and some impurity ions act as nucleation centers for crystallization. If the first portion of precipitated salt and the final portion of solution, that containing soluble impurity ions, are discarded, the fraction of salt recovered is of higher purity than the starting material.

Experimental

Reagent-grade salt was completely dissolved with heating in deionized water and filtered hot to remove the gross insolubles.

The weight ratio of salt to water was chosen so that at room temperature the solubility of the dissolved phase is exceeded by 13% of the initial weight of the salt. During cooling, vigorous agitation was applied to encourage many small nucleation centers for crystallization. The precipitated salt, 13% by weight, was filtered off and discarded. The filtrate was then boiled down, with periodic salt removal, until its room-temperature volume was reduced to that containing 11% of the initial salt weight. The remaining filtrate was discarded. The salt was oven dried in air at 110° C for 24 hours, then dried at 110° C for the same length of time under vacuum. This process produced a middle fraction of recrystallized salt with a 76% yield. Further continuation of the process using recrystallized salt as the starting material lead to a 58% recovery after the second recrystallization and a 44% recovery after the third.

At this point in the process several different schemes for further purification were used. The salt was heated in quartz under an argon atmosphere to 550° C for 48 hours. This process produced a slight black precipitate of carbon in the salt. Alternatively, the salt was treated with dry, purified HCl under the same conditions. The results were analogous although considerably more carbon was produced. When the salt was recrystallized with removal of the carbon, retreatment with HCl produced a white salt mass, free from carbon. The final product was stored in sealed containers under argon.

Purification by Ion Exchange

In this method, impurity cation and impurity anion removal were effected by means of ion exchange with the potassium and chloride ions respectively. The ions are exchanged reversibly between the solid and a liquid without appreciable changes occurring in the structure of the resin. The resin can be visualized as an elastic three-dimensional hydrocarbon network to which are attached a large number of ion active groups (18, p. 3-4). These ion active groups and the hydrocarbon network constitute an immobile unit. The chemical behavior of the ion exchange resins depend significantly on the nature of the ion active groups. Mobile ions of equivalent and opposite electrical charge to the ion active groups complete the system. These mobile ions can exchange with other ions of similar charge and give rise to the phenomenon of ion exchange.

Dowex AG-1, a strongly basic anion exchanger, was used to remove anion impurities as indicated by the following reaction:

$$\phi - N^{+}(CH_3)_2C_2H_5OHCl^{-} + X^{-} \rightleftharpoons \phi - N^{+}(CH_3)_2C_2H_5OHX + Cl^{-}$$

where $X^{-} = I^{-}$, NO_3^{-}, Br^{-}, IO_3^{-}, Ac^{-}, OH^{-}, or F^{-}.

Dowex A-1, a weakly acid cation chelation resin, was used to remove cation impurities as follows:

$$\phi - N\begin{matrix}\diagup CH_2COO^-K^+ \\ \diagdown CH_2COO^-K^+\end{matrix} + M^{++} \rightleftharpoons \phi - N\begin{matrix}\diagup CH_2COO^- \\ \diagdown CH_2COO^-\end{matrix} M^{++} + 2K^+$$

In the above reactions only the active group of the resin has been shown and X^- and M^{++} are used as examples. M^+ also exchanges in a similar manner.

The exchange of any anion or cation can be described by the usual chemical equilibria. The removal of some ions is more effective than others giving rise to selectivity values for a particular resin. However, in a resin bed of sufficient length and special design, as is the case of column operation, most limitations of selectivity can be overcome. Ion exchange as a method of purification of KCl has been investigated by Fredericks, Rosztoczy and Hatchett (26, p. 2-7). The results of this study were used as the basis for column design used in salt purification by the ion exchange method.

Experimental

Polypropylene, polyethylene, nylon, and lucite were used exclusively in all steps of this purification to prevent additional contamination from contact with glass or metal. Reagent-grade KCl was dissolved in deionized water to make a 25% by weight solution. The solution was filtered through Whatman's #1 filter paper to remove gross insolubles and the filtrate passed through separate

resin beds of Bio-Rad analytical grade Chelex 100[1], potassium form, and Dowex AG-2, chloride form, at the rate of 100 ml/minute. The ion exchange unit used was designed and built by W. J. Fredericks and L. Schuerman in our laboratories. The design was based on the earlier findings of Fredericks, Roszotczy and Hatchett. The filtrate from this column was evaporated to dryness in a vacuum oven at a pressure of 15 mm of mercury. Heat was applied simultaneously during evaporation and the temperature increased from 25° C to 75° C over a period of 48 hours. The salt was removed when the latter temperature was attained and stored in polypropylene containers.

Salt Purity: A Comparison

Analytical detection of trace impurities in the part-per-million or part-per-billion range is not possible for some ions and with others the results are upper limits to the concentration. In many instances several different criteria may be used to indicate purity. In the case of alkali halides, optical data, conductivity, trace analyses and reactions with the containing vessels help to indicate the level of foreign ions in the host material. Analyses are performed either on the starting material or on ingots produced from

---

[1]Purified Dowex A-1.

the same material.

The presence of foreign halides are indicated by a shift in the ultraviolet absorption edge while lead, thallium, hydroxide, and other ions can be observed by their characteristic absorptions in the 200-400 mμ range. For example, the presence of hydroxide in KCl gives rise to an absorption peak at 204 mμ. Rolfe (87) has studied this absorption and the well-known absorption due to hydroxide in the infrared at 2. 75 μ to assign the 204 mμ peak to OH^-. Lead ion in KCl has an absorption band at 273 mμ and the oscillator strength for this band was determined in this study. Thallium in KCl absorbs at 247 mμ and this band is also proportional to the concentration of thallium in the crystal (47).

The sensitivity of trace analyses in the part-per-billion range is quite unpredictable and either selective single ion concentrations or total impurity cation or anion concentrations are often reported. In this study an upper limit to the lead ion concentration was established using dithizone as a complexing agent.

Spectrographic analysis (26, p. 13), and EDTA back-titrations in our laboratories have been used as methods for impurity content. Other authors have employed neutron activation analysis (1) and semi-quantitative spectrographic analysis (21).

A further indication of purity is given by some of the chemical properties of the salt. Etching of the growth crucible by an active

oxygen species, perhaps O_2^- or OH^-, indicated the presence of these materials.

Conductivity has been shown to be a criterion of polyvalent cation impurity. Kelting and Witt (43) working with various concentrations of $SrCl_2$ in KCl found a marked increase in the conductivity in the extrinsic range for increasing strontium ion concentrations. However, where the possibility of polyvalent anion compensation can occur the data is not a true indication of polyvalent impurity cation content. Conductivity measurements (see Chapter VI) suggest that the salt purified by ion exchange has an impurity content comparable to that of ten-pass zone refined material.

Table 2.1 is a comparison of impurity content of KCl purified by various means. Considerable variation was found in the analyses of any one investigator due to variations in the source material. Quincy and La Valle (84, p. 5) suggested that the only way to check effective impurity removal was to analyze each sample (or lot) of raw material before purification was undertaken. More complete data is forthcoming on the purity of ion-exchange-purified salt as produced in our laboratory.

Comparisons between the various sources depend upon the nature of the growth atmosphere. Some authors (22, 77) have observed attack of the melt container during crystal growth in the presence of oxygen and water vapor. Observations in this study were the same.

Table 2.1 Comparison of the impurity content in KCl and KCl ingots purified by various means. (all values are reported in parts per million).

	Harshaw, ingot 1952 (a)	Harshaw, ingot 1962 (b)	Harshaw, ingot 1962 (c)	Anderson, vacuum distilled, ingot (d)	Pohl, zone refined ingot (e)	TTA-Hexone extraction, ingot (f)	Reagent grade KCl (g)	Fractional recrystal-lization (h) (twice)	Ion exchange purified KCl (i)	Ion exchange purified KCl (j)	Sublimed KCl (k)
Na	100	1	0.1	1	1	4	40.0		2.1		8.3
Ca	50	100	0.1	100	100	<2					
Mg	5	1	0.1	1	1	<3		<10			
Sr		1	0.1	1	1	<2					
Al	10	10		10			0.5	10-100	.04		.09
Fe	10	0.1	0.1	0.1	0.1	<.3	< 0.1		< 0.1		0.5
Cu							.03		.02		.04
Pb							< .01		<.01	<.01	<.01
Ni							<.01		<1.0		<1.0
Mo							<0.1		<0.1		<0.1
Cr									<1.0		
Total polyvalent cation						25				0.1	
Total polyvalent anion						15					

(a) semiquantitive spectrographic analysis (SQSA), Duerig & Markham (21)
(b) SQSA, Noble & Markham (76)
(c) Neutron activation analysis, Anderson, Wiley & Hendricks (1)
(d) (e) SQSA, Noble & Markham
(f) (g) Various techniques, Quincy & Lavalle (84. p. 7-12)
(h) SQSA, our laboratory, results of Fredericks
(i) Spectrographic, Fredericks, Rosztoczy, Hatchett (26, p. 13)
(j) Dithizone, ETDA back-titration, our laboratory
(k) same as (i)

Purer salt and growth atmospheres gave the least attack on the container.

The presence of hydroxide, observed by the intensity of the 204 mμ "hydroxyl" band, was observed in crystals produced from salt of varying degrees of purity. However, the band diminished as purity increased. Complete removal of the band was possible when HCl or HCl-argon was used as the growth atmosphere with salt purified by ion exchange or fractional recrystallization.

In summary, the analyses and comparisons indicate that a host lattice with little residual impurity was available for study and that the properties introduced by small amounts of lead ion would be characteristic of that material.

III PREPARATION OF SINGLE CRYSTALS

Introduction

In reality, the methods of single-crystal growth are a science tempered by art, trial and error. Recently, Lawson and Nielsen (53) have written a book on the art alone. Many methods have been devised for single-crystal growth of varied substances. Methods of growth from solution, fused melt, and vapor are numerous in the literature. The methods of growth from the melt can be further divided into moving- and stationary-crucible, Kyropoulos, eutetic melt, or Verneuil techniques.

Some 50 years ago Nacken (74) produced single crystals from a fused melt. His method employed a seed clamped in a cooled rod which allowed the seed to contact the surface of a salt melt held just above its melting point. Czochralski (14) in 1918 produced long thin crystals by starting a seed in a fine capillary tube and drawing the newly formed seed from the surface of the melt. In 1926 Kyropoulos (52, 51, 68) extended this principle and produced large single crystals by dipping the closed end of a cooled nickel rod into the melt, allowing crystallization to take place on the rod, then withdrawing the rod until only one of the crystals formed was in contact with the melt. Further cooling of the rod enlarged the size of this crystal.

During the same era, Bridgman (6), Strong (100), and Stockbarger (97, 98, 99) developed the basic idea of Tammann (101) to give us what is generally called the Bridgman method. This process consists of cooling a tube of melt at one end and allowing crystallization to progress up the tube. The lower (cooled) end was usually drawn to a fine tip and a single crystal was produced from the most favorably oriented of the first crystals formed. Due to the differences in growth rates of the various faces and the physical limitations of the container, this crystal usually succeeded in preventing further growth of the other crystals. The modifications introduced later were in the designs of the melt container and dropping the melt tube through various temperature gradients.

Apparatus for growth by these methods have been devised by many authors (50, 55, 64), each depending on the conditions peculiar to the material under consideration.

In recent years a combination of several methods has been used to produce crystals by what is generally termed the Kyropoulos technique. This method uses a separate seed (Nacken), that is continuously cooled during growth (Kyropoulos), and is pulled from the melt as growth proceeds (Czochralski). The Kyropoulos method of crystal growth was the method most applicable to this work and its basic features were used in the designs of both crystal growing apparatus built for this study.

Crystal-Pulling Apparatus

In single-crystal growth, the term "pulling" means a literal pulling of the crystal from the melt. The apparatus designed by the author produced a lowering of the melt in relation to the growing surface of the crystal. This gave the same result as pulling. A seed crystal mounted in a water-cooled rod produced the deposition site and heat differential needed for single-crystal growth. A schematic drawing of the apparatus is presented in Figure 3. 1 and further description is contained in the following paragraphs.

Rotating Cold Finger

A nickel-plated brass rod functioned as the water-cooled clamp for the seed crystal. This rod will be termed a "cold finger" in the remainder of the text. The cold finger was attached via a flexible coupling to a variable-speed direct-current motor. Rotation was possible between the velocity limits of zero and 150 rpm. Cooling was effected by a water jacket around this solid brass rod. For the jacket, two brass plugs were soldered into the ends of a large brass tube and the ends of this tube were machined to accept the cold finger, teflon-asbestos packing, and packing glands. Two brass tubes near the top and bottom of the jacket provided for water circulation. A slot was cut in the lower end of the cold finger and two

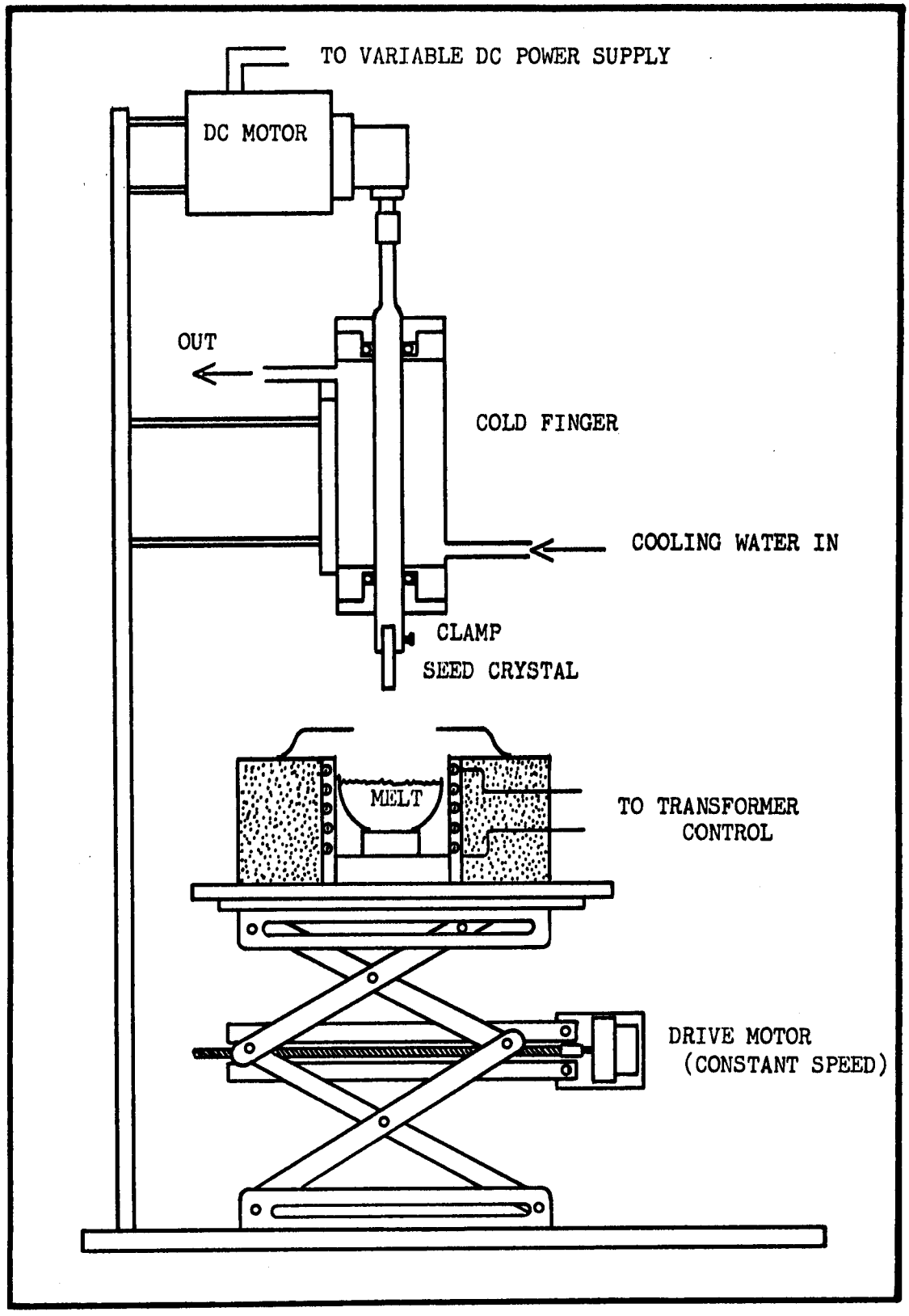

FIG. 3.1. CRYSTAL PULLING APPARATUS.

small screws, tapped through the remaining sides, were used as clamps for the seed crystal. The jacket and drive motor were attached to a Flexiframe support assembly.

Melt Furnace

The furnace housing was constructed from a section of heavy-wall Transite pipe and fitted with a Transite top and bottom. A clearance hole was cut in the top plate for the heating core. The heating element was Kanthal resistance wire wound on an alundum core and sealed in place with alundum cement. The total room temperature resistance of this heating element was 26 ohm. The core was positioned in the housing and vermiculite packed around it for insulation. Temperature control was effected by an ammeter and a Variac in the power line to the element. The furnace would accept any type of crucible up to 2-7/8" in diameter. A domed porcelain plate with a one-inch center hole was used on top of the furnace as a heat reflecting shield. This shield limited the crucible height to 3".

Furnace-Lowering Mechanism

The furnace and melt contained therein were lowered by a motor driven Lab-jack. A synchronous gear-head motor driving through a gear-reduction box produced a vertical drop rate of $1\frac{1}{4}$" to $1\frac{1}{2}$" per hour. Since the jack did not raise or lower linearly with

rotation of its drive screw, a variable drop rate resulted. The motor and gear-box were enclosed in a brass case and held in position by two long brass arms. These parallel arms slipped over and under the jack's center framing and allowed the drive unit housing to move as the drive screw turned. Only the motor shaft and the screw were rigidly coupled. By disconnecting the drive mechanism, manual motion could be introduced. To increase the stability and usable platform area of the jack, Transite bonded to Plywood, was bolted to the upper and lower surfaces of the jack.

Controlled-Atmosphere Crystal-Growing Apparatus

This apparatus also utilized the principle of melt lowering. However, to differentiate the units, this will be called a controlled-atmosphere crystal-growing apparatus. Figure 3. 2 is a photograph of the apparatus while Figure 3. 3 is a schematic diagram. The apparatus consisted of a cold finger assembly and rotator, furnace, crystal chamber and lid, lowering mechanism, and vacuum and controlled atmosphere system. Each of these components will be described in a following section.

Cold Finger Assembly

The cold finger frame work consisted of a series of parallel aluminum plates joined with four upright stainless steel rods. For

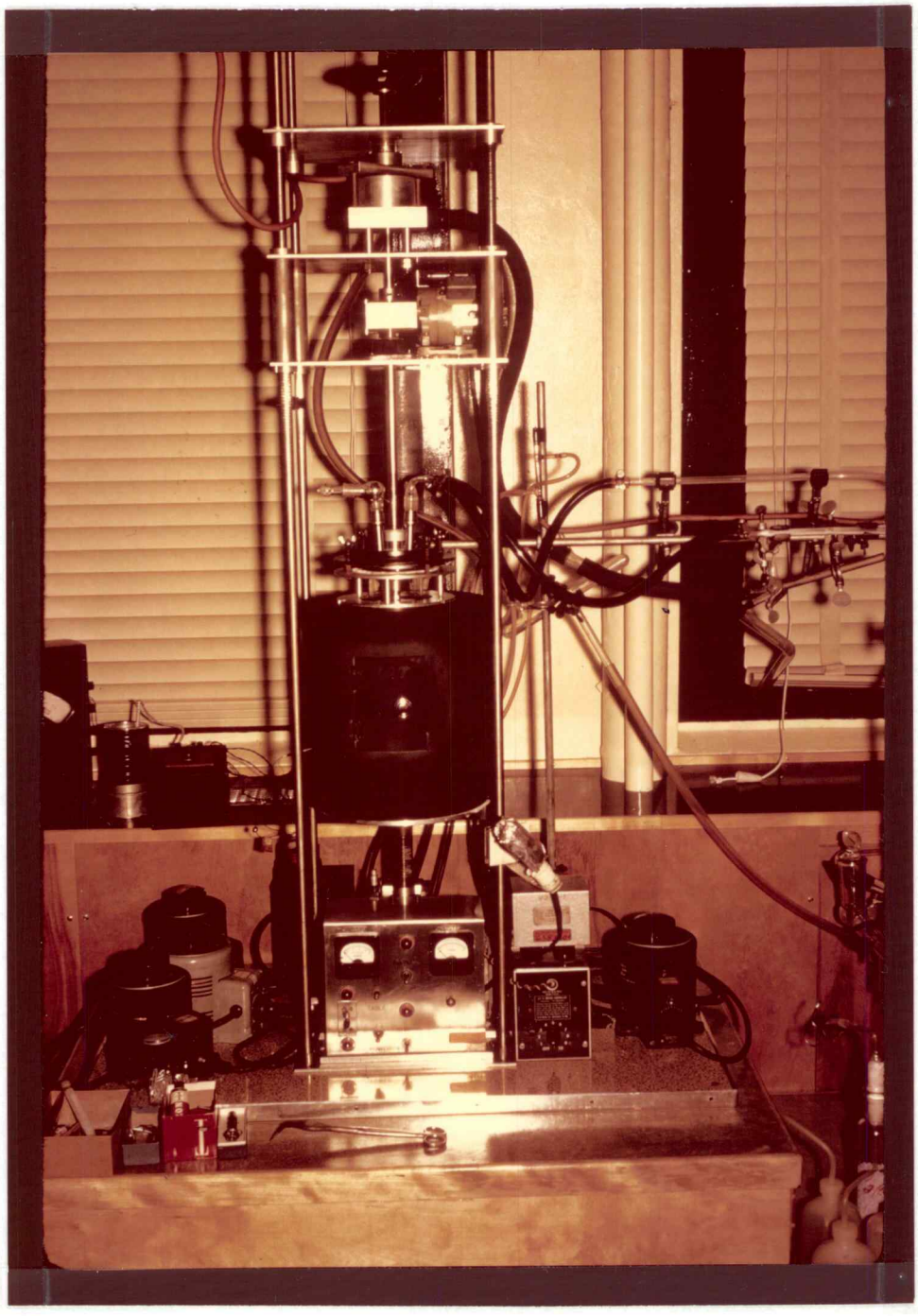

FIGURE 3.2. PHOTOGRAPH OF THE CONTROLLED ATMOSPHERE CRYSTAL-GROWING APPARATUS.

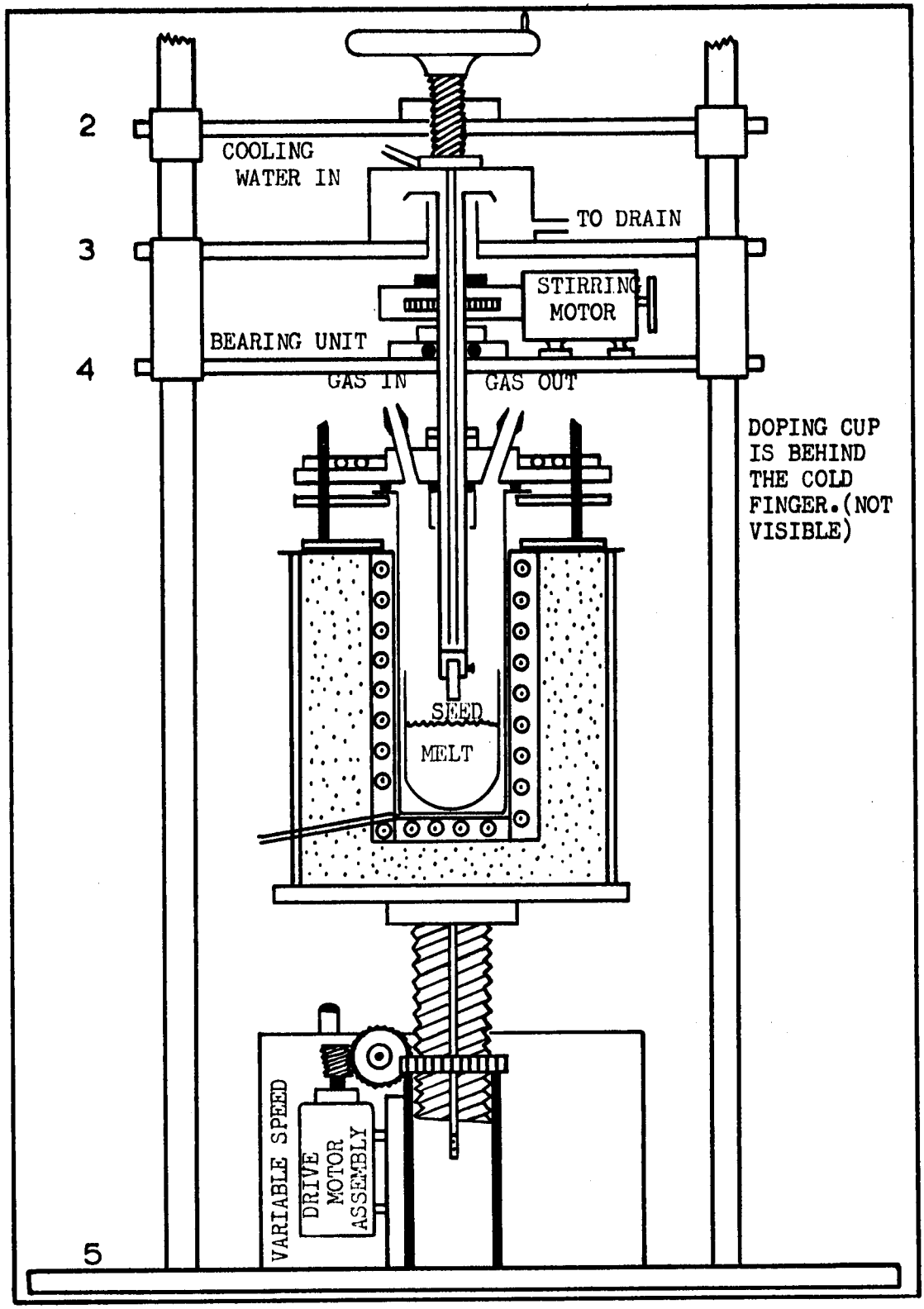

FIG. 3.3. SCHEMATIC DIAGRAM OF THE CONTROLLED-ATMOSPHERE CRYSTAL-GROWING APPARATUS.

clarity of description the plates will be numbered 1 through 5 starting from the top. Two of the plates, 1 and 5, were bolted against shoulders on the threaded ends of the stainless steel uprights. The bottom plate, 5, was bolted to a Formica-covered Plywood sheet and the entire unit mounted securely on a vacuum bench. The top plate, 1, was braced to a Unistrut channel iron framework for rigidity and alignment. The remaining plates, 2, 3, and 4, constituted a movable sandwich which slid vertically on the four stainless steel uprights. This sandwich was counter-weighted with a lead ballast for easy movement and positioning, in addition to no movement without external force. Plate 2 could be locked at any position by means of clamps at each upright above and below the plate. This plate was joined to plates 3 and 4 by means of a screw at its center. The screw passed through a nut attached to plate 2 and was connected to plate 3 by means of a ball bearing thrust bearing. Each turn of the hand wheel at the top of this screw produced a separation or approach of 0.0909" between plates 2 and 3. This screw allowed a fine adjustment of the vertical position of the cold finger after coarse positioning had been made with plate 2. Plates 3 and 4 were bolted together at the corners by means of large-diameter heavy-wall aluminum tubing. Shoulders and threads were turned on the outside ends of the tubing and spanner nuts secured the sandwich. These tubes were fitted with bronze bushings to insure

smooth movement of the sandwich on the uprights. The cold finger constructed of copper, brass or stainless steel tubing extended above and below the 3-4 plate unit. With each, a solid plug of like or compatible material was silver-soldered into the end of the tube, and a slot cut in the lower end of the plug. Two small screws tapped through the remaining sides acted as clamps for the seed crystal. The cold finger and clamp screws were plated with nickel, by an electroless method, and rhodium to insure corrosion resistance. A series of thrust and sleeve bearings built intothe gear-head unit located between plates 3 and 4 held the cold finger. A series-wound governor-controlled motor regulated with a Variac, transmitted power through a gear-reduction box to rotate the cold finger. Rotation speeds of 40 to 125 rpm were attained by adjusting the governor. As the motor was fitted with rubber vibration mountings, a self-aligning bearing was positioned below the gear box to insure concentric rotation of the cold finger. Water for cooling was introduced near the tip of the cold finger by a small aluminum tube hung inside the hollow cold finger. A disc at the top of the cold finger distributed the used cooling water into an overflow cup and hence to the drain.

Melt Furnace

A capped cylinder was fabricated from #14 gauge black steel

for the outside case of the melt furnace. The bottom was welded on, but the top, fitted with a lip and an inner flange, was removable for access to the furnace windings. A clearance hole for the furnace core was cut in the top while an opening in the side was used as a viewing port. This port was narrowed on the inside by steel plates and the outside opening was covered by an insulated door. A thick Vycor plate was fitted into the port to reduce heat losses. Kanthal resistance wire was wound on the outside of an alundum core to produce all three heating elements used in the furnace. The main element covered the bottom of the core and extended 3" up the side. The second element was wound around the upper section of the core and compensated for heat losses at the top of the furnace. The third element was mounted inside the port opening and compensated for heat losses through the port. Vermiculite was used as the packing and insulating material. The temperature was controlled by an ammeter and Variac in the power line to each element. Operation was controlled through the master panel on the lowering mechanism. Chromel-alumel thermocouples indicated the core temperatures.

A circular collar constructed of aluminum was fastened to the top of the furnace to support the growth envelope. This unit assured a positive seal of the envelope against the growth chamber lid. Four threaded posts projected upward from the top of this collar and fitted through matching holes in a cooling plate used over the chamber lid.

Springs and wing nuts on these posts secured the assembly and compressed an O-ring set in the bottom of the chamber lid against the envelope flange. A heavy asbestos gasket provided cushioning under the envelope flange.

Crystal Growth Chamber and Lid

A heavy-wall Vycor envelope containing the molten salt in a semiconductor-grade quartz crucible, was used as the growth chamber. The cold finger, doping cup, gas inlet, and gas exhaust entered the growth chamber through the lid at the top of the chamber. This lid was constructed of brass and plated with nickel and rhodium for corrosion resistance. Mounted on a hub at the center of the lid was a Wilson seal. The seal fit tightly around the cold finger yet allowed rotation and longitudinal movement. Three tubes machined to a standard-taper projected from the top of this lid and were coupled to standard-taper Pyrex fittings to provide for a gas inlet, outlet, and doping cup. Special shoulders on these tubes allowed the use of joint clamps. The cup was constructed to hold up to 3 grams of doping agent.[2] Rotation of the cup would invert the cup and drop the contents into the growth crucible.

A water cooled aluminum plate was fitted over the lid and

---

[2]Doping is used to express the addition of an impurity into the single crystal. The material added is referred to as the dopant.

bolted to the support collar as previously described. Both the cooling plate and the furnace collar aided in keeping the lid and its attendant seals cool.

Lowering Mechanism

Reduction gears coupled with a variable-speed direct-current motor produced a vertical lowering of zero to 1.4" per hour. A hub soldered at the center of the final gear in the train was bored and tapped to accept a large finely-threaded post. Each rotation of this hub produced a vertical movement of 0.0416" in the post. Rotation of the post itself was prevented by a vertical key and seat. The assembly was mounted on an aluminum plate. A large disc on top of the post functioned as a furnace platform. A microswitch positioned near the post stopped the platform at a preset lower limit. Controls and indicator lights for operation were mounted in a panel on the front of the lowering mechanism. All control passed through a master switch on the panel which controlled the platform movement, cold finger rotation, and furnace operation. Ammeters on the panel indicated the current input to the furnaces.

Vacuum and Controlled-Atmosphere System

Figure 3.4 is a schematic diagram of the vacuum system used with the controlled-atmosphere crystal-growing apparatus. Selection

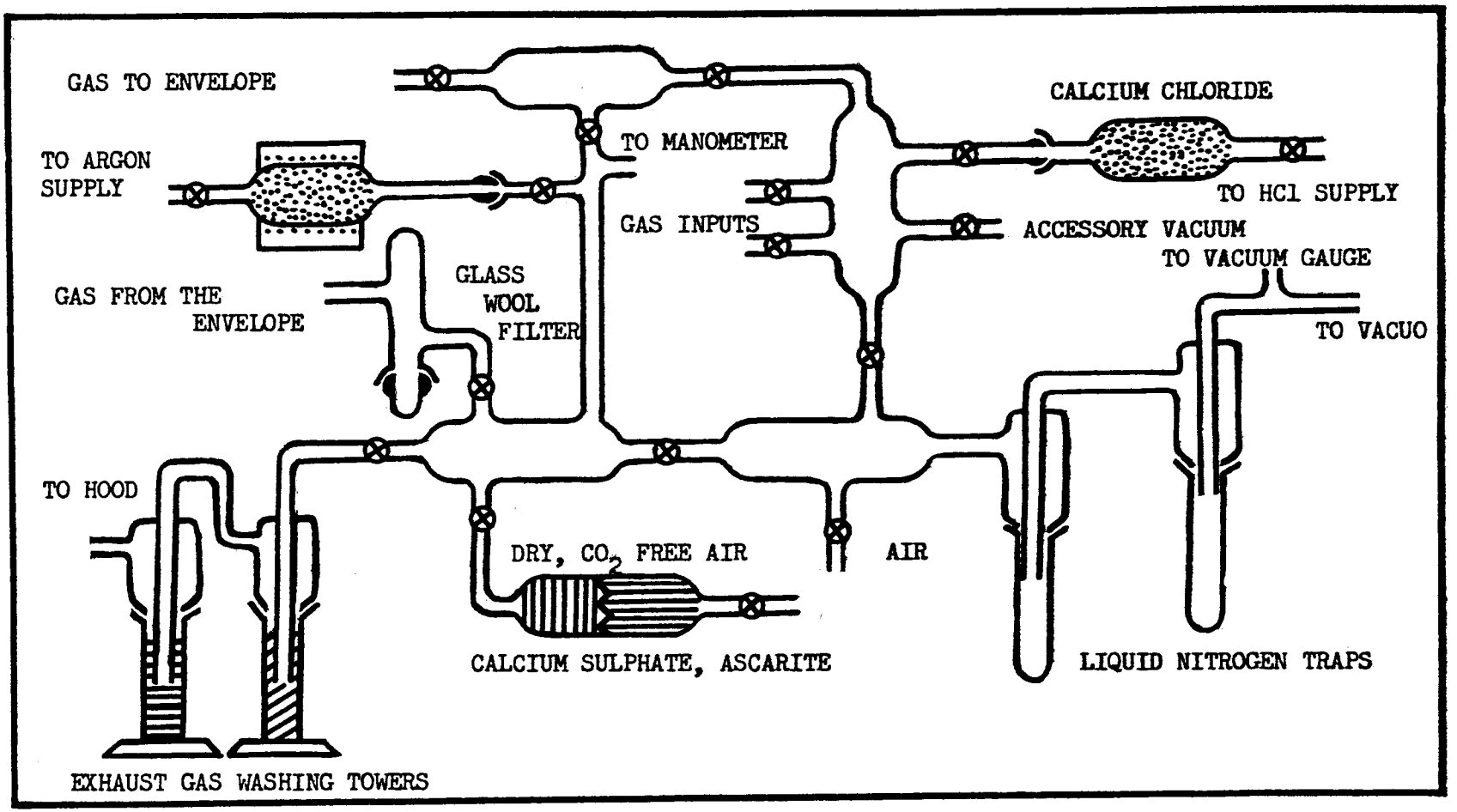

FIG. 3.4. SCHEMATIC DIAGRAM OF THE ATMOSPHERE CONTROL SYSTEM FOR THE CRYSTAL GROWING APPARATUS.

of various flow paths in the unit could introduce a vacuum, HCl, argon, HCl-argon mixture, or dry CO_2-free air into the system. Glass and vacuum stopcocks were used in the construction of the unit. Short sections of vacuum Tygon tubing were used as flexible couplings to the apparatus, the gas exhaust train, and the gas supply tanks. With this type of coupling the attainable pressure was limited to a minimum of 0.5 μ.

Prepurified research-grade argon, 99.998% minimum purity, was passed through a tube of porous copper wire heated to 400° C for residual oxygen removal. The typical impurities present in this material were (16, p. 2) 1-10 ppm nitrogen, 0-5 ppm oxygen, 0-5 ppm carbon dioxide, < 1 ppm hydrogen, and 0-6 ppm water. Purified HCl, 99.0% minimum purity, was passed through a tube of anhydrous $CaCl_2$ for residual moisture removal. A gas-washing tower filled with anhydrous $CaCl_2$ provided moisture protection on the gas exhaust train. Another tower filled to a depth of 3" with Shell Ondina oil was used to establish a positive pressure in the apparatus and prevent the back diffusion of oxygen or water vapor.

Single-Crystal Growth

Experimental

Salt as produced from any point in the purification process

could be used for single-crystal growth. Two experimental procedures were used. The first was for growth in the atmosphere, the second was for growth under a controlled atmosphere. When crystals were grown in air in a platinum or quartz crucible, the salt was heated from room temperature to about 120° C and allowed to remain at 120° C for two hours. Further heating for two hours brought the charge to 400° C. This temperature was maintained for a minimum of one hour, after which the temperature was increased and the salt melted. After melting was complete and the salt had reached a temperature of about 10° C above its melting point, the seed, firmly clamped in the cold finger, was introduced into the surface of the melt and rotation of the seed was started. After the outer surface of the seed had melted off, the seed was raised until only the lower end was in contact with the melt. In nearly all cases this method removed surface crystallites and insured single-crystal growth. Since the surface of the seed was dissolved in the melt, seed stock of comparable purity was necessary. Crystals obtained from the Harshaw Company or crystals produced by the author were used for this purpose. Adjustment of the melt temperature, the coolant flow in the cold finger, and the pulling rate established the conditions necessary for producing a large boule. Initial growth on the seed proceeded as shown below (A). By alternately increasing and decreasing the diameter of the growing crystal (B), crystals with fewer grain

boundaries and better cleavage properties were produced.

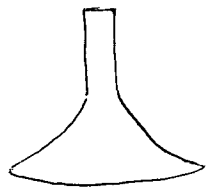

(A)

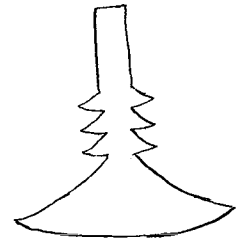

(B)

Each crystal grown was limited to 75% of the initial charge. Boules of 40 to 50 grams were most representative. Doping of the charge, and hence the crystal, could be done at any chosen time during the growth process.

The second procedure used for single-crystal growth pertains to growth in the controlled-atmosphere crystal-growing apparatus previously described. In all cases the crystals were grown from a quartz crucible set in a Vycor envelope. The metal components of the chamber lid were washed free of grease and reassembled with minimal lubrication. The envelope and crucible were stripped with concentrated HNO_3 and rinsed thoroughly in deionized water. A charge of salt, weighed directly in the crucible, was placed in the chamber, a seed clamped into the cold finger, and a known weight of doping agent introduced into the doping cup. The chamber was sealed and put under vacuum. Once the pressure of the chamber had reached 5 μ the temperature was increased to 110° C. This

temperature was maintained for 24 hours. At the end of 24 hours the vacuum was required to be $\leq 0.5\ \mu$ or the procedure was terminated. The temperature was increased to 450° C and the chamber maintained for four hours under a pressure of 0.5 μ. At 450° C the system was back filled with argon to a positive pressure of 20 mm Hg with the chosen atmosphere. Typical gas flow rates through the chamber were 3-10 liters per hour. The salt was melted and a growth procedure similar to that previously described was used. At any time the atmosphere could be changed or the relative amounts of any gas present regulated. The doping agent was introduced during the growth at a time determined by the operator. At completion the crystal-melt contact was broken and the chamber allowed to cool. Removal of the sample took place about eight hours later.

Contamination from Atmosphere and Crucible

Some of the factors that affect crystal growth, purity, and impurity distribution merited special consideration. The content of impurities in the initial salt charge was considered as a lower limit to the impurity content of the crystal produced. Although some volatile impurities will vaporize upon melting the charge, it is reasonable to suppose that further contamination occurs during growth through contact with the melt container and the atmospheres.

Crystals grown in the atmosphere are known to contain OH^-,

O_2, and $CO_3^{=}$ in one form or another (89). It was important to exclude H_2O, CO_2, and O_2 because of their reaction with the salt and possible reaction with the doping agent, lead. The total exclusion of these impurities, in addition to heavy-metal ions, was desired.

In a recent paper Fritz, Lüty, and Anger (30) have shown that air-grown KCl crystals, pure and doped with OH^-, contain two types of OH^- impurities. The first is the free OH^- which gives rise to the well known 204 mμ and 2.79 μ absorption peaks. It is probably an OH^- ion in a substitutional site. The second is a reaction product between divalent impurities and OH^-. Products of the second type lead to an erroneous value of the oscillator strength of lead ion at 273 mμ and low values for the conductivity of the sample. Further discussion of this effect is found in the sections on oscillator strength and conductivity.

Patterson (79) and Otterson (78, 77) have studied the presence of OH^- in alkali halides and suggest that reagent-grade NaCl melted for a period of eight hours in air contains about 200-300 ppm OH^-. In dry air, only 8 ppm OH^- was noted, a level comparable to that for Harshaw crystals (about 3-20 ppm). They suggest that O_2 in conjunction with moisture in the air gives rise to the OH^- in the crystals. Patterson's treatment of NaCl crystals, containing 20 ppm OH^-, with dry HCl for 48 hours reduced the OH^- level to about

1 ppm.

The author tested the effect of various atmospheres on crystal growth and found that crystals grown under argon, or argon-HCl mixtures, had little or no OH^- content. Growth atmospheres of nitrogen or argon reduced the peak significantly while HCl removed it completely. In all cases removal of O_2 and moisture was found necessary to prevent contamination from OH^-.

Investigations carried out by Fredericks (25, p. 26-34) in this laboratory as well as work by Etzel and Patterson (22) suggest possible attack (etching) of the container by the melt and consequent contamination of the crystals produced. With reagent-grade doubly-recrystallized salt or salt purified by ion exchange, the author found various degrees of attack. There was a definite relation between purity of the salt and attack of the container. The purer the salt the less the etching. In an argon atmosphere, porcelain or platinum crucibles were inferior to quartz. However, in the presence of moist air, quartz etched severely and platinum proved more durable.

The argon used was of high purity while the HCl was contaminated with chlorinated hydrocarbons and acetylene (84, p. 6). These organic materials either passed through the system unchanged or were degraded to elemental carbon during the fusion. Carbon did appear in all melts where oxygen was excluded. Its presence as a

floating scum caused some initial difficulty in starting crystal growth. The best results and highest purity of final product were obtained with the combination of salt purified by ion exchange, the use of a quartz crucible and an atmosphere of HCl or argon-HCl.

Uniformity of Doping

Variables such as crucible shape, rotation rate of the seed, and thermal heating and cooling patterns have a marked effect on the distribution and the effective segregation coefficient of lead ion in KCl. Lead ion is more soluble in the melt than in the crystal having a segregation coefficient less than one.

Numerous papers (70, 32, 8) have considered the problem of impurity distribution in a growing single crystal when the segregation coefficient is less than one. In the absence of rotation of the seed or crucible, the distribution of dopant in the crystal usually shows an inhomogeneity associated with the asymmetry of the thermal field (80). At the hottest points in the thermal field the crystal has the lowest impurity content. Experiments by Belyaev, Perlshtein, and Panova (4) denoted that in Kyropoulos-grown NaI crystals doped with TlI, a dopant concentration gradient of some 40% often appeared within a 1 cm section. This was caused by the lack of stirring as well as activator loss by evaporation. Once the distribution was set in the crystal, a seven-day anneal failed to homogenize the

crystal.

When stirring is introduced, the distribution of dopant in the growing crystal can be made more homogeneous. Studies by Turovskii and Mil'vidskii (104) indicate that primary mixing is due to crystal rotation. When the crystal alone is rotated, the impurity is drawn up from the bottom and then thrown out toward the sides of the crucible, and total melt mixing is quite thorough. Further, they found that a hemispherical crucible sets up temperature gradients and convection currents which promote a more uniform impurity distribution.

Coker (11, p. 10-11) has shown that when the seed and growing crystal alone are rotated, rotation rates of 90 rpm were necessary to insure uniform distribution of sulfate ion in a crystal. A uniform distribution of dopant in planes perpendicular to the crystal growth axis and a predictable increase along the growth axis resulted from this method. However, the author has found the problem to be more complex, as the speed of rotation of the seed (and growing crystal) has to be correlated to the thermal heating and cooling patterns of the furnace, the crucible shape, and the pulling rate, before predictions regarding homogeneity and distribution can be made. Ikonnikova and Izergin (38) found that vibration introduced into the Czochralski method even increased the growth rate and impurity content in KCl crystals grown from a KCl-$PbCl_2$ melt. If the

previously mentioned factors such as cooling and pulling rate are controlled, the segregation coefficient can be considered as a constant. Then the problem becomes one of furnishing a melt of constant composition to the growing crystal. Varonov, et al. (106) have considered the problem of uniformity throughout the boule from a theoretical standpoint. They devised a melt vessel consisting of two concentric crucibles of special shapes connected by a long small flow tube. As the crystal is pulled from the inner crucible, the outer crucible feeds the inner melt to hold a constant concentration of impurities in the melt. Parameters and considerations for vessel design are presented in that paper. Without a provision such as this, the concentration of lead ion increases as the crystal is drawn from the melt. It was observed that a uniform distribution of the dopant along the vertical axis could not be obtained without special modifications of the growth vessel.

Results

Crystals of varying purity, but all of all good optical quality, were grown in the apparatus described. Lead ion in various concentrations was introduced into these crystals. The author did not attempt the application of Varonov's principles, but found that crystals with a constant concentration of lead ion in transverse slices could be produced from a simple hemispherical melt vessel.

These crystals were of sufficient homogeneity that vessel modification was not made. This method of growth produced crystals homogeneously doped with lead ion in planes perpendicular to the vertical growth axis, but with a variation in lead ion concentration parallel to this axis. To produce these crystals, rotation of the seed and growing crystal was made in the range of 65 to 90 rpm. Rotation rates below 65 rpm lead to an uneven distribution of dopant in the transverse planes of the growing crystal.

A special type of crystal was grown in this study for the transport studies of Pb^{++} in KCl. This type contained two separate regions, one pure, the other doped with Pb^{++}. At a designated point the melt in contact with the growing crystal was intentionally doped with a known concentration of $PbCl_2$. Direct observation of the large established cross section of the growing crystal insured the presence of a flat growth interface between the crystal and the melt at the time of dopant instroduction. In a few cases a momentary separation of the two phases aided in establishing the planarity of the growth face. Immediate recontact of the two phases introduced no discontinuity in the single crystal lattice.

IV OSCILLATOR STRENGTH

Introduction

The oscillator strength of a band is related to the probability of the optical transition producing the absorption. The bell-shaped curves observed for many absorbing centers suggest that the centers may be treated as damped oscillators according to classical dispersion theory. Smakula (94) in 1927 was the first to adopt this approach. For classical damped noninteracting oscillators, for which the absorption curve has a Lorentzian shape, the following equation was obtained:

$$N_o = \frac{9mc}{2e^2} \cdot \frac{n}{(n^2+2)^2} \alpha_m \omega \qquad (4.1)$$

where N_o is the concentration of centers per cm^3, m the electron mass, e the electron charge, c the velocity of light, n the index of refraction at maximum absorbance, α_m the absorption coefficient at maximum absorbance, and ω the half-width of the absorption band. α_m is given by

$$\alpha_m = \frac{2.303}{x} \log \frac{I_o}{I}$$

where I_o is the intensity of the incident light beam, I the intensity of the transmitted beam, and x the sample thickness. When α_m is given in cm^{-1}, ω in eV, and the band shape is considered Lorentzian,

equation (4. 1) reduces to

$$N_o = 1.29 \times 10^{17} \frac{n}{(n^2+n)^2} a_m \omega \qquad (4.2)$$

This is the result for classical damped oscillators. For an atomic absorber, if the oscillator strength f is the ratio of its absorption to that of a classical damped oscillator, equation (4. 2) becomes

$$fN_o = 1.29 \times 10^{17} \frac{N}{(n^2+2)^2} a_m \omega \qquad (4.3)$$

Rauch and Herr (85), Dexter (15, 16, 17), and Konitzer and Markham (48) have considered the fundamental shape of absorption bands and suggest that interactions of the centers with lattice vibrations contribute to the width of the band. Further, the band shape is more nearly Gaussian. Attempts for a better curve fit are made using a Pekarian or double Gaussian curve. On the assumption that the band shape is Gaussian, equation (4. 3) becomes

$$fN_o = 0.87 \times 10^{17} \frac{n}{(n^2+2)^2} a_m \omega \qquad (4.4)$$

The experimental observation of the absorption coefficient and index of refraction plus a direct chemical determination of the number of centers present, leads to a value for the oscillator strength f. Even though the value of f appears to be an experimentally determined quantity, it must be remembered that the development of Smakula's equation was based on a particular model and the correlation of the oscillator strength to the area under the absorption

curve depends upon this model.

Necessary for the determination of the oscillator strength was a method of direct chemical analysis of uniformly doped samples. Dithizone was used for the chemical analysis of lead and the lead distribution was checked to insure that observed portions of each analytical sample were representative of the entire sample. The problem of impurity distribution was closely coupled with the methods of crystal growth as noted in Chapter III.

Prior to the direct chemical analysis of the lead ion present in single crystal samples, the samples had been subjected to other procedures. The samples were cut from KCl:Pb crystals of varying purity, grown under a variety of conditions. The samples, nominally 1/2" × 3/4" × 1/64", were heated to 630° ± 20° C for ten minutes and quenched to room temperature. The thickness of the sample was measured at three different positions across the platelette and the homogeneity of absorption checked. If the criteria for homogeneous doping were met, the ultraviolet spectrum of the sample was recorded and the weight measured to ± 0.01 mg on a microbalance.

The use of the crystal puller or the controlled-atmosphere crystal-growing apparatus gave single crystals of varying inherent impurity content, crystals doped completely with lead ion, and crystals which contained lead ion only in one region. These crystals were subjected to the analytical studies considered in the following sections.

Trace Analysis of Lead in KCl with Dithizone

Lead is observed in trace levels in nearly all systems. Many methods have been devised for its analysis, among them a colorimetric method utilizing dithizone. This method has been extensively investigated (3, 49, 69, 110) and gives quantitative results for lead in the 0.1-100 ppm range. The author has adopted the dithizone method to the analysis of single crystals of KCl.

As Sandell (91, p. 138) noted, organic reagents used for trace analysis show varying degrees of selectivity and rarely true specificity. In order to yield specific reactions, auxiliary means must be employed. Diphenylthiocarbazone, or dithizone, which has the following structure,

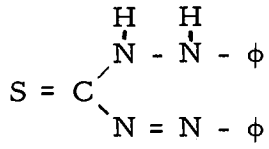

is no exception. The material reacts with many heavy-metal ions to produce brightly-colored internal complexes called dithizonates. In general, these dithizonates are soluble in an organic phase such as CCl_4 or $CHCl_3$. Divalent lead forms a characteristic cinnabar-red color in CCl_4. The complex is of the primary type as shown below:

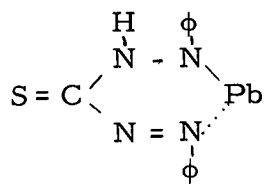

Mathre (65) has studied the formation of lead dithizonate in both CCl_4 and $CHCl_3$. Suggested in his study were the conditions necessary for a quantitative evaluation of the lead ion concentration in the 0.1-100 ppm range. He calculated the extraction constant of lead ion from an ammoniacal solution considering the following equilibria:

$Pb^{+2} + 2H_2Dz \rightleftharpoons Pb(HDz)_2 + 2H^+$ $\quad (CCl_4) \quad (CCl_4)$	$\frac{K_{25°C}}{5.6 \quad (I = 1)}$
$H_2Dz \rightleftharpoons H^+ + HDz^-$ (CCl_4)	1.4×10^{-9} (I=1)
$PbOH^+ \rightleftharpoons Pb^{++} + OH^-$	1.5×10^{-8} (I = 0)
$Pb(OH)_2 \rightleftharpoons Pb^{++} + 2OH^-$	4×10^{-11} (I = 0)
$HPbO_2^- + H_2O \rightleftharpoons Pb^{++} + 3OH^-$	3×10^{-14} (I = 0)
$Pb(CN)_4^= \rightleftharpoons Pb^{++} + 4CN^-$	5×10^{-11} (I = 0)

where H_2Dz is dithizone and I the ionic strength. In theory, the extraction was found to be favorable and experiments bear this out.

In the analysis of single KCl crystals, equilibria involving halo-complexes become pertinent. The following equilibria may exist:

$Pb^{+2} + Cl^- \rightleftharpoons PbCl^+$	$K_{25°} \sim 7.6$	(I=1)
$PbCl^+ + Cl^- \rightleftharpoons PbCl_2$	~ 4.1	"
$PbCl_2 + Cl^- \rightleftharpoons PbCl_3^-$	~ 0.4	"
$PbCl_3^- + Cl^- \rightleftharpoons PbCl_4^{-2}$	~ 0.7	"

$$PbCl_4^{-2} + Cl^- \rightleftharpoons PbCl_5^{-3} \qquad ?$$

$$PbCl_5^{-3} + Cl^- \rightleftharpoons PbCl_6^{-4} \qquad ?$$

Not all the equilibrium constants for the above are known and no attempt was made to include these equilibria in a theoretical calculation of the extraction coefficient. It is known that compounds containing $PbCl_6^{-4}$, $PbCl_4^{-2}$ and $PbCl_3^{-1}$ do exist. The determination of known amounts of lead in the presence of a large excess of KCl indicated that the quantitative extraction of lead was favorable under this condition.

Since some 20 heavy-metal ions react with dithizone, specificity must be obtained to make the reagent useful. Adjustment of the pH, addition of complex-forming agents, and absorbance measurements taken at 520 mμ are used for the analysis of lead. The fundamental process is the formation of lead dithizonate by extraction of lead ion with dithizone, from an aqueous ammoniacal solution containing cyanide and sulfite, into a CCl_4 medium. The absorbance of lead-dithizonate recorded at 520 mμ is found to be proportional to the concentration of Pb^{++} in the sample.

With the use of monochromatic light, dithizone, lead dithizonate, and the oxidation product of dithizone diphenylthiocarbadiozone, all in CCl_4, give good Beer's Law plots. The absorption curves of these materials are given in Figure 4. 1. For accurate quantitative results, the absorption measured at 520 mμ must be that of lead dithizonate

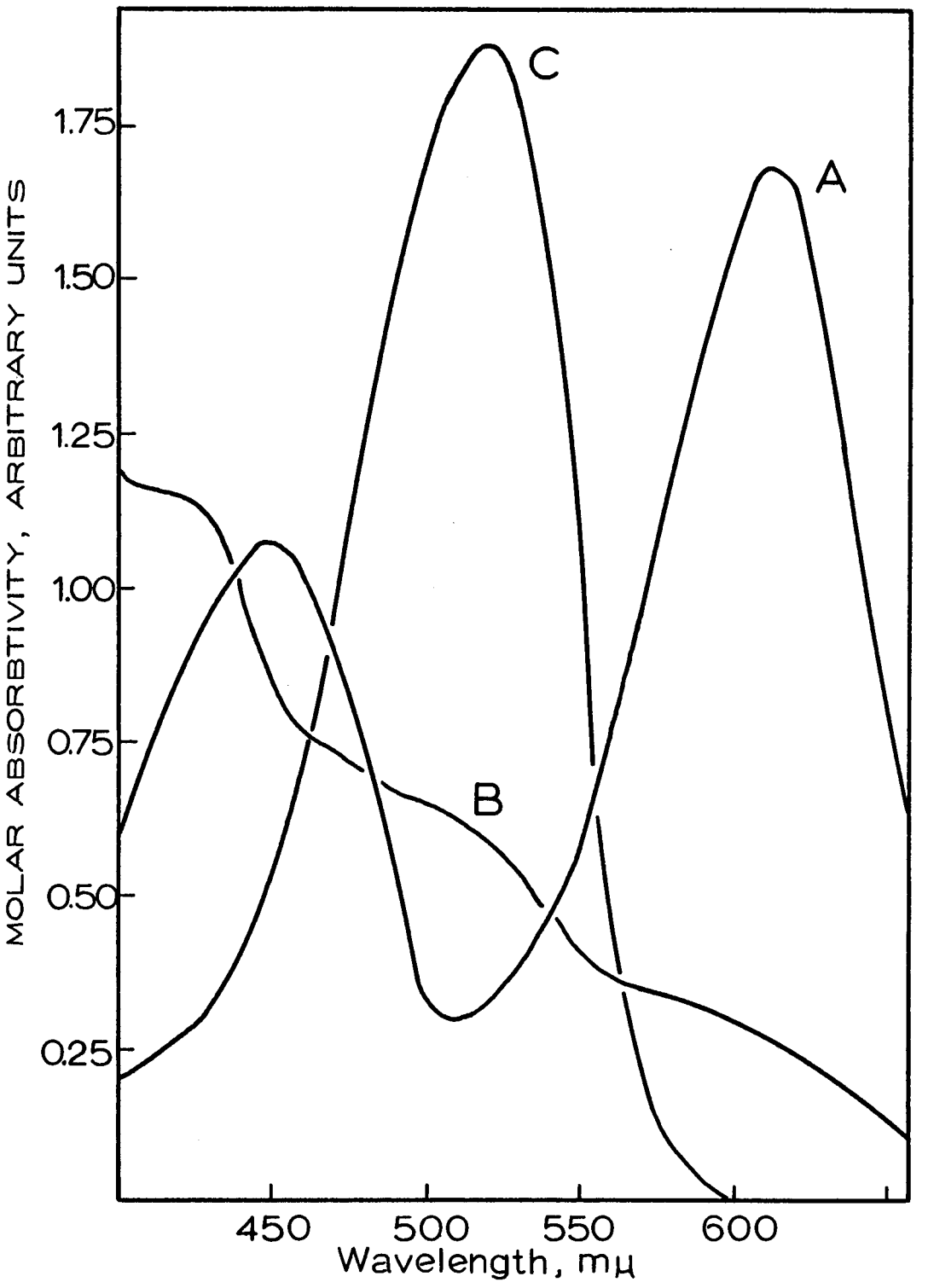

Fig. 4.1. Absorption curves of : A, dithizone; B, its oxidation product; and C, Pb-dithizonate; all in carbon tetrachloride. (23)

alone. The addition of sulfite helps to prevent the oxidation of dithizone while the addition of cyanide and pH adjustment prevent the formation of the majority of other metal dithizonates. Under these conditions, Sn^{++}, Tl^{+}, and Bi^{+++} will also be extracted. However, the amount of these ions present in the samples was negligible.

Mathre's methods of reagent purification were used in conjunction with longer, light-protected extraction times to make the system suitable for the analysis of lead without the removal of the KCl. The extensive methods of purification used are summarized briefly.

Reagent Purification

The sensitivity of the dithizone method for lead required the reagents to be free from heavy-metal contamination and trace substances which would cause oxidation of the complexing agent. Dithizone is oxidized to diphenylthiocarbadiozone under weak oxidizing conditions and the presence of the oxidation product in dithizone-carbon tetrachloride solutions gives a yellow brown color which interferes with the quantitative determination of lead. Purification of the reagents eliminates these problems.

Water. Distilled water was passed through a 20 mm by 500 mm column of Dowex AG-50 ion exchange resin at the rate of one litre per hour to give a lead-free product.

Carbon Tetrachloride. Reagent grade CCl_4, supplied from the

J. T. Baker Co. or Matheson-Coleman-Bell Co. was allowed to stand with a few drops of Br_2 for two weeks, after which it was shaken twice with one tenth its volume of 10% NaOH, refluxed for four hours with one tenth its volume of 10% NaOH, cooled and washed free of alkali. The CCl_4 layer was refluxed for one half hour with one tenth its volume of 10% hydroxylamine hydrochloride, washed free of the hydrochloride, dried over Drierite, and distilled in Pyrex from a mixture of Drierite and CaO. The product was stored in the dark at 40° F. CCl_4 purified in this manner caused less than 1% decrease in the absorbance of freshly formed lead dithizonate during a period of one hour. No attempt was made to reclaim or reuse the CCl_4.

Dithizone. Matheson Co. reagent grade #CB992 dithizone was used without further purification. Solutions of this prepurified material in CCl_4 showed but a trace absorbance at 450 mμ, the point of maximum absorption for the oxidation product.

Deoxygenated, purified CCl_4 was used to prepare 0.01% (w/v) and 0.001% solutions of dithizone in CCl_4. These solutions were stored in the dark at 40° F and the 0.001% solution was prepared shortly before use by dilution of the 0.01% solution.

Nitric Acid. Redistilled concentrated HNO_3 free of oxides of nitrogen was suitable for use when diluted 1:100 with deionized water.

Ammonium Hydroxide. A 28% solution of NH_4OH was prepared

by passing pure ammonia gas into deionized water until saturation occurred. Dilution with deionized water lowered the concentration to 8 M.

Potassium Cyanide. A 50% solution of reagent-grade KCN, suitably free from K_2S, a complexing inhibitor, was extracted with 0.01% dithizone in $CHCl_3$ until the organic layer showed no further indication for lead. Washing with pure $CHCl_3$ removed the remaining dithizone and the KCN solution was diluted to the concentration level required.

Sodium Sulfite. A 10% solution of reagent-grade Na_2SO_3 was extracted at pH = 8 with a 0.001% dithizone-CCl_4 solution until the heavy-metal ions were removed. Excess dithizone was removed by shaking with pure CCl_4 and $CHCl_3$.

Lead Nitrate. Lead nitrate was purified by fractional recrystallization. Three recrystallizations from deionized water containing 0.01 mole HNO_3 per litre produced a 50% yield. The recrystallized product was dried in air at 110° C for 24 hours and desiccated for two weeks in a vacuum over KOH. This product was used for all standard lead solutions.

Ammonia-Cyanide-Sulfite Solution

This solution was the basic medium for the analysis. Sufficient purified water was added to 725 ml of 8.0 M NH_4OH and 30 ml of 10%

KCN to make one liter of solution. One and one half grams of sodium sulfite were added to the solution and storage was made in polyethylene to prevent contamination from the container.

pH Control

Buffers were prepared from a saturated solution of potassium bitartrate, pH = 3.57, and 0.05 M borax, pH = 9.18. pH measurements were made on a Beckman Zeromatic pH meter and analyses were made at pH = 10.8 ± 0.1.

Glassware

All glassware used in this study was Pyrex glass. Wherever feasible, polypropylene was used to prevent contamination. All glassware used was washed well with Labtone detergent solution, rinsed with distilled water, stripped with concentrated HNO_3, washed with distilled H_2O, triply rinsed with deionized H_2O and drained dry.

The glass wool used as filter plugs was purified before use by extracting with 0.01% dithizone solution, stripping with concentrated HNO_3, and washing three times with deionized water. It was dried at 150° C for 24 hours and stored in polyethylene.

Experimental

A series of standard solutions was prepared from $Pb(No_3)_2$

dissolved in 1:100 HNO_3. By means of 0.00100% and 0.0100% Pb in HNO_3, a series of standards from 1-80 γ Pb was prepared and used to establish a standard curve. Using microburettes, a known amount of lead in 10 ml of 1:100 HNO_3 was introduced into a 125 ml black-coated separatory funnel. To this was added 10 ml of ammonia-cyanide-sulfite solution and the pH adjusted to 10.8. (A periodic check was made on the pH to insure the required value. The solutions used were fresh and matched so that equal volumes of the 1:100 HNO_3 and the ammonia-cyanide-sulfite solution gave a pH of 10.8 ± 0.1.) A 10 ml or 25 ml portion of fresh 0.001% dithizone-carbon tetrachloride solution was pipetted into the separatory funnel. The volume used depended on the amount of lead thought to be in the sample. The solution was shaken on a mechanical shaker (200 shakes per minute) for 15 minutes and the phases allowed to separate. The nonaqueous layer was drawn off through a filter plug of purified glass wool into 1 cm Pyrex cells and the absorbance at 520 mμ obtained by means of a Beckman Model DU Spectrophotometer using CCl_4 as a reference. Exposure to strong light was prevented during extraction by the black coating on the separatory funnels and minimal exposure occurred before absorbance readings of the solution were obtained.

When studies were made using additive concentrations of pure KCl, the KCl was dissolved in 1:100 HNO_3 solution prior to its use.

In the case of solid crystal samples, they were dissolved in 10 ml of 1:100 ml HNO_3 and allowed to stand for a minimum of 15 minutes. This step increased the extraction rate as it was thought that the $PbCl_x^{(-x+2)}$ species present in the crystal have to be converted to an aqueous species before reacting with dithizone. The samples from this point were treated in a manner analogous to that for the analysis of standard solutions. A blank determination was run with each set of eight samples or standards as a check for contamination and oxidation of the complexing solution.

Discussion of Results

A plot of the concentration of lead dithizonate in CCl_4 versus absorbance, Figure 4. 2, demonstrates that absorbance is directly proportional to the concentration. Two curves are shown, one for a 10 ml CCl_4 layer, the other for a 25 ml CCl_4 layer. The extended portion of these curves, shown in the inset, was for conditions of moderate supersaturation. The solubility of lead dithizonate in CCl_4 at 25° C is 12 ppm (w/v) Pb or 5.7×10^{-6} M and is marked by the vertical line on the plot. Sandell (91, p. 567) has suggested that supersaturations up to 3. 5 ppm Pb behaved normally. However, the system in the presence of KCl seems reliable only to saturation, as indicated by the failure of Beer's Law beyond this value. All trace analyses made in this study were at or below the saturation

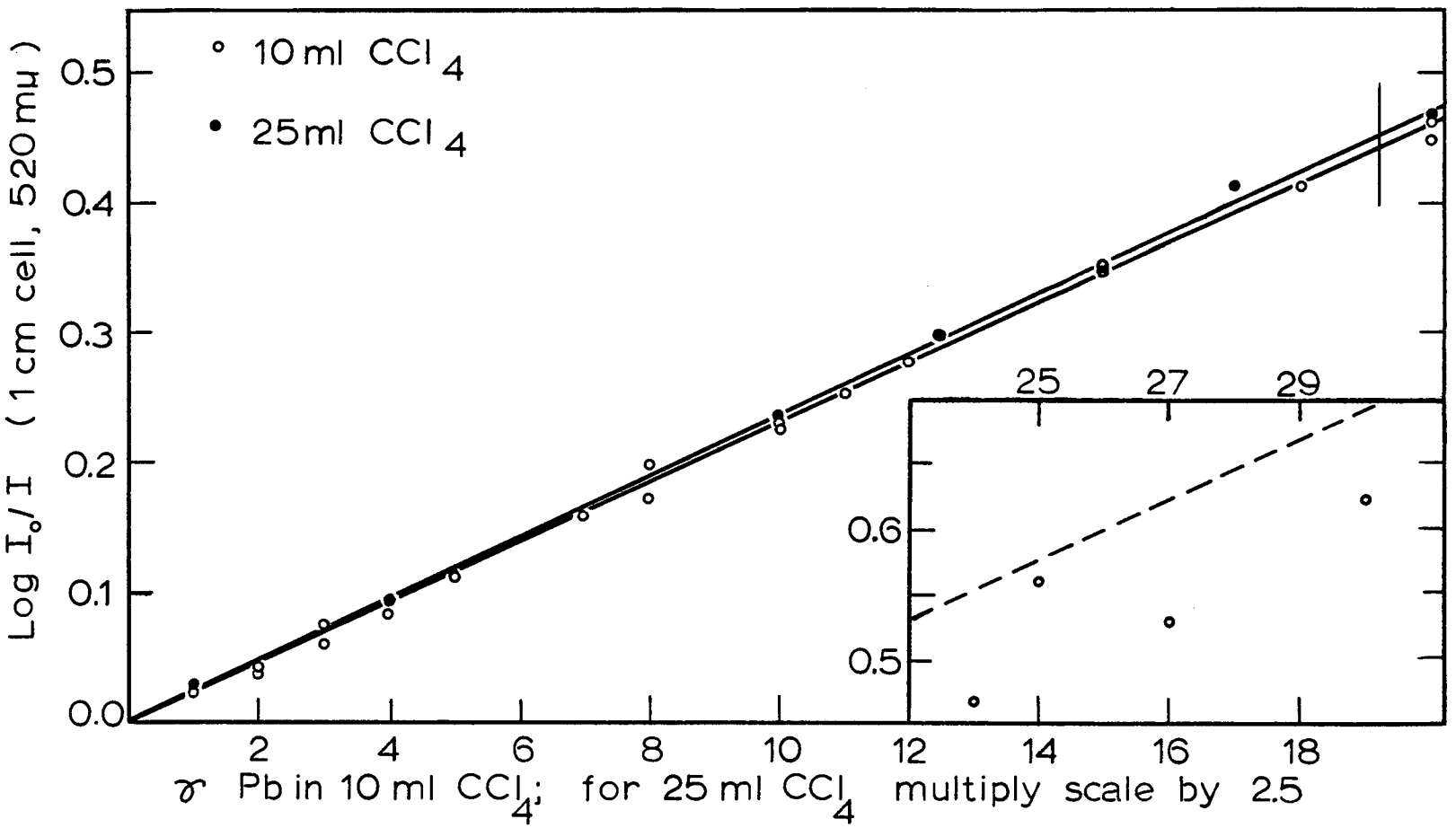

FIG. 4.2 . Determination of lead in KCl single crystals with dithizone in CCl_4 . Insert shows the region of supersaturation of Pb-dithizonate in CCl_4 . Dotted line is extrapolated from the unsaturated region.

value.

The extraction of lead in basic solutions using carbon tetrachloride is rapid in the absence of KCl. The presence of Pb^{++} in a KCl matrix affected the kinetics of extraction significantly more than the extraction equilibrium. The extraction rate was decreased by a factor of ten. In the presence of purified KCl, the extraction of Pb^{++} added to the solution was comparable to that for the standard solutions. Table 4. 1 gives representative data for the percent recovery of known lead samples in the presence of a large excess of KCl. It is suggested that unless the crystal sample remains in 1:100 HNO_3 for a sufficient length of time, the following equilibrium becomes the rate-controlling step for extraction:

$$PbCl_x^{(-x+2)} \rightleftharpoons Pb^{++}_{aqueous} + xCl^-.$$

Variations in the pH of the ammonia-cyanide-sulfite solution from the value of 10. 8 lead to errors of the magnitude shown in Table 4. 2. Besides variations of the pH, interference from other reacting metals, heavy metals in the reagents and solutions, instability of standard solutions and dithizonates, oxidation of dithizone, supersaturation, and incomplete extraction were sources of error. Table 4. 3 gives an evaluation of the errors found, based on known amounts of Pb taken for analysis. The data presented in this table suggests the analysis is good to ± 5% in the 0-10 ppm range and to ± 3% in the 10-70 ppm range.

Table 4. 1 Recovery of Pb in the presence of large amounts of KCl. (0. 001% dithizone in CCl_4, 1 cm cell)

Concentration of KCl present	Pb taken, γ	Pb found, γ	% error
0. 05% Pb in KCl	20	19. 3	-3. 5
	40	40. 1	+0. 25
	60	60. 3	+0. 5
500 mg KCl per sample	40	40. 1	+0. 25
	60	58. 5	-2. 5
	60	58. 5	-2. 5
	70	69. 3	-1
	50	51	+2
365 mg KCl per sample	10	9. 9	-1
	0	0	0
0. 1% Pb in KCl	10	9. 32	-6. 8
	20	19. 7	-1. 5
	30	30	0
	40	39. 5	-1. 25
	50	50. 4	+0. 8
	60	61. 2	+2. 0
	70	70. 8	+1. 1

Table 4. 2 Error from variation of pH of solution from recommended value of 10. 8 (65, p. 81). (10 ml of ammonia-cyanide-sulfite solution, 10 ml of 0. 001% dithizone in CCl_4)

pH	Pb taken	Error	
		5	25
10. 2		+0. 19	+0. 06
10. 4		+0. 10	+0. 03
10. 6		+0. 03	0. 00
10. 8		0. 00	0. 00
11. 0		-0. 03	0. 00
11. 2		-0. 03	-0. 03
11. 6		-0. 05	-0. 30

Table 4.3 Determination of lead with dithizone in carbon tetrachloride. (10 ml CCl_4, 1 cm cell) (a), (10 ml or 25 ml CCl_4, 1 cm cell) (b)

Pb taken, γ	Pb found, γ	% error
	(a) Mathre (65, p. 77)	
4.15	4.18	+0.8
5.78	5.69	-1.6
6.42	6.46	+0.8
8.50	8.55	+0.6
12.10	11.98	-1.0
15.40	15.56	+1.0
27.2	27.4	+0.7
	(b) This work	
1.00	1.03	+3.0
3.00	3.10	+3.3
4.00	4.00	0
5.00	4.75	-5.0
6.00	5.66	-5.7
8.00	8.02	+0.25
9.00	8.52	-5.3
10.00	9.92	-0.8
12.00	12.01	+0.08
13.00	12.90	-0.77
14.00	13.57	-3.1
15.00	14.03	-1.1
20.0	19.7	-1.5
30.0	29.5	-1.7
40.0	41	+2.5
50.0	50	0
50.0	49	-2
60.0	61.6	+2.7
60.0	61.7	+2.8
70.0	69.3	-1

Homogeneity

Scanning Absorption Cell

To determine the impurity distribution in crystals and to define the interfacial position between pure and doped regions of single potassium chloride crystals, a scanning absorption cell was designed and built. The cell and light cover were designed for use in a Beckman DK-1 Recording Spectrophotometer and are shown in Figure 4. 3. The basic function of the unit was to drive a sample past a fixed slit to allow the observation of differences in absorption in various portions of the sample. In addition, the cell was suitable for other room-temperature absorption measurements on crystal samples.

The cell consisted of three parallel plates mounted on a common base and fitted with a drive unit to elevate the sample. The reference side of the cell remained fixed at all times and the sample side had only vertical movement. A 0. 2 rph synchronous, gearhead motor transmitted power through a friction coupling to a stainless steel shaft mounted in two shielded ball bearings. By use of a friction coupling, a knob at the other end of this shaft could be turned to override movement and reposition the sample at any point. A pinion gear fixed on this shaft drove a rack mounted on the sample

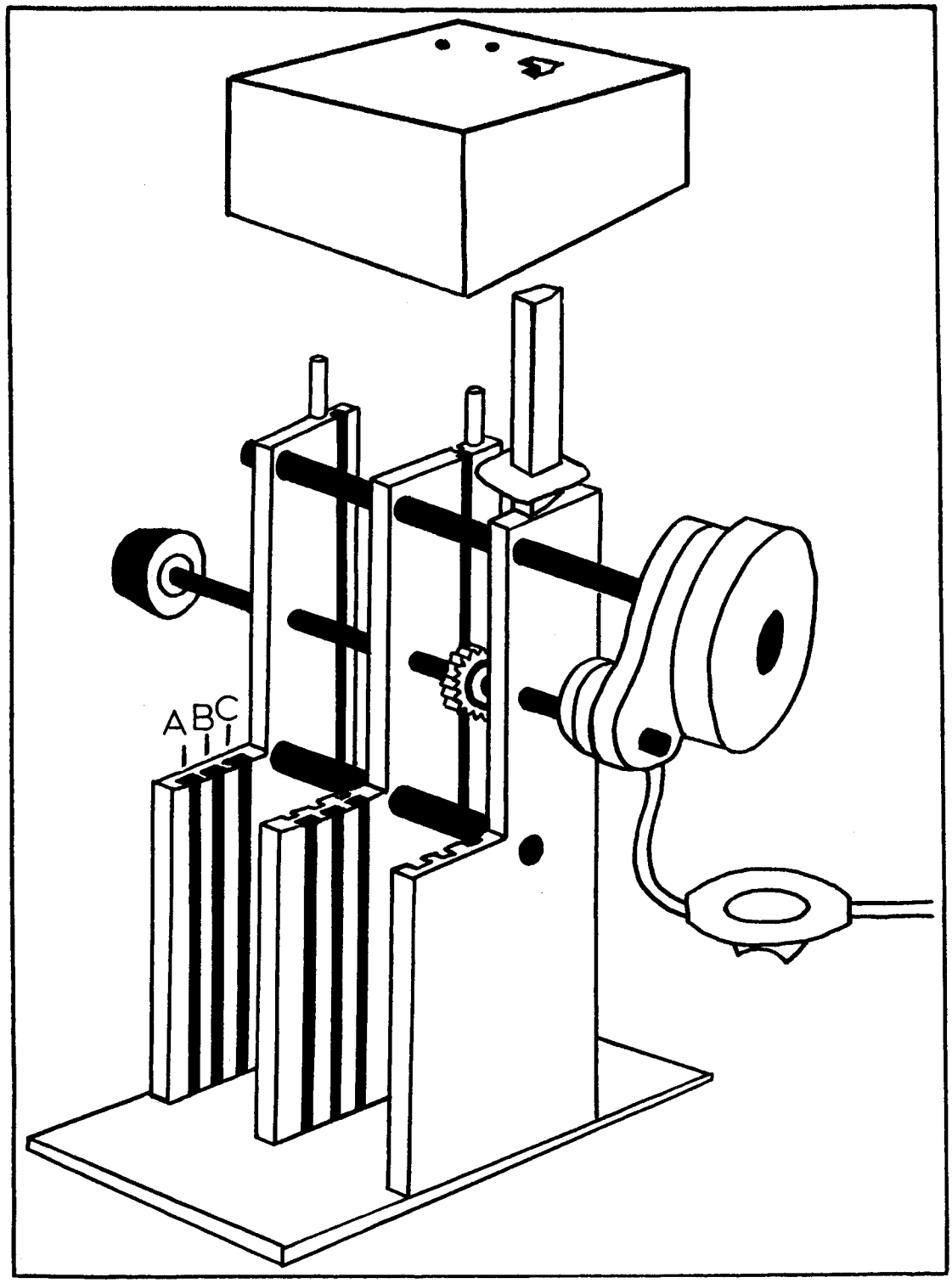

FIG. 4.3. SCANNING ABSORPTION CELL AND COVER.

backing plate, thus converting rotation to linear vertical movement. This plate was elevated at the rate of 0. 5 mm per minute, moving the sample and its mount past the spectrophotometer beam. The upper portion of this plate extended through the cover and was engraved with a vernier scale in 0. 1 mm divisions. This vernier traveled parallel to a stationary scale which was mounted on the cell frame proper and indexed the position of the sample with respect to the spectrophotometer beam. An on-off switch with a neon indicator light controlled the power for operation.

The light cover was constructed of black Bakelite and fitted with felt strips on all edges where light leaks were possible. It was positioned over the cell in a reproducible manner by aligning holes in the cover with two 3/16" diameter pins which fitted through the cover.

Figure 4. 4 shows the sample and reference mounts, and examples of the slits used. The mounts were designed to clip over the top of the backing plate and sit in a groove at the base of the plate. These mounts were fitted with silicon-bronze clips so that a large degree of flexibility in accommodating sample thickness was obtained. Sample width was limited by the dimensions of the cell and the cell compartment. Samples up to $1\frac{1}{2}$" thick and 7/8" wide could be accommodated.

Matched pairs of slits were machined to limit the vertical and

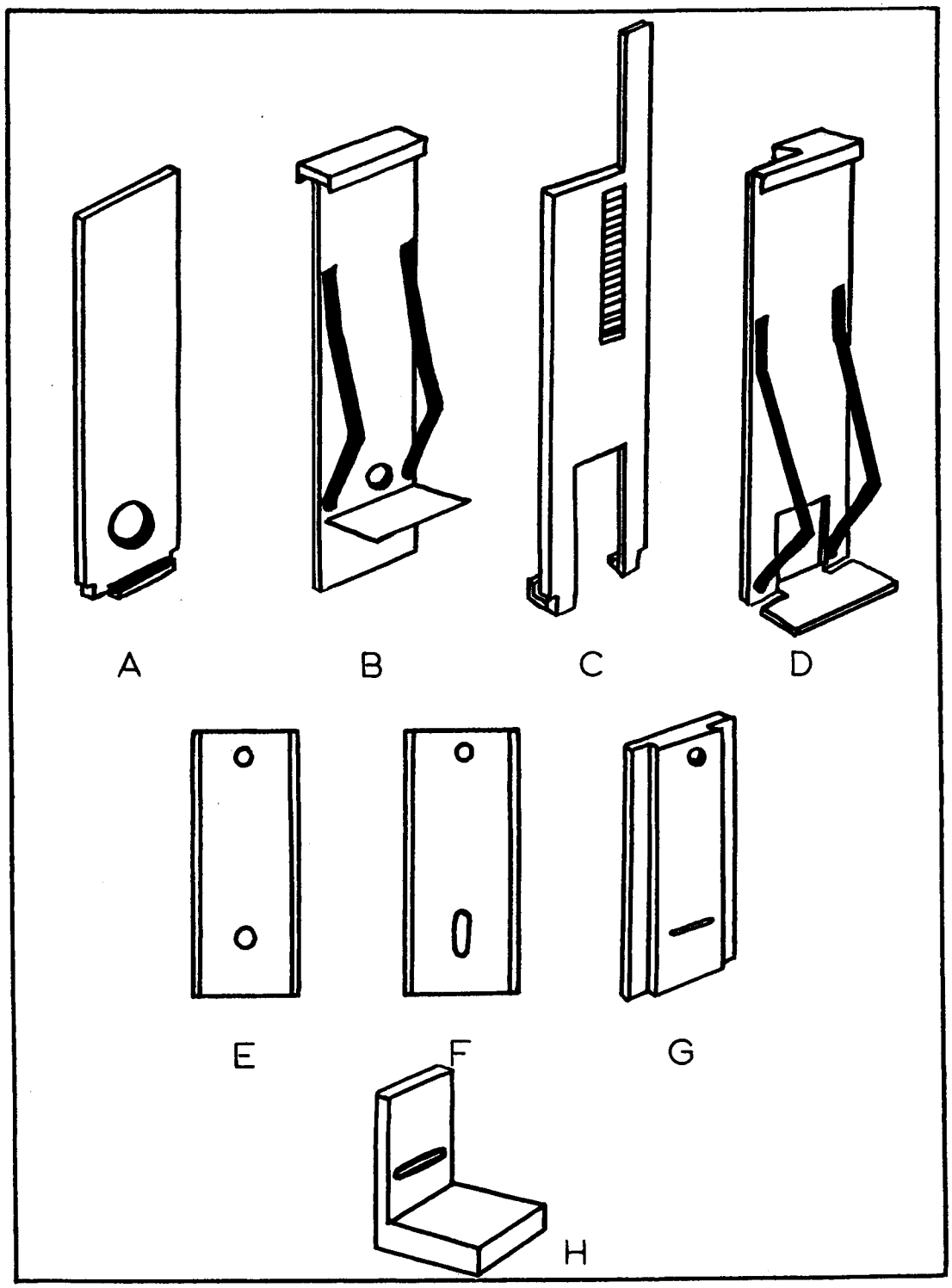

FIG.4.4. REFERENCE BACKING PLATE,(A), AND SAMPLE MOUNT,(B), SAMPLE BACKING PLATE, (C), AND MOUNT,(D), VARIOUS SLITS,(E-H).

horizontal dimensions of the spectrophotometer beam reaching the sample. Vertical control slits of 0. 15 mm, 0. 25 mm, 0. 407 mm, 0.762 mm, and 1. 59 mm; horizontal control slits of 1. 59 mm, 3. 97 mm, 4. 77 mm, and 6. 35 mm; and circular apertures of 0. 407 mm, 2. 38 mm, and 4. 77 mm width were machined to fit the cell. By a suitable combination of these readily interchangeable slits, circular or rectangular light beams of various dimensions could be chosen. These slits were inserted at positions A, B, or C as indicated in Figure 4. 3. In addition, special pairs of slits were made to be placed directly behind the sample when it was desirable to make the effective vertical slit width smaller than that obtained with the above combinations.

Most of the cell components were made of brass. The primary exceptions were the light cover, the motor and the bearings. All brass parts were treated to produce a nonreflective black coating suitable for optical work (37, p. 129). After cleaning with petroleum ether and concentrated NaOH, the pieces were etched lightly with HNO_3 and then treated at 80° C in an aqueous solution of $Pb(C_2H_3O_2)_2$ and $Na_2S_2O_3$. An ammoniacal solution of $CuCO_3$ also gave satisfactory results and this solution was used on some of the component pieces. Both coatings were subject to fading and were periodically renewed. Wherever this chemical method of blackening was non-applicable or impracticable, a coat of flat black paint was used.

Linear motion of the sample past the spectrophotometer beam was reproducible to ± 0.04 mm. Although the limit of vertical movement of the scanning cell was over 2 cm, the limit of usable motion was 1.4 cm. By rotating a sample 180° in the holder, a sample of 2.8 cm in diameter could be observed.

Experimental

The samples were quenched to room temperature from 620° C. A continuous scan of absorbance as a function of position across the sample was made by observing the sample absorbance at 273 mμ and 350 mμ. The absorbance of Pb^{++} at 273 mμ was assumed proportional to the concentration for this scan. Since a pure KCl crystal or one containing lead ion is transparent at 350 mμ, a scan at this wave length gives the absorbance due to light scattering and reflective losses. An evaluation of the homogeneity is given from a plot of corrected absorbance, $(A_{273\,m\mu} - A_{350m\,\mu})$, versus position in the sample.

A slit 6.35 mm wide by 0.15 mm high was used to evaluate homogeneity. The effective slit width was about 0.45 mm (see Chapter V), but this width was not critical in checking homogeneity across a 2.8 cm section.

Typical data derived from the scanning cell is shown in Figure 4.5. Produced in this figure are the scans at 273 mμ and 350 mμ

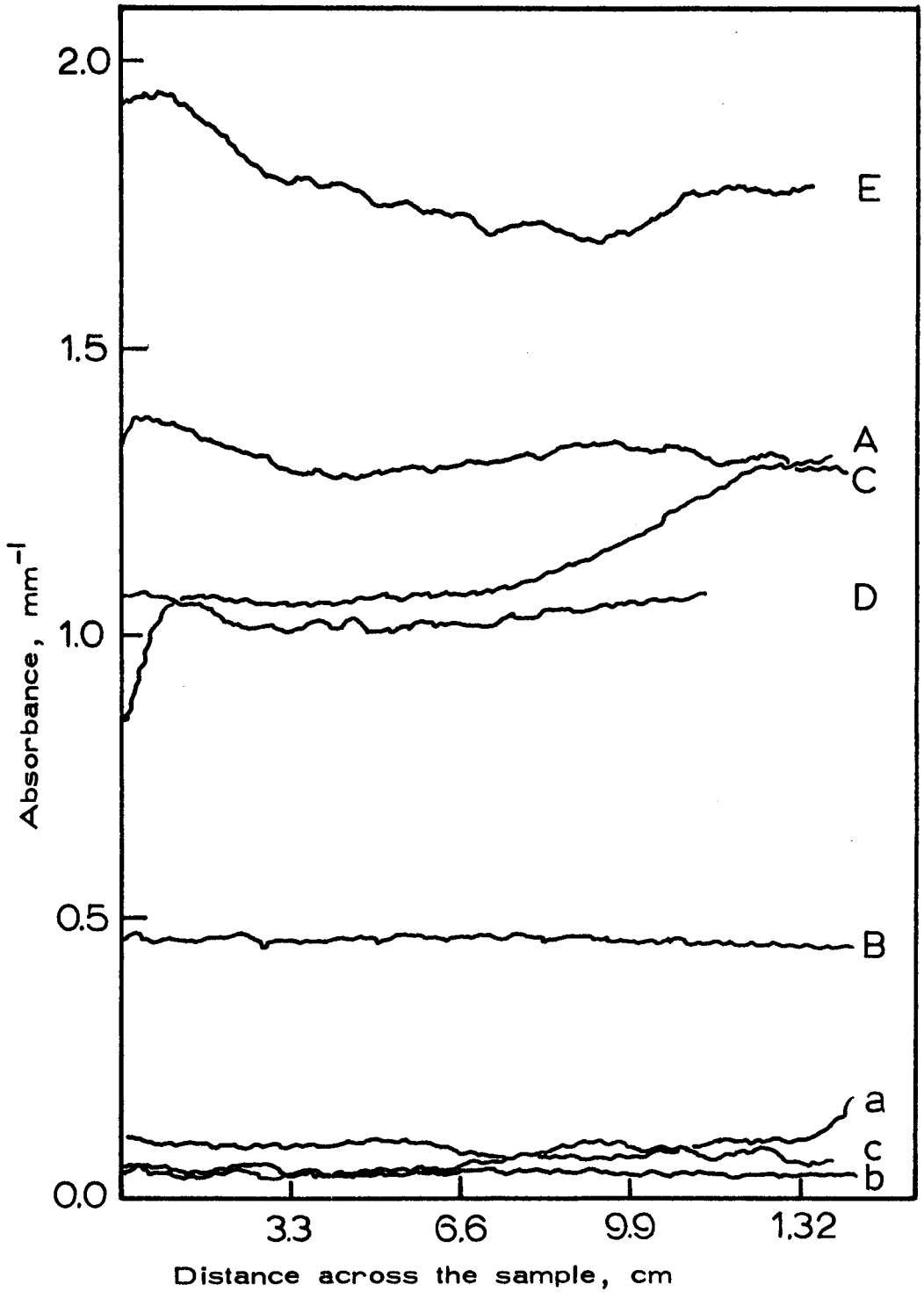

Fig. 4.5. Typical homogeneity data (Scanning absorption cell). A,B,C,D, taken at 273 mμ; a,b,c, taken at 350 mμ. d and e (350 mμ) are not shown.

for several samples. The corrected absorbance ($A_{273\ m\mu} - A_{350\ m\mu}$) for each example is given in Figure 4. 6. It is well to note that after correcting for scattering and reflections, the resultant curve shows a higher degree of homogeneity than would be suspected from an observation of the 273 mμ scan alone. Experiments made on pure crystals indicate that in an optically good sample, the correction made for scattering and reflection varies no more than 2% in the wave length range of 273-350 mμ. The correction used is good to that degree of accuracy. Having established the degree of homogeneity for a sample, it can be subjected to the necessary steps for direct chemical analysis.

Absorption spectra for each sample were recorded on a Beckman DK-1 Spectrophotometer. A few spectra were taken on a Cary Model 14 Spectrophotometer. These are designated by a C after the sample number.

Incorporation of Lead Ion in KCl Crystals

Some early authors tacitly assumed that the 273 mμ band (hereafter termed the A band) assigned to lead ion in KCl is proportional to the concentration of Pb in the sample. However, in the early period of this study, the author noted a variation in A band intensity with thermal history. After growth, the crystal samples were quenched from various temperatures to observe the change in A

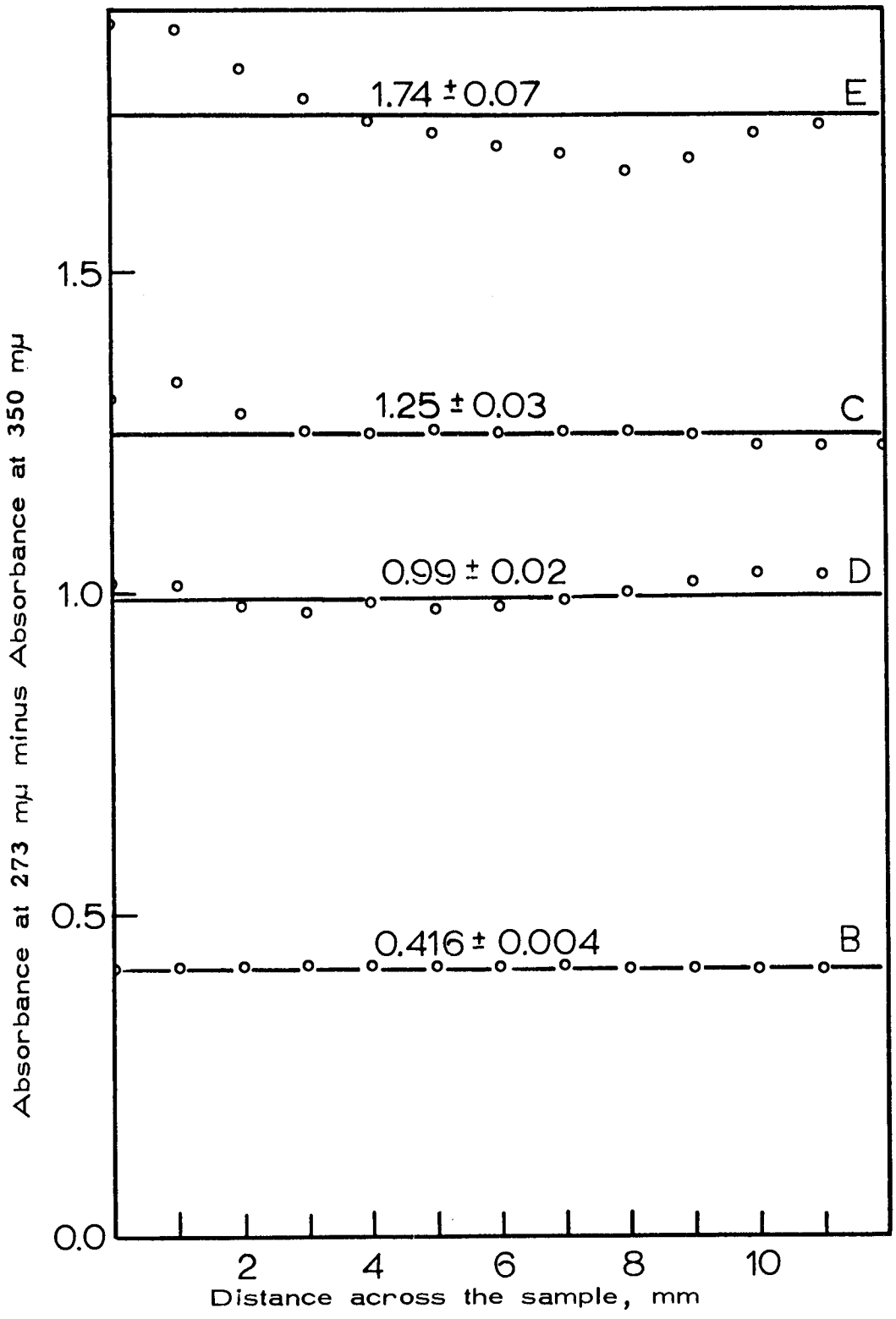

Fig. 4.6. Corrected homogeneity data. Point analysis of the continuous curves given in figure 4.5. Samples B,C,D,E.

band intensity. A brief study of the A band intensity with variation in temperature and length of heat treatment was undertaken. Figure 4. 7 shows the effect of heat treatment on representative crystals. Of the crystals investigated, those grown in air exhibited the largest thermal sensitivity. The crystals grown under HCl or HCl-argon generally showed less than a 10% increase in A band height after quenching. If samples were left at elevated temperatures for long periods of time, the intensity of the A band decreased due to the loss of $PbCl_2$. Limiting the heat treatments to temperatures and times such that the loss of $PbCl_2$ was insignificant, it was observed that the height of the A band reached the maximum value in shorter heat-treatment times the higher the treatment temperature. Although no quantitative evaluation was made on the time required to reach maximum A band intensity, it was observed that above 530° C, the melting point of $PbCl_2$, the maximum was attained rapidly.

Some conflict arises on the thermal sensitivity of the A band. Sibley, Sonder, and Butler (93) observed no change in the A band when samples were quenched from as high as 650° C. In contrast, Neubert and Reffner (75) had denoted a better dispersion of lead ion in KCl when they quenched to room temperature from 625° C. Again, Burstein et al. (7) noted sensitivity to thermal history in NaCl:Pb, while Kaifu (41) found little alteration of the A band with thermal

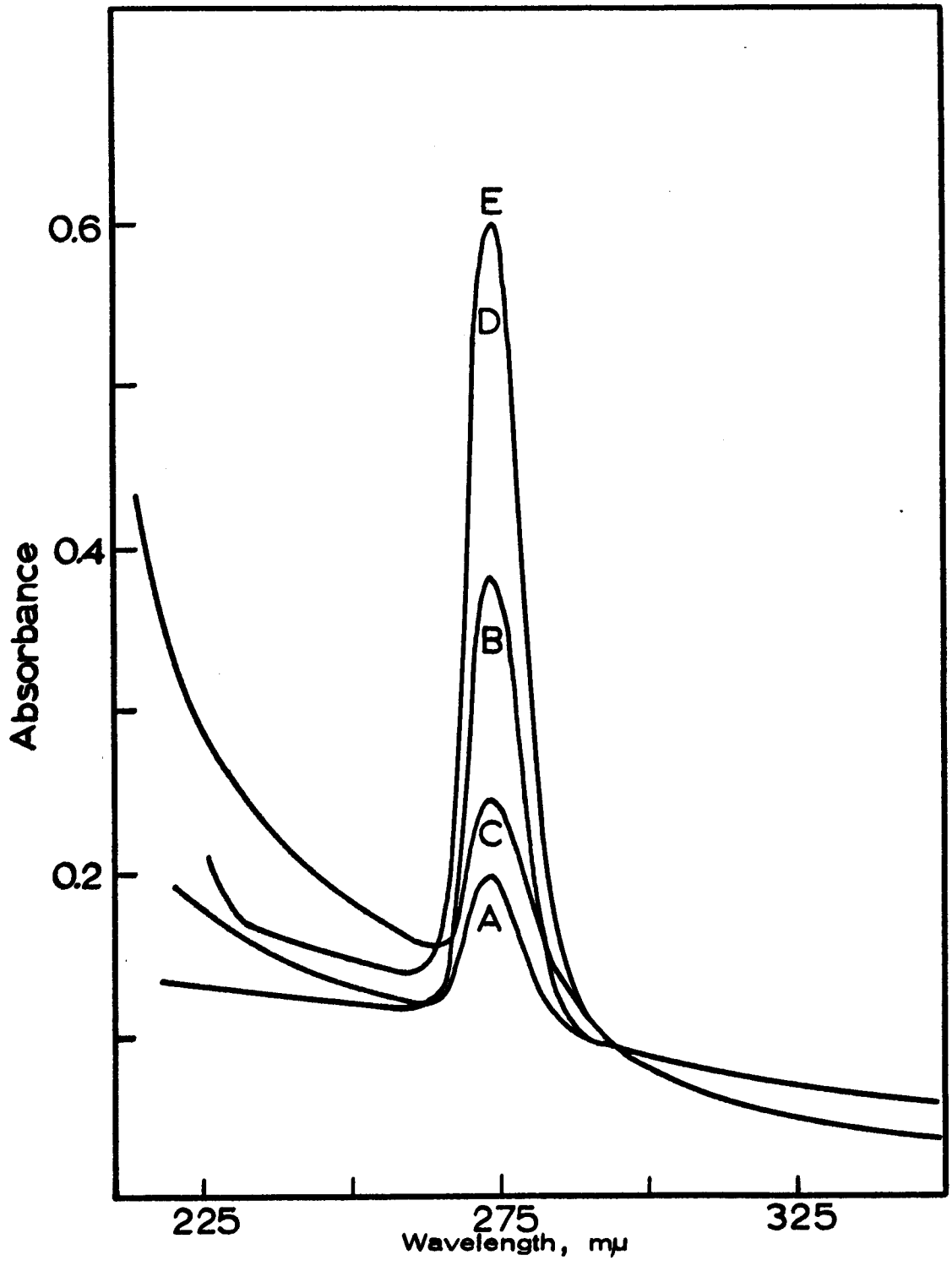

Fig. 4.7. Thermal sensitivity of air-grown KCl:Pb crystals. A, as grown; B, after quenching from 620°C; C and D are the same results for a different Pb concentration; E is sample C after a second quenching from 620°C to room temperature.

treatment in KCl:Pb, KBr:Pb.[3]

The height of the A band is not well correlated to the solubility of $PbCl_2$ in the growing crystal. As mentioned in Chapter III, vibration increases the solubility of $PbCl_2$ in a growing crystal. However, the increase in $PbCl_2$ is not directly correlated to the increase in A band intensity. This is clearly an indication that lead ion is incorporated into KCl at more than one type of site.

Burstein et al. (7) observed that the A band in NaCl:Pb showed considerable temperature instability compared to KCl:Pb and suggested that because of the lower solubility of Pb^{++} in NaCl, aggregation takes place. The KCl-$PbCl_2$ system does form solid solutions over a wide concentration range while NaCl-$PbCl_2$ does not. Thus valid comparisons can not always be made between the two systems.

A series of Russian authors (34, 67, 39, 66) have considered the possibility of Pb^{++} occupying more than one type of site in KCl. It is suggested that Pb^{++} present in the crystal at special sites such as on a dislocation baffle or a boundary of a mosaic block has no characteristic absorption. Work by Melik-Baikazyan, Zavodovskaya, and Treskina (67) suggest that during extending annealing of NaCl:Pb and KCl:Pb crystals at 350° and 600° C the A band first increases and then decreases with the simultaneous formation of a

---

[3] KCl:Pb signifies $PbCl_2$ as a dopant in KCl.

new band at about 250 mμ. Long annealing times (50-70 hours) produced a spectrum identical to that of $PbCl_2$. These authors suggested a connection between the band at about 250 mμ and a new chemical compound, say $PbCl_4^{-2}$ or $PbCl_6^{-4}$, as proposed by Fredericks and Scott (27). However, based on x-ray coloration investigations in this laboratory, the center causing the 254 mμ absorption is more probably the Pb^{+1} ion. This band appeared in less than 5% of the samples which were not subjected to x-ray coloration.

In addition to the presence of lead ion at nonabsorbing sites, the author has noted several bands in the region of 250-270 mμ, which appear as shoulders on the 273 mμ band. Figure 4.8 shows these bands and their removal by heat treatment. The bands are of low intensity and are generally found in crystals with a high concentration of lead ion. These bands and the entire base line at wave lengths less than 273 mμ decrease when the crystal has been quenched from a sufficiently high temperature. Although a complete study was not made on these bands, it is suggested that they originate from Pb^{++} near another Pb^{++} site, Pb^{+}, and reaction products of lead and oxygen. Quenching did not remove these bands entirely in crystals with a high concentration of lead. This would indicate stable compounds of lead and oxygen or association of lead ions in neighboring sites. The intensity of the band at 259 mμ was greater for crystals grown in air than in crystals grown from argon or HCl. In some

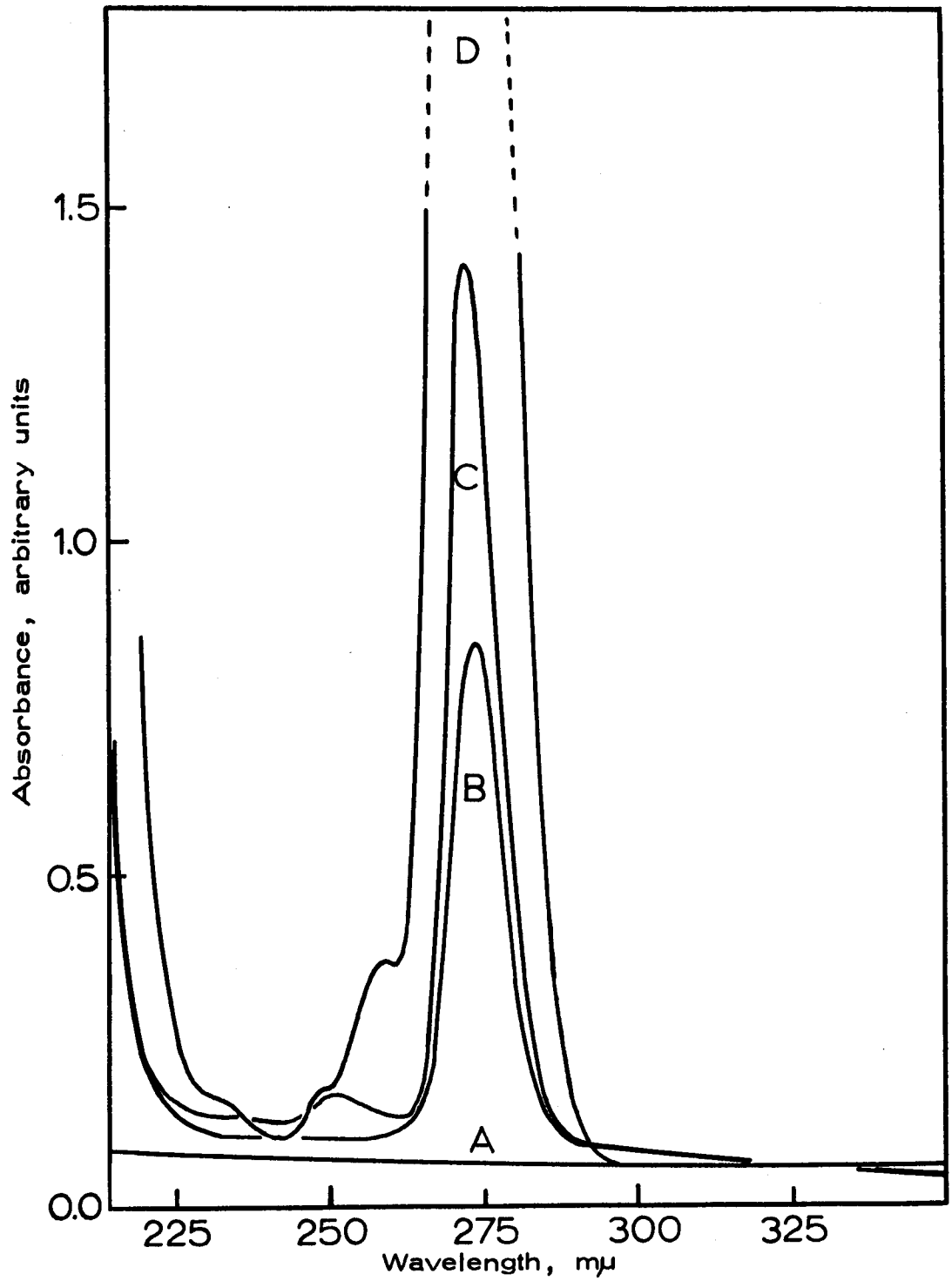

Fig. 4.8. Absorption spectra of KCl and KCl:Pb showing the presence of side bands in the 250-273 mμ region. A, pure KCl, B, KCl:Pb quenched from 620°C, C, KCl:Pb, moderate concentration, D, KCl:Pb, high concentration.

air-grown crystals, it was impossible to remove this band by quenching. A band at 254 mμ was observed in a few samples. This band has been observed in NaCl:Pb and KCl:Pb by several Russian authors (34, 39, 33, 67). The absorption due to lead on dislocation baffles, on the boundaries of mosaic sites, or in the Pb^{+} state have been proposed to account for this absorption. The author's work with x-ray coloration suggests that Pb^{+} is more probable. The presence of lead at some other site is definite. However, the interpretation of the observations is open to discussion and clarification.

The question of normal versus special sites is still open. There is no doubt that lead ion is present in the crystal in some form other than that which causes the A band absorption. In view of growth conditions alone, the author suggests that the distribution of lead ion in KCl is partially a function of growth conditions.

One of the decisive factors governing the solubility of a foreign cation in a single crystal is the size of the impurity cation. The greater the difference between the radii of the host cation and that of the impurity cation, the larger the heat of mixing and the more difficult it becomes for a crystal to capture the impurity cation from the melt. The radius of K^{+} is 1.33 Å while that of Pb^{++} is 1.32 Å. Based on size difference alone, the lead ion can fit into a substitutional or interstitial site in the crystal. Because the sizes are almost identical, it is probable that Pb^{++} can be found

anywhere a K^+ is observed.

The charge on an ion incorporated into single alkali halide crystals has been considered by Brauer (5). Divalent ions can be incorporated in the monovalent or divalent state. A prediction of the valence state is found from the value of the second ionization potential of the divalent ion. If the value is above 22 eV, the ion will probably be incorporated into KCl in the monovalent state. Since lead has a second ionization potential of 14.96 eV, it is expected that it will be present as Pb^{++} in KCl single crystals. This postulate is for normal incorporation and does not mean that other metastable valence states can not exist.

This work has demonstrated that, in the crystals studied, the A band intensity increases with heat treatment at the expense of other bands. Although the instrumentation was not quantitatively reliable below 220 mμ, qualitative data showed that the 213 mμ band and 196 mμ band assigned to lead ion in KCl did not decrease with heat treatment. Observations indicate that the intensity of the A band is not a true criterion of the total amount of Pb^{++} ion present in the crystal.

With the thermal treatment indicated earlier, the author was able to maximize the A band absorbance and determine directly the amount of Pb^{++} present in the crystal.

Before considering the values found for the oscillator strength

of the A band, a brief consideration of the shape of the band will be presented.

Band Shape Analysis

A plot of absorbance versus energy or wave length is called an absorption spectrum. Spectra, in general, consist of a series of absorptions or bands which are characteristic of the absorbing centers. The symmetry and shape of each particular band can be examined if the absorbance due to that center alone can be measured. Each band is an absorbance superimposed upon a background absorbance. This background, often called the "base line", is caused by scattering points in and on the surfaces of the crystal and by reflective losses at the crystal faces. In practice, the absorbance due to a center alone, the band shape, and band asymmetry are evaluated by subtracting the background from the overall absorbance value. Fortunately, pure potassium chloride crystals of good optical quality have a well defined base line that shows but a slight change in absorbance in the 350-200 mμ wave length region. Subtraction of the base line from the observed absorbance gives the absorbance due to the absorbing centers alone. The shape of the A band determined in this manner is given in Figure 4.9.

Kaifu (41) has studied the A band shape at temperatures below -50° C and found that at these temperatures it was approximately

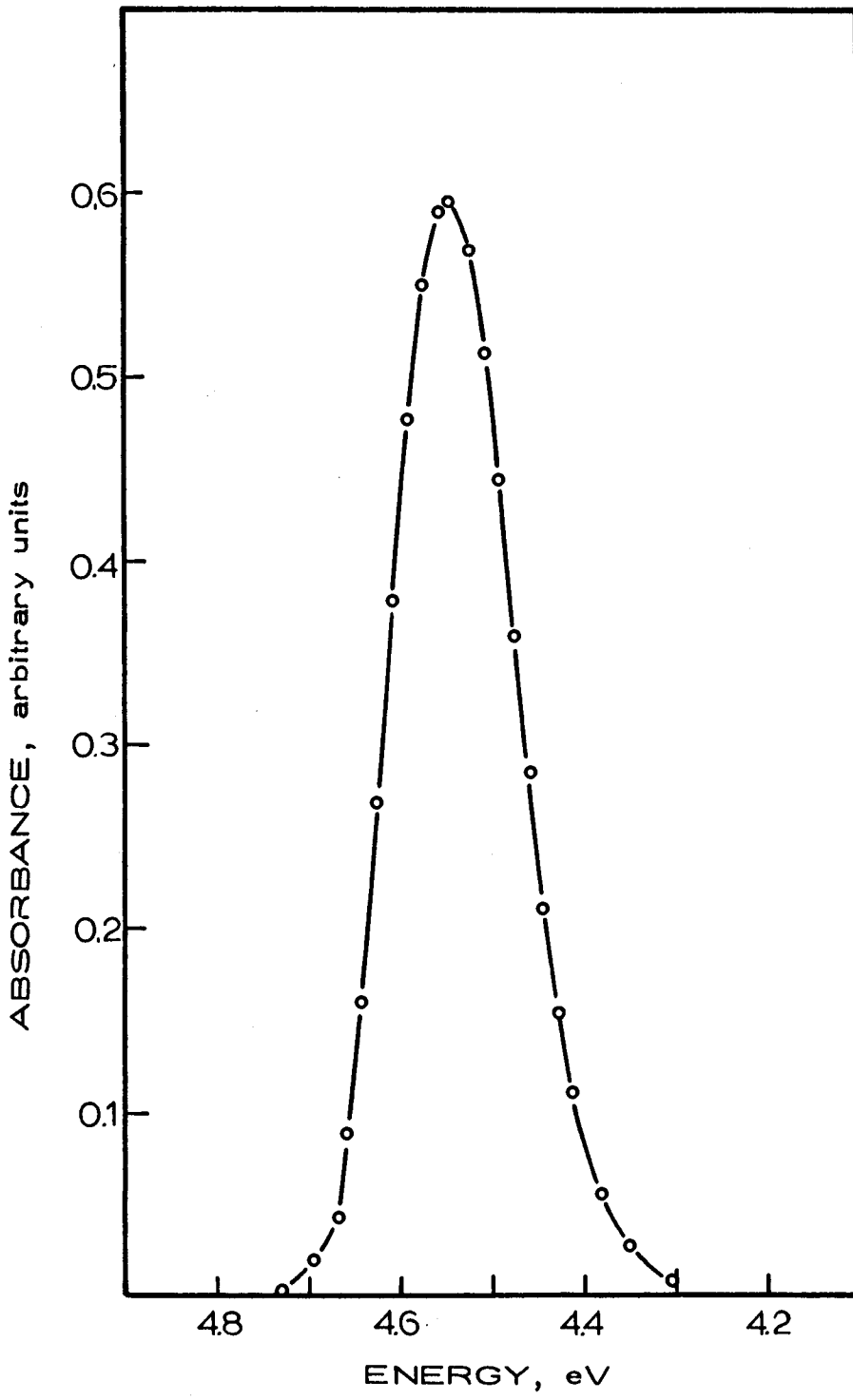

Figure 4.9. Shape of the A-band in KCl:Pb. Note the asymmetrical shape of the band.

Gaussian in shape. The analysis of the shape of the A band for Pb^{++} in KCl is analogous to Konitzer and Markham's (48) treatment of the F center.

We can write

$$G = \frac{a}{\sqrt{\pi}} \exp\{-a^2(\varepsilon-\varepsilon_A)^2\}$$

for the normalized Gaussian distribution of absorbance as a function of energy. Where a is a constant, and ε_A the energy at the band maximum. A plot of log of relative absorbance against $(\varepsilon-\varepsilon_A)^2$ for the A band should give a straight line of slope $a^2/2.3$ if the band is truly Gaussian. Figure 4.10 is such a plot for the A band.

The red side of the absorption curve is very well represented by a Gaussian curve with a = 0.2484. However, this value for a does not produce a good fit to the experimental curve on the violet side of the band. Although a better fit on the violet side is obtained using a = 0.2363, the curve on this side is not Gaussian. Figure 4.11 is a plot of relative absorbance versus $(\varepsilon-\varepsilon_A)$ for the experimental curve and the double Gaussian curve using $a_{red} = 0.2484$ and $a_{violet} = 0.2363$. The curve is better described by this double Gaussian shape. However, this method of description is not founded as yet in theory and to date, no theoretical models have been proposed to suggest such a shape.

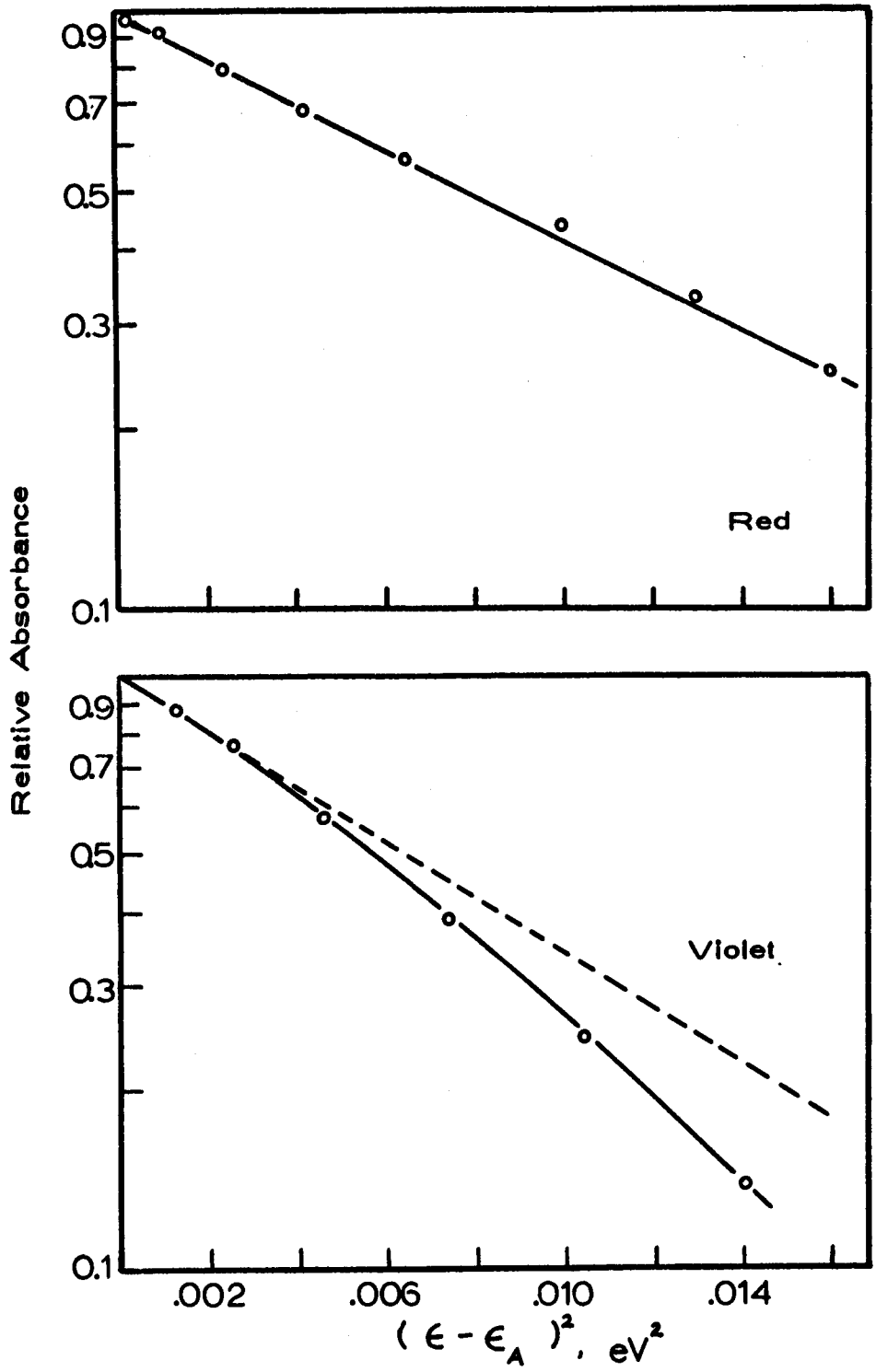

Fig 4.10 Graph of log (relative absorbance) versus $(\epsilon - \epsilon_A)^2$ at 298°k (——); The non-Gaussian shape of the violet side of the band is evident. The Gaussian curve (---) was fitted to the top of the band.

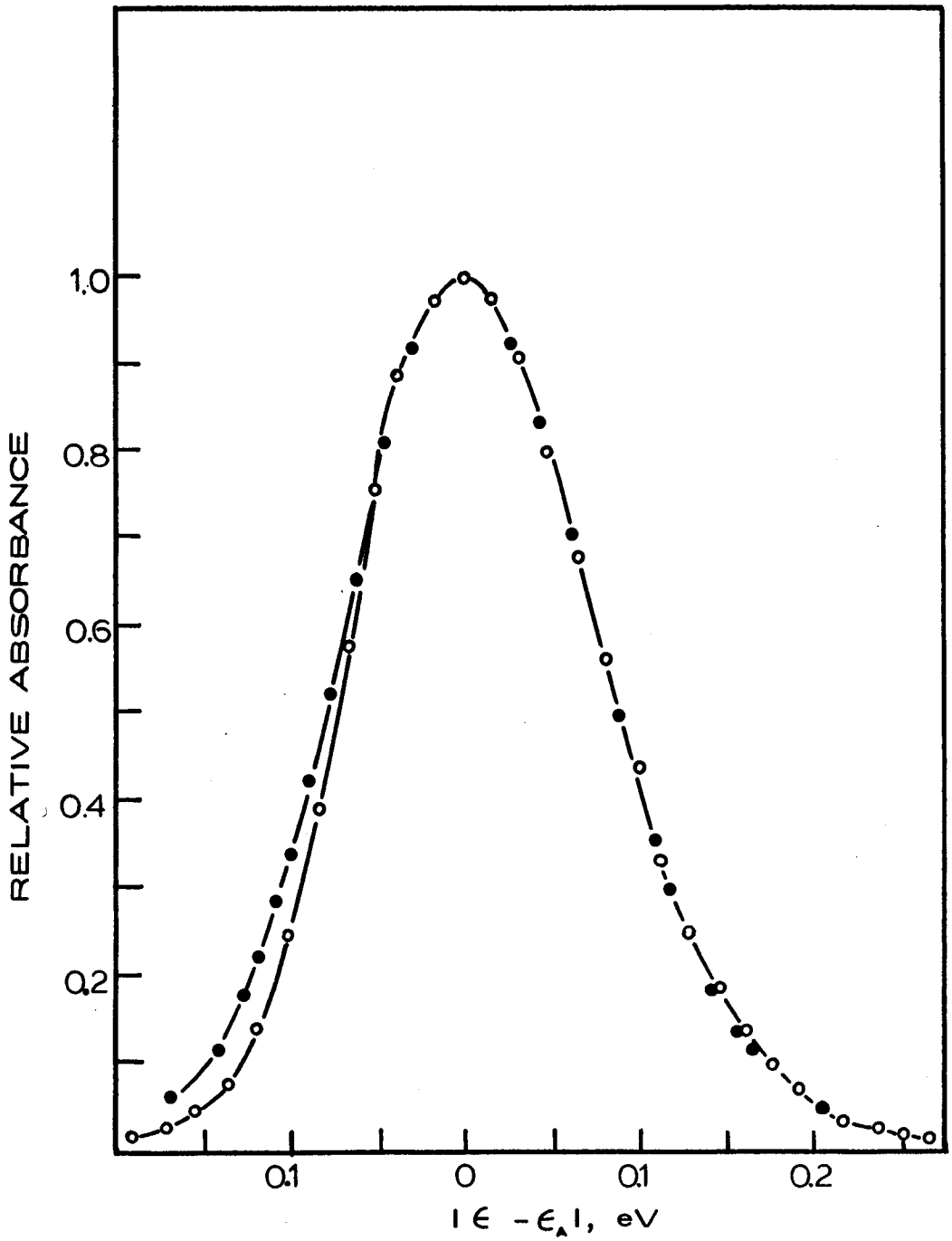

FIGURE 4.11. COMPARISON OF THE A-BAND SHAPE (o) AGAINST A DOUBLE GAUSSIAN SHAPE (•). NOTE THE A-BAND ASYMMETRY. DATA TAKEN AT 298°K.

Oscillator Strength Evaluation: Summary and Discussion of Results

Using the methods previously described, the author found varying results for the value of the oscillator strength of the A band. The concentration of Pb^{++} was determined directly with dithizone and the oscillator strength evaluated from equation (4. 4).

Table 4. 4 lists the values for the half-width of the band determined for 12 samples. The average value of the half-width was used in equation (4. 4) to determine the oscillator strength. Included in the table are the wave lengths at half-band height $\lambda_{\frac{1}{2},\ \text{violet}}$ and $\lambda_{\frac{1}{2},\ \text{red}}$ for each sample.

Table 4. 5 presents the data used for the determinations of the oscillator strength and the amount of lead found in each sample. The values for the oscillator strength are not shown in this table because of the wide variation observed in the results. Compared with the 3-5% error observed in standard samples determined by direct chemical analysis, the results for f show considerably more scatter.

Some insight into the problem arises when the samples are grouped by source and in degree of increasing purity. Table 4. 6 gives the oscillator strength values found for crystals grown in air or argon with recrystallized KCl. Table 4. 7 is for samples grown

Table 4.4 Half-band width of the A band.

Sample	A band absorption	$\lambda_{\frac{1}{2}}$, violet, mμ	$\lambda_{\frac{1}{2}}$, red, mμ	Half-width eV
4	0.354	268.4	278.0	0.160
6	1.072	268.2	278.0	0.163
7	0.181	267.9	277.9	0.167
8	1.234	268.2	278.0	0.163
11	0.861	268.4	278.2	0.163
12	0.871	268.3	278.0	0.161
13	0.722	267.3	276.7	0.159
18	0.497	268.2	278.3	0.167
20	0.714	268.5	278.2	0.162
29	0.571	268.4	278.2	0.163
29-C	0.566	268.4	278.1	0.162
51	0.501	268.3	278.1	0.163
			average	0.162
			standard deviation ±	0.002

Table 4.5 Concentration of lead in KCl crystals. (Table includes sample thickness and A band absorbance.)

Sample	Weight, g	Thickness, cm	A band absorbance, cm^{-1}	Absorbance of lead dithizonate in CCl_4, cm^{-1}	γ Pb
1	0.6010	0.1173	5.27	0.462	20.02
2	0.2441	0.0594	1.67	0.036	1.6
3	0.3518	0.0846	13.49	0.360*	30.5
4	0.3031	0.0856	4.14	0.136	5.93
5	0.7405	0.1367	11.63	0.464*	39.6
6	0.5121	0.1052	10.57	0.346*	29.4
7	0.2451	0.0681	2.66	0.091	3.95
8	0.9993	0.2065	6.26	0.408*	34.7
9	0.3119	0.1120	4.50	0.150	6.55
10	0.1953	0.0518	19.80	0.273*	23.1
11	0.3774	0.0927	9.29	0.395	17.15
12	0.2809	0.0876	10.08	0.350	15.2
13	0.1699	0.0417	41.06	0.380*	32.2
14	0.5599	0.1384	11.54	0.346*	29.4
15	0.6124	0.1453	8.44	0.298*	25.3
16	0.6669	0.1557	8.35	0.358*	30.4
17	0.6652	0.1892	3.36	0.284	12.4
18	0.3270	0.0795	6.10	0.338	14.73
19	0.4719	0.1313	12.83	0.356*	30.2
20	0.3573	0.0902	8.09	0.341	14.83
21	0.4687	0.1290	10.82	0.572	24.8
22	0.3007	0.0826	8.80	0.352	15.3
23	0.3031	0.0846	14.80	0.377*	31.9
24	0.1444	0.0386	37.04	0.247*	20.9
25	0.1378	0.0368	41.85	0.312	26.4
26	0.1482	0.0345	26.17	0.426	18.52
27	0.1410	0.0366	32.51	0.416	18.08
28	0.2695	0.0734	19.79	0.195	16.4
29	0.2463	0.0594	9.61	0.296	12.88
30	0.2495	0.0635	11.11	0.342	14.84
31	0.3712	0.0991	12.79	0.262	22.1
32	0.1513	0.0942	17.60	0.232	10.1
33	0.1424	0.0973	19.63	0.198	8.6
34	0.0972	0.0315	31.05	0.231	10.05
35	0.0846	0.0279	30.54	0.201	8.75
36	0.1138	0.0406	29.85	0.264	11.5
37	0.1422	0.0465	26.09	0.279	12.1
38	0.1050	0.0394	43.05	0.427	18.6
39	0.1595	0.0559	14.31	0.187	8.10
40	0.1771	0.0691	17.03	0.258	11.2
41	0.0881	0.0384	13.99	0.110	4.8
42	0.3511	0.0970	4.23	0.149	6.5
43	0.3309	0.1638	7.32	0.225	9.76
44-C	0.7721	0.2116	5.99	0.481	20.9
45-C	0.4822	0.1318	4.17	0.166	7.22
46-C	0.4959	0.1615	7.01	0.349	15.2
47-C	0.8530	0.2332	4.85	0.441	19.2
48-C	0.3314	0.0927	7.04	0.250	10.88
49-C	0.5603	0.1834	7.61	0.381	16.55
50-C	0.4877	0.1763	5.00	0.219	9.5

* 25 ml CCl_4 phase

Table 4.6 Oscillator strength of A band in KCl:Pb. Values for crystals grown from reagent or recrystallized KCl in air or argon.

Sample	Oscillator strength	Average value and standard deviation	Growth specifications
3	0.067		Reagent-grade KCl,
18	0.059		grown from Pt in air.
19	0.087		
20	0.085	0.075± 0.012	
21	0.089		
22	0.075		
23	0.061		
1	0.069	0.069	Recrystallized KCl, from Pt, in air.
7	0.072	0.072	Reagent KCl, from Pt, air
4	0.092		Recrystallized KCl, argon,
5	0.094		no special heat treatment.
6	0.080		
8	0.078		
9	0.093		
10	0.078		
11	0.089		
12	0.081		
13	0.094		
14	0.095		
15	0.089	0.086 ±0.007	
16	0.079		
17	0.078		
29	0.080		
30	0.081		

Table 4.7 Oscillator strength of A band in KCl:Pb. Values for crystals grown from high purity KCl in HCl, HCl-argon, or argon atmospheres.

Sample	Oscillator strength	Average Value and standard deviation	Growth atmosphere
36	0.13	0.13	HCl, argon
24	0.11		HCl, argon, containing some O_2
25	0.095	0.10 ± 0.08	
26	0.091		
27	0.11		
28	0.14	0.14	HCl, argon
31	0.093	0.093	HCl
32	0.11		
33	0.14	0.125 ± 0.02	
2	0.11	0.011	HCl, argon
37	0.13	0.13	HCl
34	0.13	0.13	HCl, argon
35	0.13		
39	0.12	0.12	Argon
40	0.12		
41	0.11		
43	0.11		Argon
46-C	0.10	0.11	
49-C	0.11		
50-C	0.11		
38	0.11		Argon (strong crucible attack)
42	0.099		
44-C	0.096	0.10 ± 0.01	
45-C	0.12		
47-C	0.093		
48-C	0.093		
		0.11 ± 0.02	

from high purity KCl in argon and HCl. A direct correlation between the observed value of f and the purity of the crystal is noted. Crystals grown in air from reagent-grade KCl gave the lowest values, while those grown from high purity KCl in HCl, HCl-argon, or argon atmospheres gave the highest. The values of f for a particular crystal showed a variation of ± 10%, a value not unexpected from the nature of lead ion incorporation.

In addition, this data support strongly the postulates of Fritz, Lüty, and Anger (30), that OH^- reacts with divalent cations to give a reaction product which does not contribute to the conductivity. If O_2 or OH^- reacts with lead ion to give a product which was either inactive in the ultraviolet or produced an absorption other than at 273 mμ, the maximum absorption at the A band position would be decreased. However, the lead ion would still be present, with the net result being a decrease in the apparent value of f for the A band. This interpretation correlates the wide separation of values of f determined to date. Kaifu (41) produced crystals grown in the air by the Kyropoulos technique from reagent-grade materials. His value for f is 0.075 ± 0.008. Sibley, Sonder, and Butler (93) used higher purity KCl and produced crystals from a nitrogen atmosphere. They determined f to be 0.11. The precision of all reported values, including the author's, is comparable.

It is evident from Tables 4.6 and 4.7 that a higher value for f

is obtained when HCl, argon and high purity salt are used. A comparison between the absorption curves of crystals of varying purity indicates a flatter background absorbance and more symmetrical absorption bands for crystals of higher purity. The presence of bands other than the 273, 213, and 196 mμ bands suggests that all the lead ion is not at the 273 mμ sites. The previous discussions on impurity distribution of lead ion at special sites, such as dislocations, mosaic boundaries, and the like, account for the variation in the value of f.

Previous discussions on impurity distribution and growth conditions, in addition to the comparisons made with other papers suggest that an f value need be determined for each set of conditions used for crystal growth. Only then can the results from various samples of independent laboratories be compared quantitatively.

We find the best value for the oscillator strength of the A band to be 0.11 ± 0.02. This result is higher than that found by Kaifu and the same as that of Sibley, Sonder, and Butler. The author proposes that the true value for f is larger than 0.11. Faster quenching rates, higher heat-treatment temperatures, and better salt purity increase the observed value for f. Incomplete removal of bands caused by the presence of lead ion at other sites drives the observed value for f downward. Further investigations will no doubt produce a larger value for f.

V TRANSPORT OF LEAD ION IN KCL

Introduction

When an electric field is established across an ionic crystal, the charged particles in the crystal move and carry current through the system. The carriers at moderately high temperatures, 200° - 700° C, in these ionic solids are the ions themselves. In general, the ions are more mobile and less tightly bound than the electrons and transport of these ions produces the effect of current flow through the crystal.

Transport under the influence of an electric field, or electrolysis, was observed in solids as early as 1888 (108). Early investigators such as Tubandt and Lorenz (102) verified Faraday's Law for cation carriers in the silver halides and found the Ag^+ carries more than 99% of the current in these solids. Dendritic formations in the electrolyzed solids plagued the early authors. These dendrites were formed either from the reduced cation of the material under study or from the metal electrodes in contact with the sample. A solution to the problem of dendrite formation was brought about by the use of substances like $BaCl_2$ (45) or graphite (27) between the electrode and the crystal under study.

Smekal (95) surveyed the field of electrical conduction in

single crystals and presented a review of the subject in 1928. A few years later, the determination of transference numbers in the alkali halides and the lead halides was undertaken by Tubandt, Reinhold, and Liebold (103), and a more detailed study on KCl and KCl:Ca was undertaken in 1951 by Kerkoff (45). These studies showed that while lead chloride and lead bromide are essentially anionic conductors, the alkali halides remain cationic conductors until about 450° C. Above this point anion conduction becomes significant.

Although the diffusion of copper, nickel, and platinum into NaCl during electrolysis had been observed by Lukirsky, Scukareff, and Trapensnikoff (58), deliberate electrolysis experiments did not follow until later. The electrolysis of KCl single crystals containing lead ion was first undertaken by Lehfeldt (54) in 1933. He found that after samples had been subjected to electrolysis, or electrolytic purification, their conductivity decreased. This work was primarily on conductivity, but his observations suggested that impurity metal ions might be readily transported through an alkali halide crystal. The diffusion and migration of $^{137}Cs^{+}$ in NaCl single crystals by Chemla (10) demonstrated that foreign metal ions are transported through single crystals under the influence of an electric field.

Fredericks and Scott (27) studied directly the problem of transport of Pb^{++} in KCl and observed an apparent movement of the lead ion toward the anode during electrolysis. They proposed a

complex of the type, $PbCl_x^{(-x+2)}$ as the species undergoing transport. They suggested that vacancy clusters would account for the transport of a complex of this size.

Theory

Since the carriers in ionic solids are the ions themselves, their transport affects both conductivity and diffusion. An understanding of the process of electrical conduction in alkali halides demands a knowledge of the mechanisms of diffusion responsible for the migration of these ions. The basis for all the proposed mechanisms of diffusion is the ability of an ion in a crystalline lattice to gain sufficient energy to change its site. These jumps from one site to another produce diffusion in ionic solids. The mechanisms of diffusion that will be described briefly are the vacancy, interstitial, ring and interstitialcy models.

Vacancies or unoccupied lattice sites are known to be present in all crystals. If an ion leaves its site and jumps into a vacancy, it has diffused by the vacancy mechanism. The vacancy at the new site can then accept another ion and the mechanism perpetuates. The interstitial mechanism describes the motion of an ion from an interstitial site to a neighboring interstitial site. The ring mechanism describes the motion of three or four ions rotating as a group. This mechanism produces diffusion by carrying the ion through a

series of group rotations, eventually displacing the ion from the original region. An ion in an interstitial position diffuses by the interstitialcy mechanism if it pushes one of its nearest neighbors into an interstitial position and occupies the site vacated by the neighboring ion.

These mechanisms are widely applied to conductivity and diffusion in solids when the diffusing species is an atom or an ion. Spatial arrangement of the ions, electrostatic forces between them, and other factors determine the mechanism in each type of material. The author refers the reader to a more complete treatment of these mechanisms and their applications (31, p. 26-32).

The phenomena of ionic conductivity and diffusion can be discussed without assuming a detailed mechanism. Assuming only that the ions move in a random-walk motion, the well known Nernst-Einstein (57) equation was developed. It is

$$\frac{\mu}{D} = \frac{q}{kT} \qquad (5.1)$$

where μ is the mobility, D the diffusion coefficient, q the charge on the ion, k the Boltzmann Constant, and T the absolute temperature. In addition, we can write

$$\sigma = nq\mu$$

where σ is the conductivity, n the concentration and q the charge on the carriers. Combination of these two equations gives another

form of equation (5. 1):

$$\frac{\sigma}{D} = \frac{nq^2}{kT} \qquad (5.2)$$

This relationship allows an indirect calculation of the diffusion coefficient from conductivity measurements. At first glance, one expects μ and D to be related by the Nernst-Einstein relationship. In fact, this equation was approximately verified by Chemla (10) for monovalent ions in NaCl. However, the ratio μ/D is not always equal to q/kT. Lidiard (57, p. 336) reporting on the work by Teltow on Zn^{++} gives (μ/D) observed as $= 5.05 \times 10^2$ cgs esu, whereas (2q/kT) is 7.06×10^3 cgs esu. He suggests that results such as this are to be expected if Zn^{++} diffuses as a Zn^{++}-vacancy complex whose time-average charge is approximately the same as the host cation. Parallel results have been observed with both divalent and trivalent cations.

A more detailed analysis of the problem indicates that equation (5. 1) is not valid for all systems because of the correlation effect. The microscopic movement of ions being transported in a crystal can be described by a series of discrete jumps. In general, an ion does not follow random-walk motion but shows a greater probability of jumping back into the site it has just vacated. Corrections to equation (5. 1) are given by correlation factors. Manning, in a series of papers (63, 61, 60), Lidiard (56), Friauf (29) and others are actively investigating these factors. Modifications introduced

into the Nernst-Einstein relationship by means of correlation factors help to resolve the differences between observed and true mobilities. The correlation factor differs for each type of lattice and every type of diffusion mechanism. Manning (62) has modified the Nernst-Einstein relationship for divalent impurities diffusing in a face-centered-cubic, monovalent sub-lattice. When diffusion in an electric field takes place by a vacancy mechanism, the following equation is found:

$$\frac{\mu}{D} = \frac{2e}{kT} \cdot \frac{8.15\,k_1}{2\omega_1 + 5.15k_1} \qquad (5.3)$$

where k_1 and ω_1 are the jump frequencies for exchange of the vacancy with the surrounding host ions. k_1 is for jumps in which the vacancy moves away from the impurity, while ω_1 is for jumps in which the vacancy moves to another site neighboring the impurity. As Manning pointed out, care must be taken in applying this equation. It is valid primarily in homogeneous crystals when the number of vacancies introduced by the divalent cation is small in comparison to the total number of vacancies. Also, the effect of inhomogeneity, vacancy-impurity complexes and divalent ion concentration are not yet fully understood. If the vacancy is tightly bound to the impurity ion, and with every jump of the impurity ion the vacancy returns to a site neighboring the impurity, μ/D goes to zero. When the attraction is weak, only an upper limit of μ/D is given by equation (5.3).

Some authors (19, 20, 109) have suggested that divalent cations

can exist in the host crystal as a complex of the ion and a vacancy. The time-average charge on this complex then determines the magnitude of the electric field effect. If Pb^{++} is present in a substitutional site and is not associated with a vacancy, we would expect transport of Pb^{++} toward the cathode. Any association either with vacancies or anions of the host lattice would change the time-average charge on the complex and field effects might be reduced or their direction reversed. Thermal dissociation can also change the net charge on the complex and the transport direction of the species. Complex formation between a lead ion and a positive-ion vacancy can be represented by the following equation:

$$Pb^{++} + \boxplus \rightleftharpoons [\, Pb^{++} \; \boxplus \,]^{+}$$

The resulting complex is electrically "neutral". That is to say, it has no excess charge in relation to the charge on the host cations. Any time-average dissociation of the complex produces a charged species which is transported by the field. The amount of drift in the field would be proportional to the probability of dissociation of the complex.

Banasevich, Luré, and Murin (2) observed that the effective charge on a divalent ion associated with a vacancy was approximately "zero". Association is used here in a general sense and is used to describe complete or partial association. The effective charge is

that in excess of the charge on the host cation. Considering jump probabilities of the associated ion with and against the field, they suggested that the current due to associated ions in a crystal should be proportional to

$$i \propto \frac{e(z-2)aE}{kT} \tag{5.4}$$

where z is the charge on the cation, E the field strength, and a sample thickness. From equation (5.4) it is expected that for a completely associated divalent ion, i would be zero. A further extension of this work by Murin, Banasevich, and Grushko (73), gives the effective charge on an associated complex as

$$(ze)_{\text{effective}} = 0.86 \frac{\tau_D}{\tau_K} \tag{5.5}$$

where τ_D is the time between jumps for the impurity-cation complex and τ_K is the average lifetime of the complex. For complete association $\tau_K \gg \tau_D$ and $(ze)_{\text{effective}}$ is zero. If the complex dissociates to some degree, then equation (5.5) can be used to estimate the effective charge on the complex.

Complexes involving only lead and chloride ions can be represented by $PbCl_x^{(-x+2)}$. The motion of these complexes has been considered by Fredericks (25, p. 82-92) as requiring vacancy clusters to allow the diffusion of this relatively large complex. The results of the author's study would suggest that a mechanism of this type does not occur in KCl:Pb. The reader is referred to Fredericks's

work for a complete description of the proposed mechanism.

Electrolytic Transport

The electrolytic migration of ions in alkali halides can not be considered as an isolated process, because an electric field affects diffusion by exerting a direct force on the charged ions and by establishing a flow of vacancies or interstitial ions in the crystal. Simultaneous diffusion and electrolytic transport occur in the crystal with the net movement of ions being described by a combination of diffusion and transport effects.

One of the problems of transport in alkali halides is that of evaluating the drift mobility of an impurity ion in an electric field. The Nernst-Einstein relationship does not hold for aliovalent impurity ions in a monovalent lattice structure, so the conductivity and the diffusion coefficient are not directly related by this equation. If the problem is considered as one of diffusion, and then modified to include the effect of an electric field, electrolytic transport can be quantitatively described. We can write the one-dimensional diffusion equation in its generalized form (13, p. 4),

$$\frac{\partial c}{\partial t} = D\frac{\partial^2 c}{\partial x^2} \qquad (5.6)$$

where c = concentration
t = time
x = distance from the origin
D = diffusion coefficient

to describe the diffusion alone. Chemla (10) extended this equation to include diffusion in the presence of a steady electric field and (5. 6) became

$$\frac{\partial c}{\partial t} = D\frac{\partial^2 c}{\partial x^2} - \mu E\frac{\partial c}{\partial x} \qquad (5.\ 7)$$

where E is the field and μ the mobility of the impurity cation. Equation (5. 7) is written for the consideration of cation transport; the sign of the term $(\mu E \frac{\partial c}{\partial x})$ becomes positive when anions are being considered. The application and solution of equation (5. 7) depends on the nature of the boundary conditions established in the experimental samples. Two basic types will be considered. The first is diffusion and electrolytic transport from a plane source, the second that from a semi-infinite extended source.

Plane Source

The initial concentration of divalent ions, C_o, is deposited in an infinitely thin layer, at $x = 0$, upon a semi-infinite sample. That is, a sample of dimensions sufficiently large so that the edges are far from the regions where transport will be measured and edge effects can be neglected. The initial condition is that $C(x, t) = 0$, for all $x > 0$ and $x < 0$. If μ and D can be considered constant, the integral of (5. 7) for this case becomes

$$C(x, t) = \frac{C_o}{(\pi Dt)^{\frac{1}{2}}} \exp\left\{\frac{-(x-\mu Et)^2}{4Dt}\right\} \qquad (5.\ 8)$$

Construction of concentration versus distance curves permits the calculation of μ and D. Figure 5. 1 shows the form of the profile for two different values of t. The direction of displacement of the profile depends on the nature of the carrier, anion or cation, and the direction of the field. The shapes of the pure diffusion profiles, A or A', are not distorted by the electric field, but simply displaced an amount equal to (μEt). The displaced curves are shown as B and B'.

Chemla applied equation (5. 8) to his study of the diffusion and electrolytic transport of radioactive impurities in NaCl and KCl crystals. Banasevich, Lure', and Murin (2) used the same technique to follow the diffusion and transport of Ca^{++} in $NaCl:CaCl_2$ solid solutions. Both experiments involved diffusion and transport from a plane source.

The determination of μ from transport experiments requires a solution to equation (5. 7). The solution of this equation, equation (5. 8) gives the value of D and μ from an observation of the concentration profiles. Although equation (5. 8) is mathematically simple, the solution C(x, t) for some boundary conditions requires complex graphical methods of analysis. This is true, for example, of transport from a semi-infinite extended source.

Some authors have noted erosion of the diffusion profile and erroneously high values for the impurity concentration at x = 0.

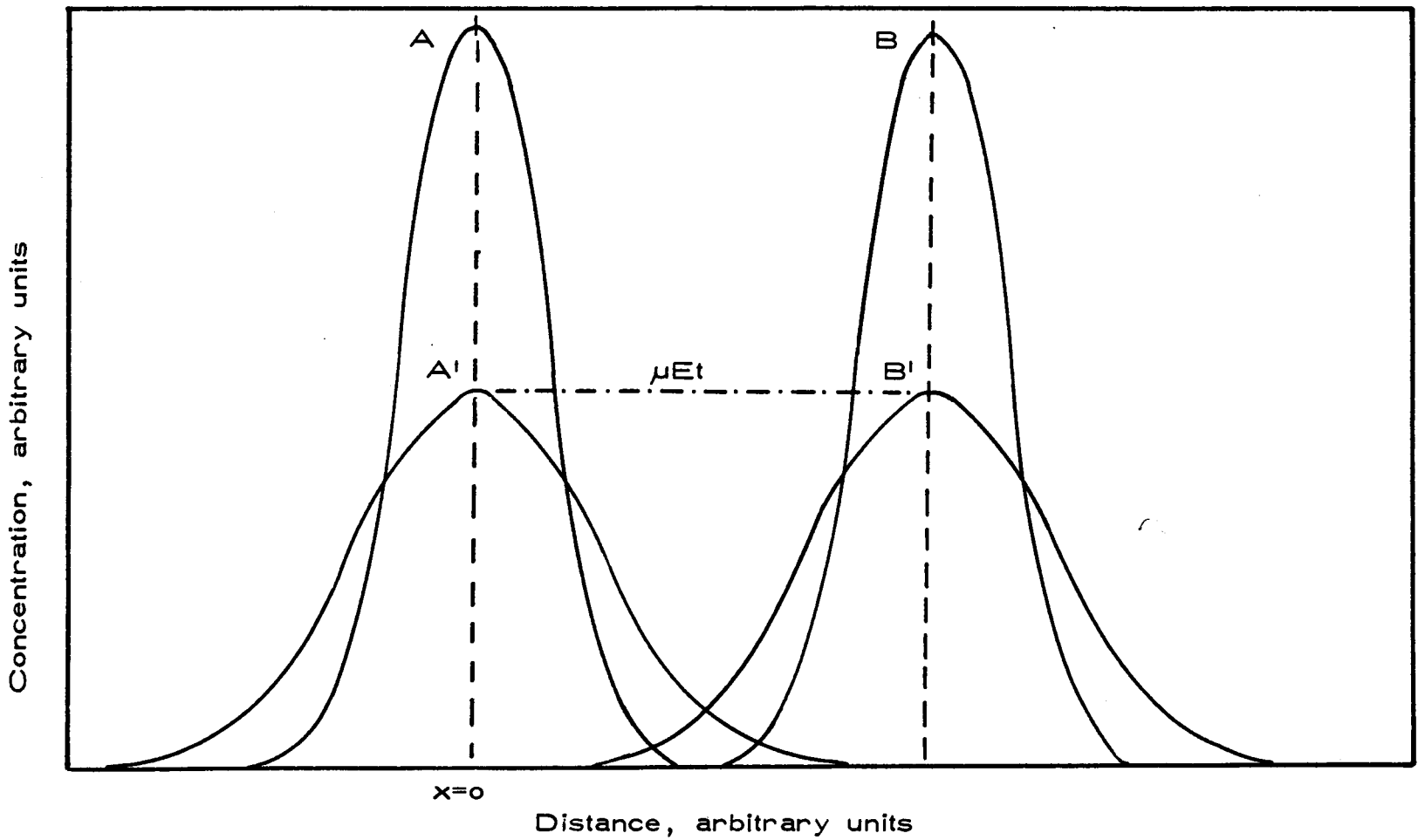

Fig. 5.1. Concentration-distance curves for diffusion and electrolytic transport from a plane source. A and A' are for diffusion; E=O. B and B' are for diffusion and electrolytic transport with a field effect of μEt.

Either of these difficulties present a problem in the determination of μ and D. Malkovich (59) has shown that the ratio μ/D can be determined in an alternate manner by eliminating the need for the determination of the exact location of the maximum or the original concentration. This approach circumvents measurements in the junction region, x = 0, where high diffusivity paths and surface diffusion have been observed. Malkovich's treatment of the problem is as follows. If two samples are joined at a plane source and electrolytic transport takes place in both, they will differ only in that the field effect is either parallel or antiparallel to the diffusion effect. Equation (5. 7) can then be used to describe each sample. Thus

$$\frac{\partial C_A}{\partial t} = D\frac{\partial^2 C_A}{\partial x^2} - \mu E \frac{\partial C_A}{\partial t} \qquad (5.9)$$

and

$$\frac{\partial C_B}{\partial t} = D\frac{\partial^2 C_B}{\partial x^2} + \mu E \frac{\partial C_B}{\partial t} \qquad (5.10)$$

where the concentration distributions will be $C_A(x, t)$ and $C_B(x, t)$ respectively. The system can be diagrammed as:

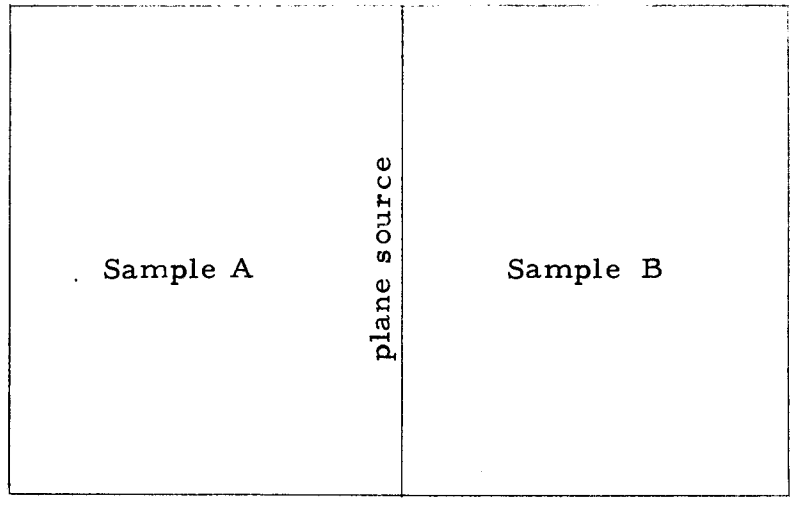

With each side, x is taken as the absolute value of the distance from the plane source at x = 0. Both sides of the sample have identical initial and boundary conditions. The plane source at x = 0 is common to both and considered as an instantaneous source at t = 0. To establish a relationship between the two concentration distributions let us write

$$C_A(x, t) = C_B(x, t)\, f(x) \tag{5.11}$$

and solve for f(x). Substitution of equation (5.9) into equation (5.11) gives

$$f\frac{\partial C_B}{\partial t} = D\frac{\partial^2 C_B}{\partial x^2} f + 2D\frac{\partial C_B}{\partial x} + D\frac{\partial^2 f}{\partial x^2} C_B - \mu E f\frac{\partial C_B}{\partial x} - \mu E C_B\frac{\partial f}{\partial x}$$

or

$$f\frac{\partial C_B}{\partial t} - Df\frac{\partial^2 C_B}{\partial x^2} = (2D\frac{\partial f}{\partial x} - \mu Ef)\frac{\partial C_B}{\partial x} + C_B\frac{\partial}{\partial x}(D\frac{\partial f}{\partial x} - \mu E) \tag{5.12}$$

Using equation (5.10), the left side of equation (5.12) is equal to $\mu Ef\ \partial C_B/\partial x$. Thus

$$2(D\frac{\partial f}{\partial x} - \mu Ef)\frac{\partial C_B}{\partial x} + C_B\frac{\partial}{\partial x}(D\frac{\partial f}{\partial x} - \mu Ef) = 0$$

and $$D\frac{\partial f}{\partial x} - \mu Ef = 0$$

The solution of this equation is

$$f = A\ \exp\{\frac{\mu E}{D}x\}$$

where A is a constant which can be taken equal to one.

If we multiply this solution by $C_B(x, t)$, the resultant product,

$$C_B(x, t)\ \exp\ (\frac{\mu Ex}{D}) \tag{5.13}$$

will be one of the solutions to equation (5.9), that of $C_A(x, t)$. We can write

$$C_A(x, t) = C_B(x, t)\ \exp\ (\frac{\mu Ex}{D}) \tag{5.14}$$

Since the solution to the diffusion equation is unique, equation (5.14) will be valid for all x and t, if it holds for the boundary conditions and at t = 0. At t = 0, equation (5.14) can be satisfied only if

$$C(x, 0) = 0 \quad \text{for all } x \neq 0.$$

For equation (5.14) to hold on the boundaries, one boundary must be such as to capture ions (C=0) and the other must be in the plane

$x = 0$. At $x = 0$, $C_A(x, t) = C_B(x, t)$ for all t.

Under these conditions equation (5. 14) can be written as

$$\ln\left\{\frac{C_A(x, t)}{C_B(x, t)}\right\} = \frac{\mu E}{D} x$$

or

$$\frac{\mu}{D} = \frac{1}{E} \frac{d}{dx} \ln\left\{\frac{C_A(x, t)}{C_B(x, t)}\right\} \qquad (5. 15)$$

and μ/D can be found from the slope of a plot of $\ln\left\{\frac{C_A(x, t)}{C_B(x, t)}\right\}$ versus x.

If the transport profile is well defined beyond the region around $x = 0$ an evaluation of the profile shift, μEt, can give a value of μ. Combination of this value and the value of $\frac{\mu}{D}$ determined from equation (5. 15) gives us both μ and D.

Extended Initial Distribution

This case describes transport from a semi-infinite region of a uniformly doped crystal into a semi-infinite region of pure crystal. The samples can be separate sections placed in contact or a single crystal containing an impure and a pure region separated by a plane of infinite extent. The initial concentration distribution is then:

$$C(x, o) = \begin{cases} C_o \text{ for } x < o \\ o \text{ for } x > o \end{cases}$$

The solution to equation (5. 7) based on one-dimensional transport then becomes

$$C(x, t) = \frac{C_o}{2}\{1 - \mathrm{erf}\,(\frac{x-\mu Et}{2\sqrt{Dt}})\} \qquad (5.16)$$

A construction of concentration versus distance curves permits evaluation of μ and D. Figure 5.2 shows the theoretical concentration-distance curve for transport starting with an extended initial distribution. Again, the shape of the profile is not changed by the action of the field, but the entire concentration curve is uniformly displaced with a velocity of μE. μ can be determined from the displacement of the observed profile, μEt, and equation (5.16) used to evaluate D.

Transport Apparatus

To study the transport of ions in ionic crystals at high temperatures, a controlled-atmosphere transport unit was designed and assembled. Figure 5.3 is a photograph of this unit. The primary function of the unit was to hold a sample at an elevated temperature, in a controlled atmosphere, while a DC field was applied across the sample. The unit consisted of a furnace and controller, regulated power supplies, coulometer, transport clamp, envelope, and controlled-atmosphere gas system. Each part will be discussed in a following section.

Furnace System. A Marshall High Temperature Testing Furnace, a Barber-Coleman Series 620 Power Controller, with silicon

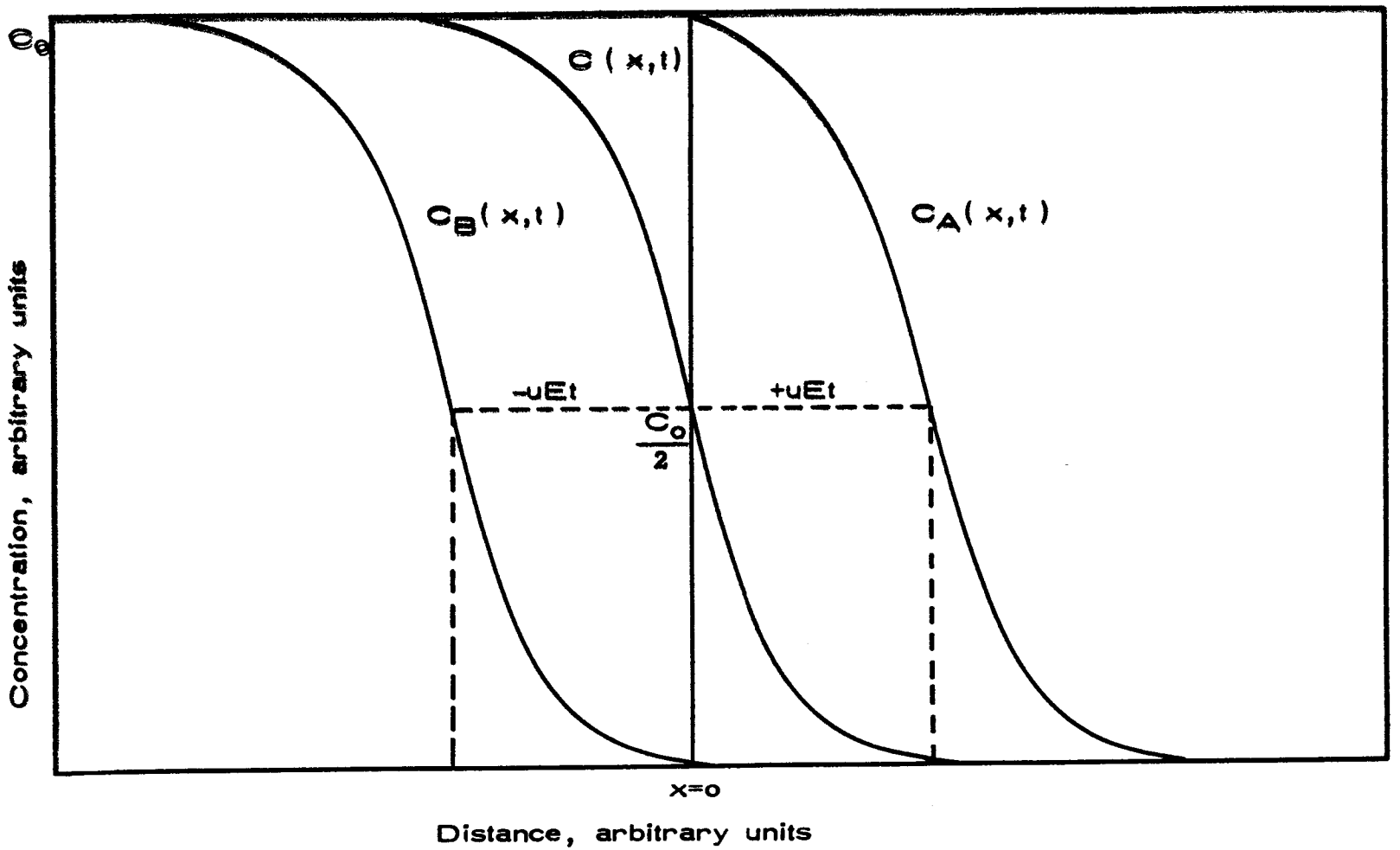

Fig. 5.2. Concentration-distance curves for diffusion and electrolytic transport from an extended initial distribution. C_A is for ions showing a positive field effect; C_B for ions showing a negative field effect.

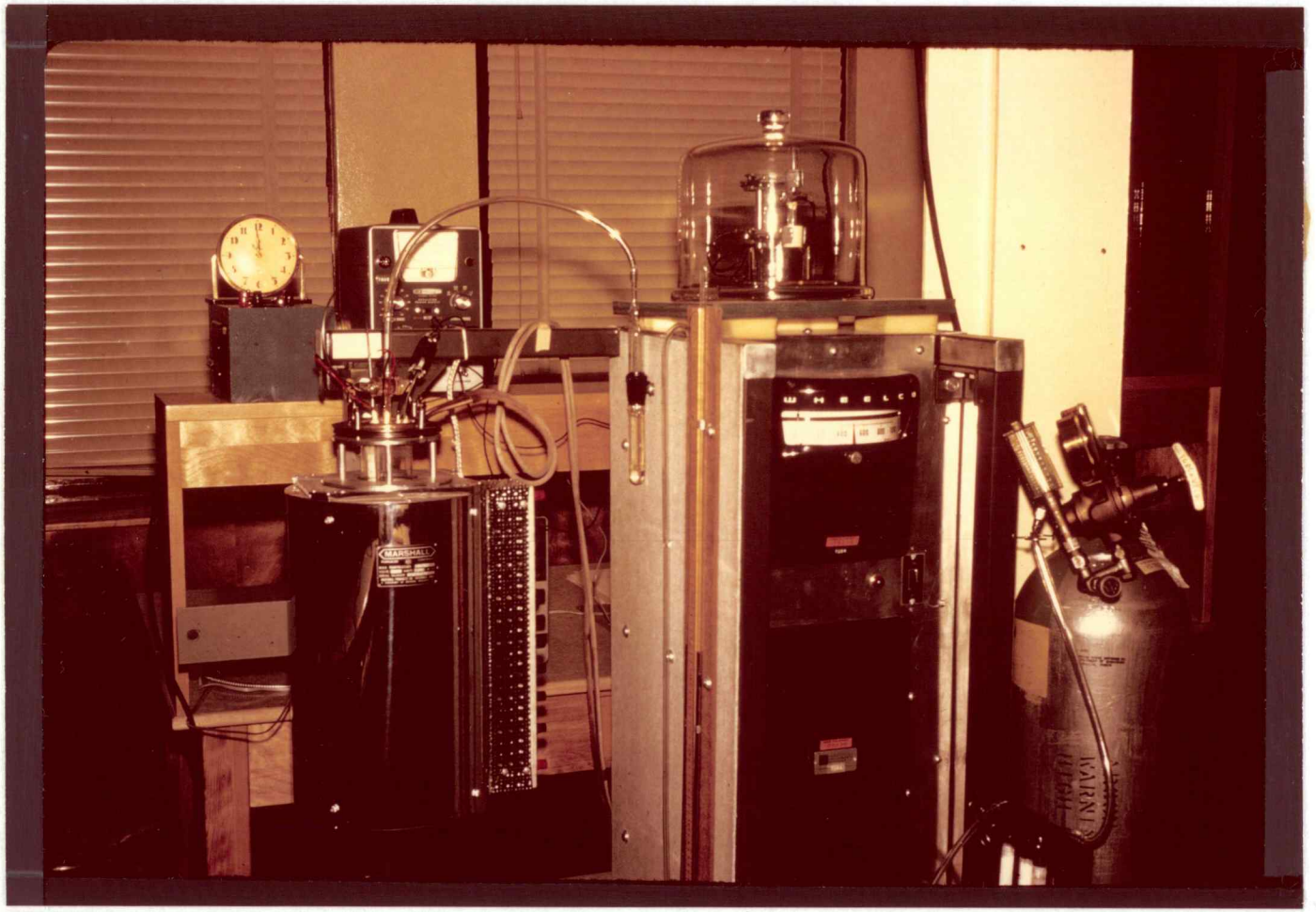

FIG. 5.3. PHOTOGRAPH OF THE CRYSTAL TRANSPORT APPARATUS.

controlled rectifiers, and a Wheelco Temperature Indicator were the primary components of the furnace system. Transite plates adapted to the ends of the furnace were fit snugly against the transport envelope to reduce heat leaks. A mounting collar at the top of the furnace was used to provide support for the envelope and insure a positive seal of the transport unit to the envelope flange. Four threaded pins, projecting upward from this collar, fitted through matching holes in the top plate of the transport unit. Spring-loaded wing nuts bolted the top plate against the envelope flange and an asbestos gasket was used under the flange for cushioning. Temperature indication and control was attained by a jacketed chromel-alumel thermocouple inserted into the furnace case. The temperature of the sample was followed by two chromel-alumel thermocouples placed in the sample chamber.

Regulated Power Supplies. Two power supplies were used in this study to furnish regulated voltage in the range 0-400 volts DC. A Heathkit Model IP-20 Transistor Power Supply furnished controlled voltage in the range 0-50 volts DC while a Heathkit Model IP-32 was used for voltages between 50 and 400 volts DC.

Coulometer. A coulometer built on the basis of the recommendations of Rosa and Vinal(90) was used in this study. A platinum dish acted as the cathode and a pair of silver electrodes were used as anodes. An alundum extraction thimble was placed between the anodes

and the cathode to collect any anode sludge. Reagent-grade silver nitrate and deionized water in a 13% by weight silver nitrate solution were used in the coulometer. This solution was reused until the concentration reached 9%. The cathode dish, set on a burnished brass plate, was mounted on a Formica base and the entire unit was covered with a black bell jar for protection from light and dust.

Transport Clamp. The clamp held a sample between two electrodes across which a DC field could be applied. Stainless steel was used in the construction of the clamp itself, whereas the electrodes and lead-in wires were copper or stainless steel. The clamp and the closed-atmosphere Vycor envelope are shown in Figure 5.4. The clamp was fitted at one end with a variable-position backing plate and at the other with a fixed plate. The movable backing plate was center-mounted on a ball joint to compensate for any irregularities in the sample or other components of the clamp assembly. A series of insulators, mica, quartz, and porcelain were used to isolate the electrodes from the backing plates. The metal electrodes were separated from the crystal by reactor grade carbon blocks. These blocks were used to prevent dendritic growths of potassium in the crystal samples. Fredenhagen and Coderbach (24) have shown that interstitial compounds such as KC_4 and KC_{16} are formed and it is suggested that reactions leading to these compounds prevent dendritic growths in the crystal. The graphite blocks were cut to

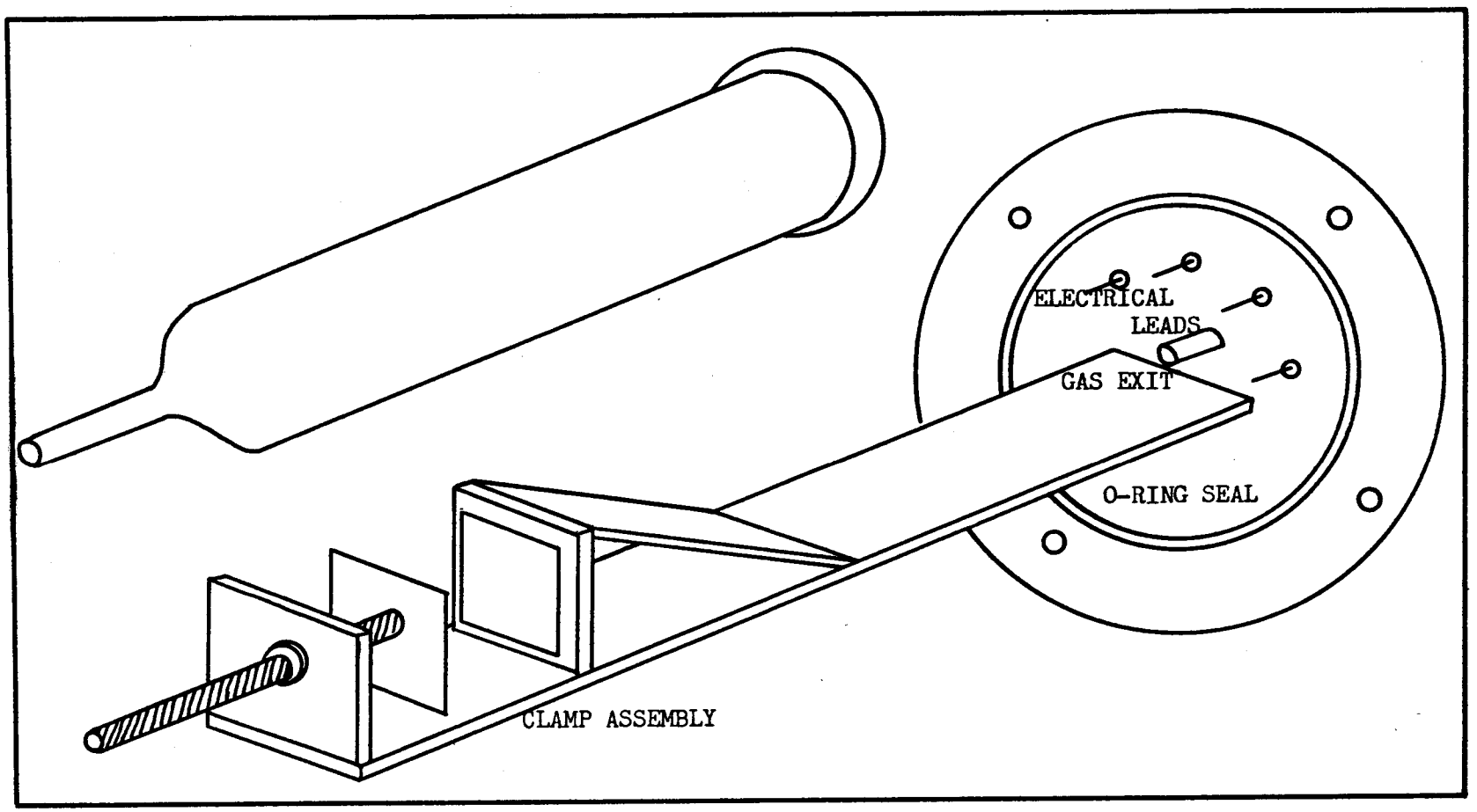

FIGURE 5.4. TRANSPORT CELL AND ENVELOPE.

size, polished, and hand-lapped to insure a smooth, flat surface. Two chromel-alumel thermocouples near the sample indicated the temperature of the crystal. Details of the assembly are shown in Figure 5. 5.

The lower surface of the top plate, of the transport unit, was fitted with an o-ring to seal against the envelope flange. All electrical and thermocouple leads in the transport clamp were insulated with alundum or quartz tubing and passed out through holes in the top plate. Isolation from the plate was accomplished with quartz sleeves. The wires and sleeves were sealed in place with an insulating epoxy resin. A Pyrex stopcock and tubing sealed into this plate functioned as a gas exhaust. A circle of copper tubing was silver-soldered to the upper surface of the plate to provide water-cooling of the plate and the attendant seals.

Controlled-Atmosphere Gas System. Research-grade argon, minimum purity 99. 995%, was used as the transport atmosphere. Reduced reagent-grade copper oxide wire, maintained at 400 ° C was used as an oxygen scavenger, while sodium hydroxide and anhydrone were used as drying agents in the argon supply. An exhaust bubbler using Shell Ondina oil was used to prevent back diffusion of air. Gas flow was regulated by a needle valve and flow meter in the argon line. The gas system is shown in Figure 5. 6.

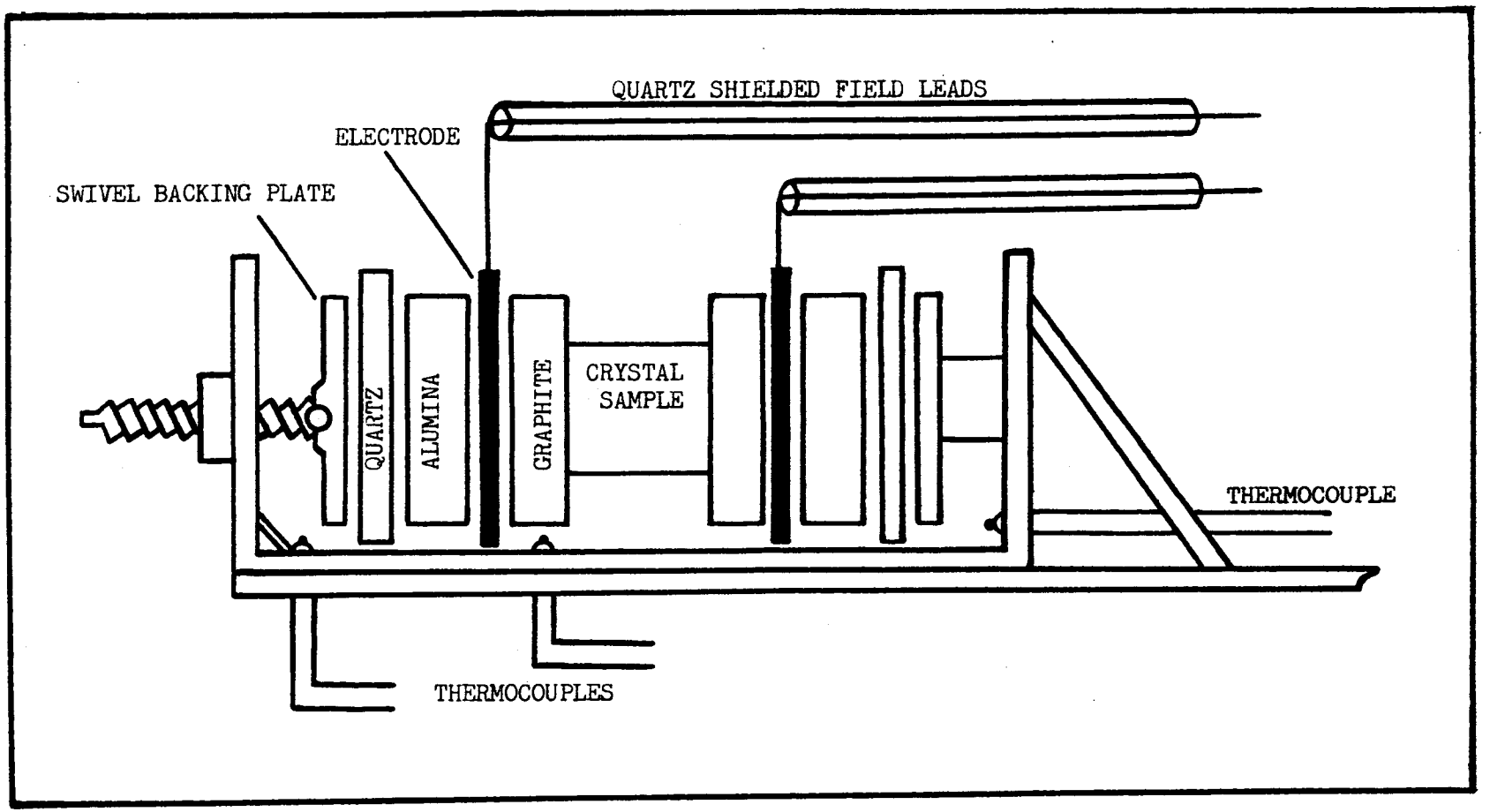

FIG. 5.5. SCHEMATIC DIAGRAM OF THE TRANSPORT CELL CLAMP, ELECTRODE ASSEMBLY AND CRYSTAL STACK.

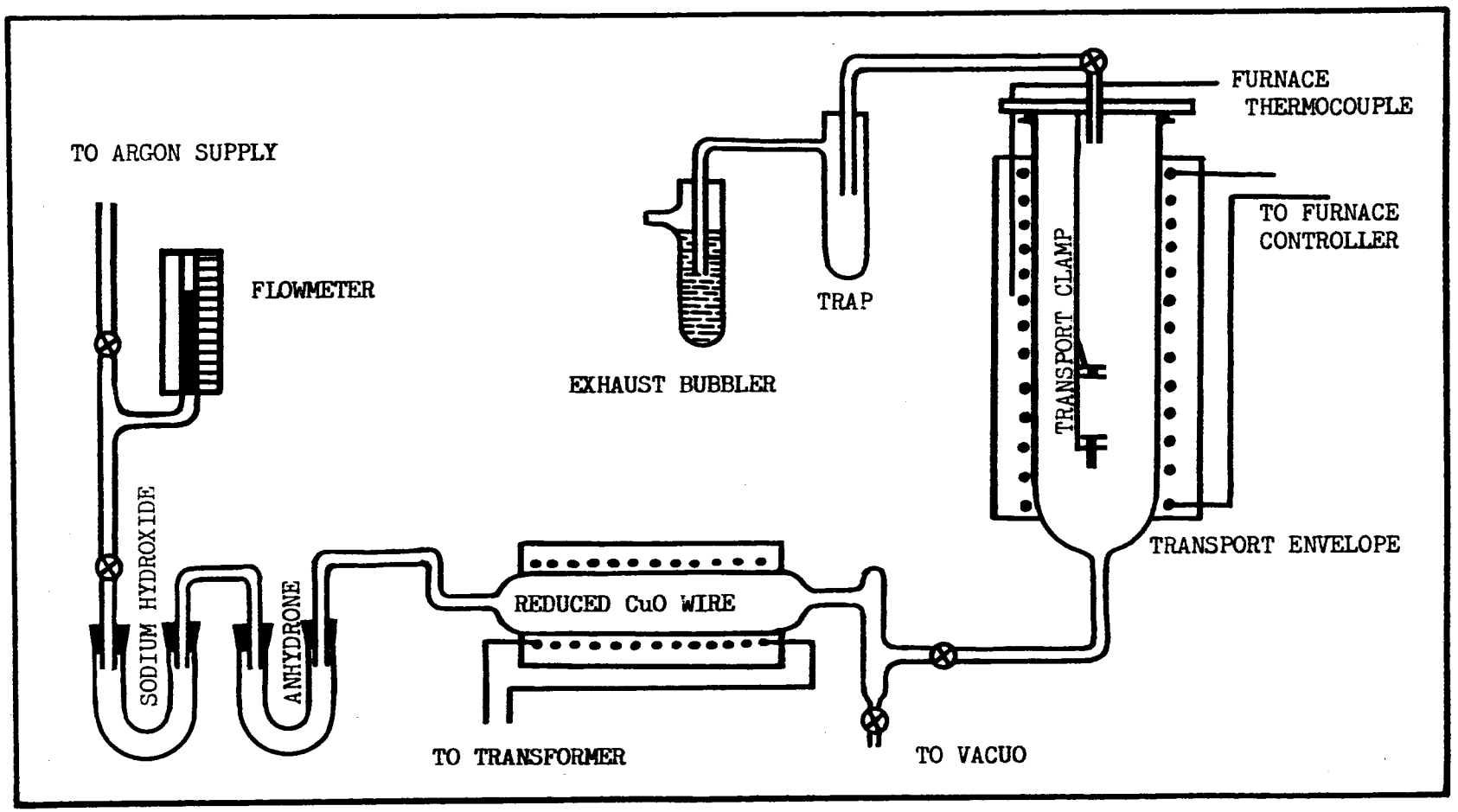

FIG. 5.6. SCHEMATIC DIAGRAM OF THE CONTROLLED ATMOSPHERE SYSTEM FOR THE TRANSPORT CELL.

Experimental

Several experimental schemes were used to study the transport of lead ion in KCl. Basically, they all included a crystal or crystal stack composed of three different regions as shown below:

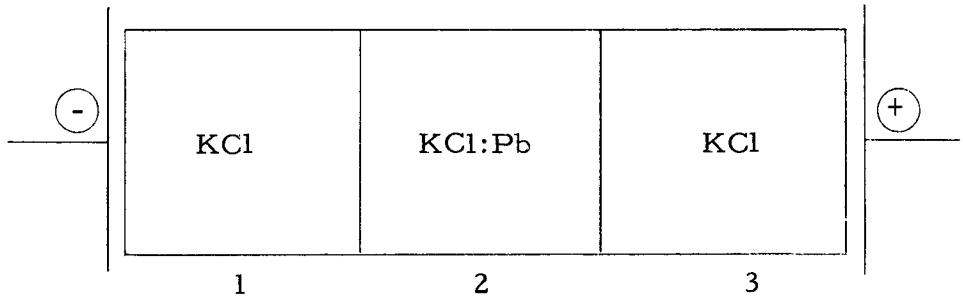

In some cases, region 2 was an infinitely thin layer (experimental approximation) and in others the junction between region 1 and 2 or between 2 and 3 was integral. That is, a crystal was used in which only part of the crystal was doped with lead ion. This crystal will be termed a "dual" section or "dual" crystal in this work. The various sections of the stack were cut to size and the dimensions of each section were measured with a micrometer. Three readings were taken on the thickness and the results averaged. The nominal size for each of these sections was $1 \times 1 \times 0.3$ cm. An examination was made of the fit between adjacent sections and only samples with flat and parallel surfaces were used. When the concentration of lead was low, an absorption spectrum of the KCl:Pb zone was

determined directly. In other cases, slices cut from the faces of these sections were used to evaluate the lead ion concentration. Absorption measurements on very thin plates immediately adjacent to two sides of the KCl:Pb region gave a good evaluation of the concentration of lead ion present in the sample.

The crystal sections of regions 1 or 3 were indexed to establish a reference line other than that of the junctions or the crystal edges themselves. A sharp fiducial line was placed on the side of the sample, parallel to the junctions between the regions. A traveling microscope was used to locate the position of the junctions with respect to this reference mark. The reference line, made with a finely-honed stainless steel razor blade, scattered light sufficiently at 350 mμ to give a sharp index of its position on an absorption spectrum.

The 350-200 mμ absorption spectrum of the end regions were checked for any absorptions due to impurities. The absorption at 350 mμ and 273 mμ was recorded for samples which contained an integral junction of KCl and KCl:Pb regions. Measurements of this type were made in the scanning absorption cell with a 0.058 to 0.15, by 6.35 mm slit. Bleaching experiments and measurements made with light in the visible range showed that the effective slit width was two to three times the nominal value. This effective width was due to light scattering at the edges of the slit and the nonparallel nature of the spectrophotometer beam. The operation of the cell was described earlier in Chapter III. The type of data derived from this

application of the cell is shown in Figure 5. 7. Curves of absorption at 350 and 273 mμ versus distance across the sample are given. Note the definite and sharp absorption made by the fiducial mark on the sample surface.

The common observation on all samples was the absorption spectrum from 350-200 mμ. From this, the concentration of lead was followed by observing the A band previously described. The presence of lead in any of the three regions was evaluated before and after diffusion, and with or without electrolytic transport. Samples were prepared from stock of the same or comparable background. One sample was subjected to diffusion, while the other underwent diffusion and electrolytic transport. The results of the two samples were compared and conclusions drawn regarding the field effect.

When samples with an integral junction between the KCl and the KCl:Pb regions were used, a "dual" crystal, the shape of the initial junction or boundary was observed by viewing the sample after x-ray coloration. The crystal was x-rayed lightly (680 roentgen/minute) for two minutes on each side, on the four sides perpendicular to the plane of the junctions. The difference in coloration rate between the pure KCl region and the KCl:Pb region produces a large difference in the color of the two regions. By observing this difference on all four sides and the penetration profile into the crystal, an indication of junction planarity was made.

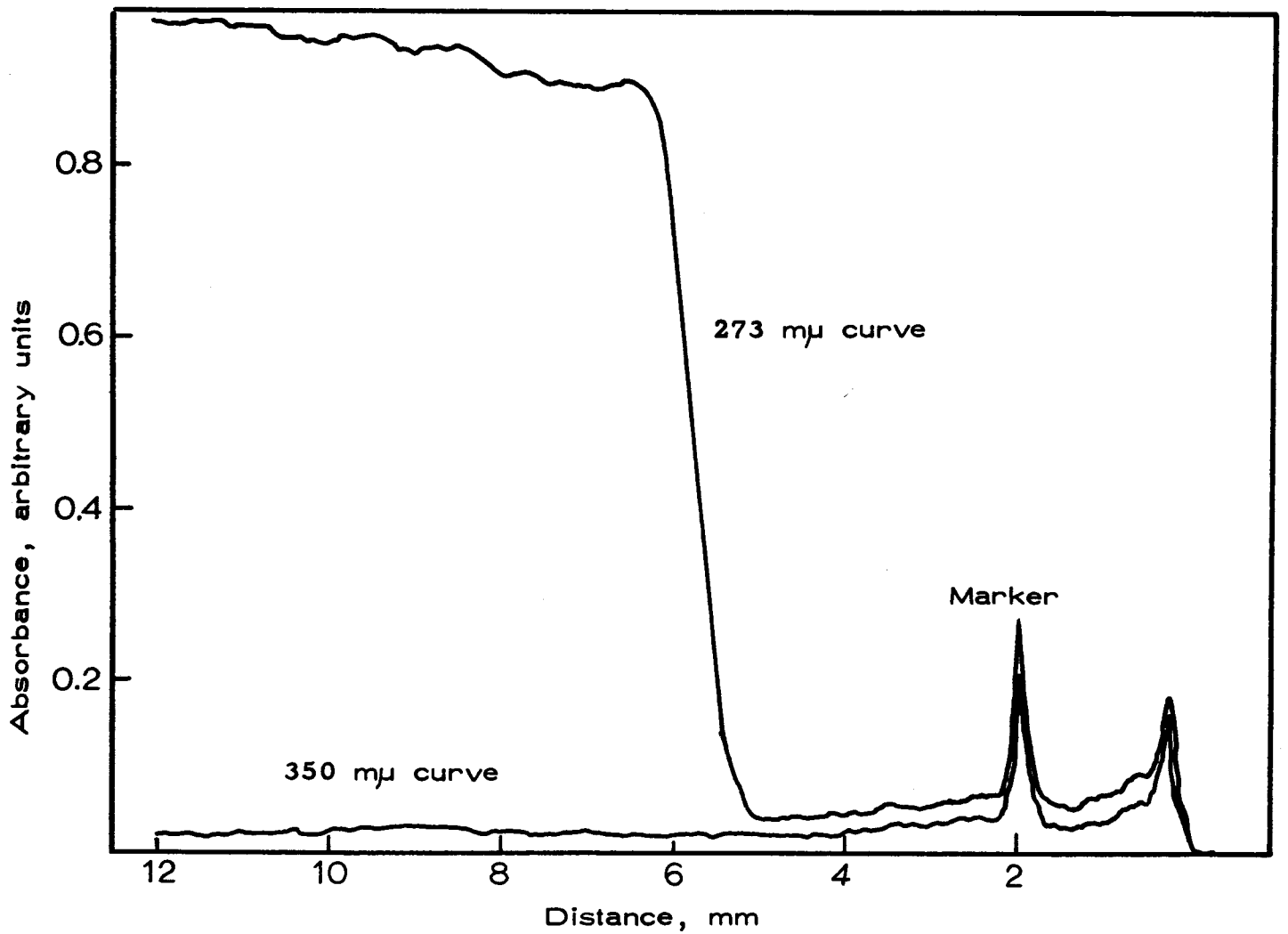

Figure 5.7. Typical transport profile determined in the scanning absorption cell.

Heating to 500° C for 15 minutes removed all effects of the x-ray coloration process and restored the sample to its original condition. The regions of the sample were aligned in cubic symmetry to allow cleavage of the entire crystal without separation at the junctions. The stack was placed in the clamp and sufficient pressure was placed on the crystal to insure good contact between the various surfaces. The crystal clamp was placed in the envelope and evacuated in 50 μ pressure. The envelope was back filled, flushed, and a positive pressure of 20 mm Hg above atmospheric was established. A continuous flow of 3-10 liters of argon per hour was maintained during the balance of the experiment.

The temperature was increased in a reproducible manner to the designated temperature over a period of one hour. During the warm-up period, the coulometer was weighed and prepared for use. When the chosen temperature was reached, a DC voltage from the power supply was applied across the stack and the timing circuit was started. The crystal was maintained at a particular voltage and temperature for a prescribed length of time. Transport was studied in the temperature range 450°-580° C. Experiments were not performed above 580°C because the loss of lead by vaporization was significant. Above 580°C contamination of the sample and the clamp readily took place. The procedure was repeated for simple diffusion experiments, except that no potential was placed across the crystal

stack.

The temperature of the furnace was observed by means of the controlling thermocouple, while that of the crystal itself was measured potentiometrically. Periodic checks were made on the temperature, the current flow, and the DC voltage; any trends were recorded. At the end of the experiment, the field was removed and the envelope was cooled by a forced draft of air. A temperature of 300° C or less was reached within 5 minutes, and 80° C within 20 minutes, after the field had been removed. The system was opened to air and the crystal removed for further observation.

Several types of measurements were now made. The entire stack could be observed at 350 mμ and 273 mμ in the scanning absorption cell as previously described or sections could be cut from the stack, either parallel or perpendicular to the direction of the field. Sectioning of the samples was done with a new razor blade and gentle but firm pressure. With very thin sections, it was often necessary to wedge the blade gently into a corner and position the blade during the cut so that the cleavage front travelled at 45° to the edge of the crystal. The slices were checked for homogeneity and their 350-200 mμ absorption spectra recorded. Because the methods used in analysis varied significantly, the particulars will be given in the results and discussion.

Experimental Particulars, Results and Discussion

Twenty three samples of KCl:Pb were observed in this transport study. Since several different techniques had been used to evaluate the transport of lead ion in KCl, the results and discussions will be presented in separate sections. The following notation will be used throughout the remainder of this chapter. D-1 would be a sample undergoing diffusion only. T-1 would be a sample undergoing simultaneous electrolytic transport and diffusion under conditions similar to those for D-1. It is to be noted that the concentration profiles are given in absorbance per millimeter versus distance instead of concentration versus distance. The concentration is related to the absorbance per millimeter by equation (4. 4). If we assume that the 273 mμ band for lead ion in KCl represents all the lead present in the crystal, the concentration of lead C_{Pb}, expressed in mole percent lead, is given as

$$C_{Pb} = 8.92 \times 10^{-4} A \qquad (5.17)$$

where f was taken as 0. 11, n as 1. 58 and ω as 0. 162 eV. This assumption is not strictly valid (see Chapter IV) because difficulty arises in relating the actual concentration of the lead ion absorbing at 273 mμ to the observed absorbance.

When initial concentration of Pb^{++} in the center region was very low, the diffusion and transport profiles showed little change,

and the observation of the profile movement was limited by the sensitivity of the experimental method. To observe a significant diffusion profile, it was desirable to have a high initial concentration of $PbCl_2$ in the center region. However, the concentration range observable by this spectrophotometric method was limited by the minimum attainable sample thickness, 0.01 cm, and the oscillator strength of the A band. The workable concentration range was 10^{-5} to 10^{-3} mole % Pb in the samples.

Absorption by an Inhomogeneous Medium

The volume surrounding an integral junction between a pure and a lead doped region of a crystal is one of inhomogeneous absorption. The pure region has little or no absorption at 273 mμ, while the region containing lead ion has an appreciable absorption at this wave length. Sectioning of the sample after diffusion or diffusion and electrolytic transport has taken place, parallel to the field direction, produces samples of this type. Jones (40) has studied absorption by inhomogeneous systems and shows that the absorption observed when a medium of known absorption coefficient covers a fraction of the slit area is less than the product of the fraction of the slit area covered and the absorption coefficient of the medium. Thus, even on the assumption that absorption is proportional to concentration, the profiles observed from the scanning absorption cell can not

be taken per se as concentration profiles. Jones's theory predicts a nonlinear relationship between the absorbance and the percent of the slit covered by the medium. Two cases can be considered which pertain to measurements made with the scanning absorption cell. If the scanning slit width is small in relation to the total width of the transport profile and the absorption gradient over the width of the slit is near zero, the corrections are small and the error negligible. If the scanning slit width is comparable to a width of the profile in which the absorption gradient is not zero, Jones's corrections may be applied.

Transport profiles as determined by the author are described by the latter case. The large value of the slit width used, 58-150 μ, in relation to the width of the diffusion profiles, 100-700 μ, indicated that correction of the absorption profiles were necessary before diffusion constants could be determined. However, the absorption curve shape observed by the author did not compare favorably with that predicted by Jones. The theoretical curve and an experimental curve for an absorbance of 0.87 are compared in Figure 5.8. It is suggested that the convergent nature of the incident beam and scattering effects produce the differences between the two curves. Application of Jones's corrections would be, at best, a rough approximation and no attempt was made to use them. No diffusion constants were determined because the absorption profiles could not be

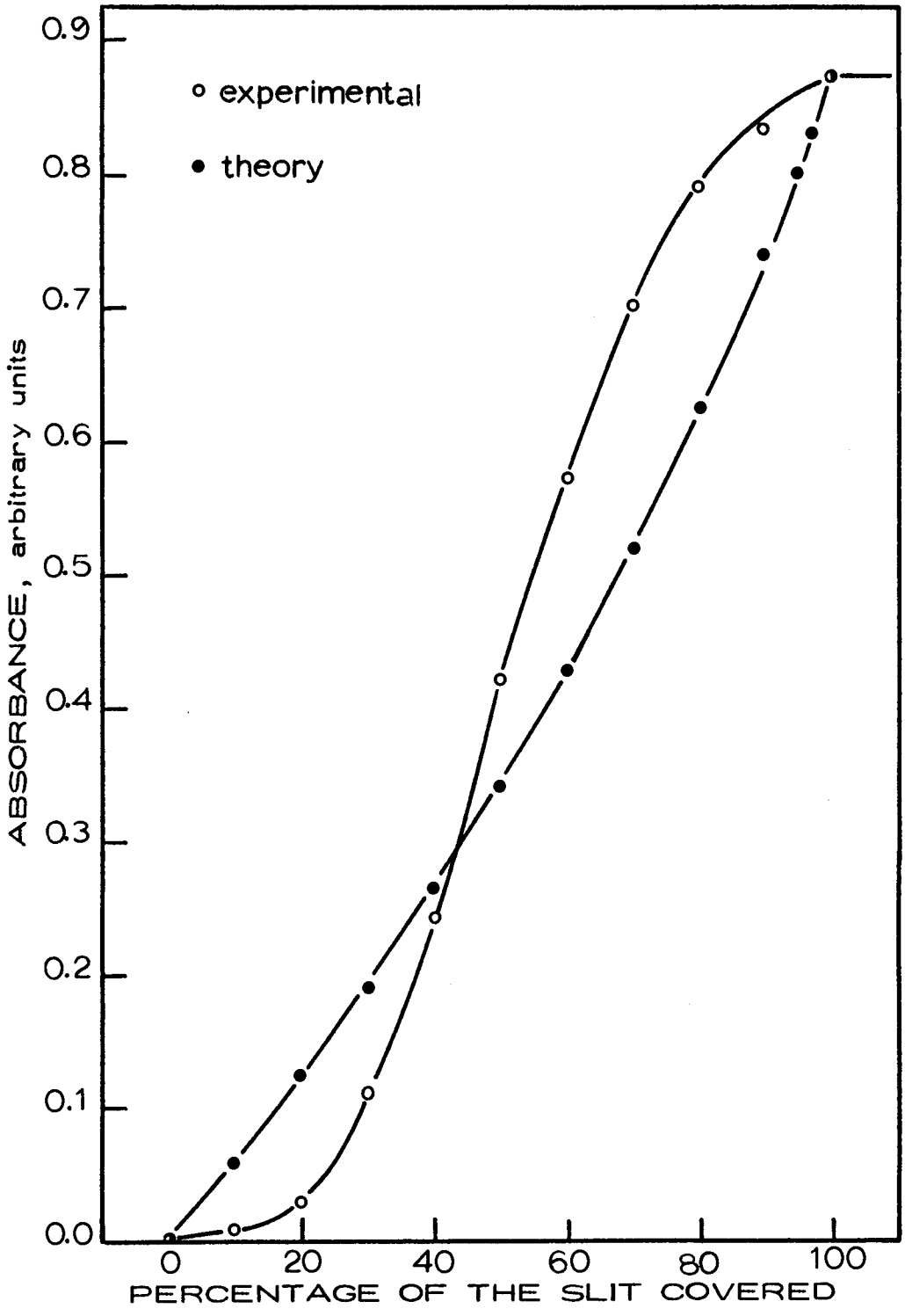

Fig. 5.8. Comparison of the absorption curve (A=0.87) predicted by Jones's theory with an experimental curve.

corrected to true concentration profiles. Recently, Reisfeld, Glasner, and Honigbaum (86) have made measurements on the diffusion of Tl^+ in KCl using a slit system similar to that of the author, except 10 μ in width. Since their diffusion profiles were 200-300 μ, Decius and Fredericks[4] suggest that diffusion coefficients determined from this type of spectrophotometric data must be corrected for inhomogeneous absorption.

Although diffusion coefficients could not be evaluated in this study, the effect of an electric field on the sample could be observed. Since the shape of the diffusion profile is not altered by an electric field, a comparison of experiments with and without the presence of the field should give a quantitative value for the profile shift due to the presence of the electric field. The errors in each profile are the same type and would cancel.

The arguments regarding slits and inhomogeneity pertained only to experiments in which the sample was evaluated by sectioning parallel to the electric field axis and observed in the scanning absorption cell. Absorption measurements made on sections cut perpendicular to the direction of the field are not subject to the difficulties described. A summary is made in Table 5. 1 of the types of sectioning used for each sample. Supporting evidence describing

---

[4]J. C. Decius and W. J. Fredericks, Professors of Chemistry, Oregon State University. July, 1965. A personal communication.

Table 5.1 Sectioning method used in the analysis of transport samples.

Crystals sectioned parallel to the field axis	Crystals sectioned perpendicular to the field axis
D-1	D-3
T-1	T-4
D-2	T-6
T-2	T-9
D-3	T-10
T-3	T-14
T-4	T-15
T-5	T-16
T-6	T-17
T-7	F-T-6
T-8	
T-9	
T-10	
T-11	
T-12	
T-13	
T-14	
T-17	
T-18	
D-18	
D-20	
F-T-6	

the motion of Pb^{++} in KCl was derived from both types of sectioning.

Diffusion and Transport from a Plane Source

Four experiments were performed where the $PbCl_2$ diffused from a plane source. A KCl crystal was cut to the required size and split in the center. The faces exposed by this split were coated with $PbCl_2$ either by evaporation of $PbCl_2$ onto the surface, or by evaporation of an ethanol-$PbCl_2$ mull. The faces were realigned and the crystal subjected to migration studies. Samples chosen for study were of sufficient area that the loss of $PbCl_2$ at the outside edges of the junction did not affect the inner area chosen for study. The experimental conditions are presented in Table 5.2 and the observed absorption profiles in Figures 5.9 and 5.10. Since the diffusion and electrolytic transport profiles are superimposed in each sample figure, the direction of the field is shown in the upper corners of each diagram. Pairs of samples were subjected to identical conditions during diffusion, and simultaneous diffusion and electrolytic transport. The solubility of $PbCl_2$ in KCl single crystals was exceeded at the junction surface, where the $PbCl_2$ had been deposited, and the crystal in this region had a characteristic white color due to precipitated $PbCl_2$. Beyond this center region, the characteristic A band for Pb^{++} was observed. No

Table 5.2 Experimental conditions for diffusion and electrolytic transport from a plane source.

Sample	D-1	T-1	D-2	T-2	D-20
Temperature, °C	555	554	578	576	530
Time, minutes	1205	1205	1200	1200	940
Potential, volts	0	30	0	30	0
Field, volts/cm*	0	43.4	0	38.7	0
Charge passed, equivalents x 10^4	0	0.57	0	0.53	0
Thickness, mm	8.77	6.92	7.73	7.76	-
Distance, marker to plane source, mm	1.89	1.64	1.95	1.21	vapor diffusion sample
Distance, plane source to anode, mm	4.14	3.58	4.41	3.17	-

* Calculated assuming constant conductivity throughout the sample

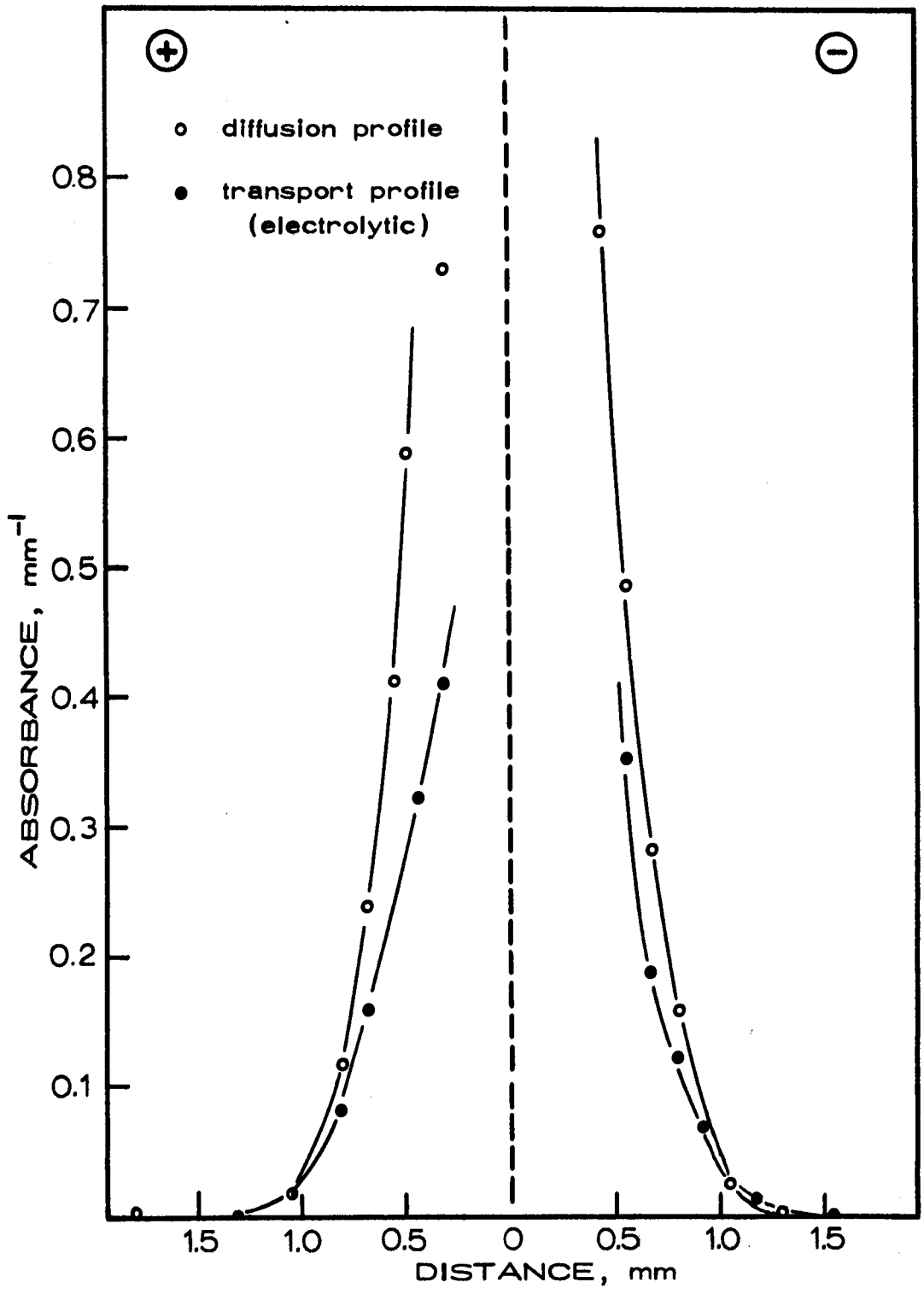

Fig. 5.9. Diffusion and electrolytic transport profile of D-I and T-I. Plane source is shown by the dotted line.

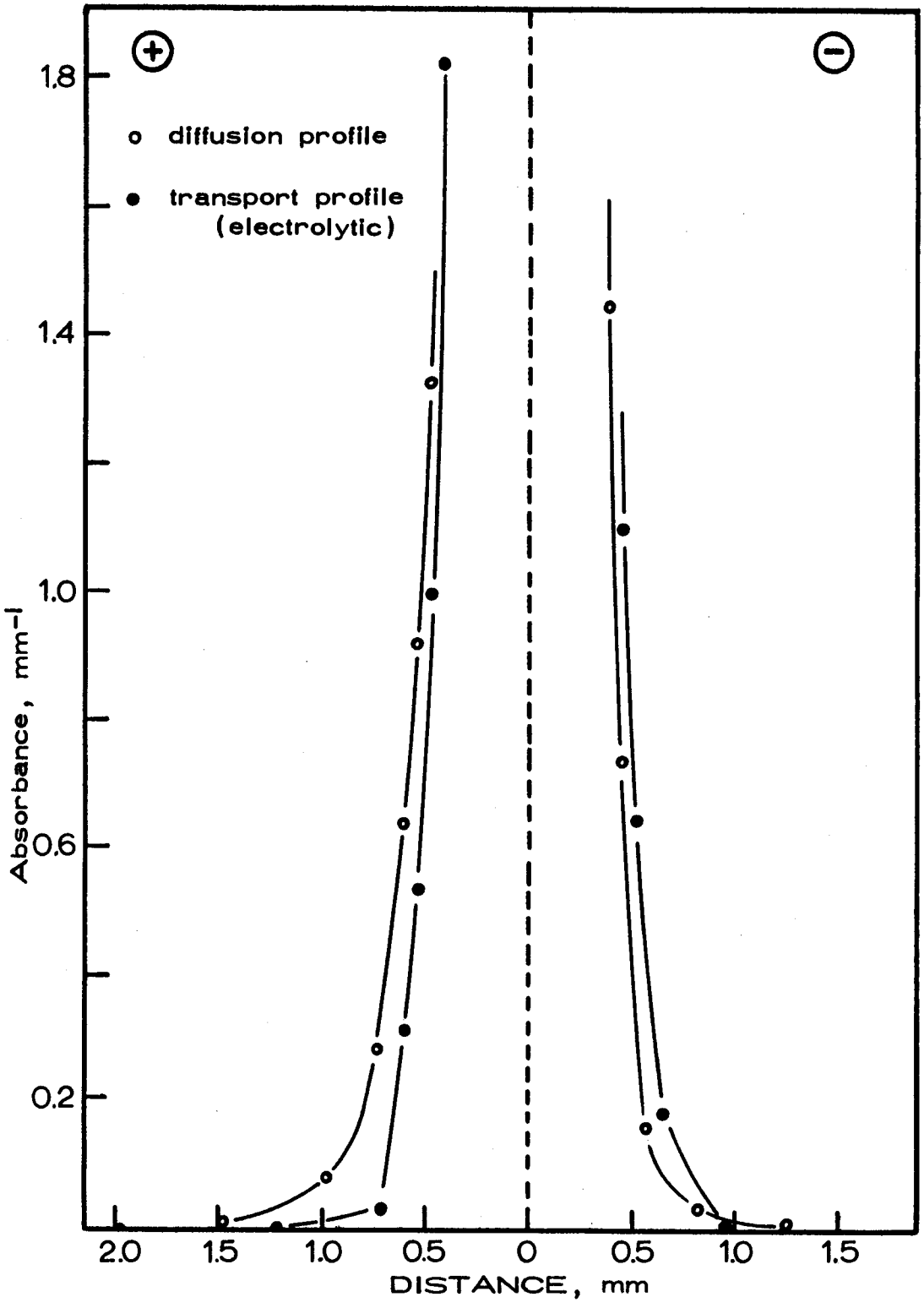

Fig. 5.10. Diffusion and electrolytic transport profile of D-2 and T-2. Plane source is shown by the dotted line.

spectrophotometric data could be taken within the opaque region, but measurements made with a traveling microscope confirmed the fact that the original plane source had not shifted with respect to the reference marker. Experiments D-1 and T-1, where the $PbCl_2$ plane source had been deposited by evaporation, showed no significant movement of Pb^{++} under the influence of the field. Experiments D-2 and T-2, where the $PbCl_2$ plane source was deposited from an ethanol mull, gave analogous results. In the latter pair of experiments, the original distribution of $PbCl_2$ on the junction surfaces was somewhat uneven, whereas the distribution on the former showed a variation of less than 10%. In experiments D-2 and T-2 the $PbCl_2$ was deposited on only one of the junction faces and the concentration profiles after diffusion were unsymmetrical. These results reflected this single coating. The lead diffused farther into the surface on which it had been coated, then into the surface in immediate contact with it. The vapor pressure of pure solid $PbCl_2$ at 525°C is 0.39 mm, so it is reasonable that vaporization will occur and the concentration of $PbCl_2$ will become uniform on both faces. However, the $PbCl_2$ on the coated face begins to diffuse with a higher initial concentration and therefore shows a greater diffusion distance than the uncoated face during the same length of time. A similar argument applies for inhomogeneity in the surface coating.

Samples D-1 and T-1 were coated uniformly with $PbCl_2$ on both

of the surfaces and the results show that diffusion from this plane source was the same in both directions. T-1, in which a field was applied across the crystal, indicates that there was no appreciable field effect on Pb^{++} in KCl. This would indicate that lead ion diffuses into the sample and forms a complex whose time-average charge is approximately the same as the host cation or that, even though charged, its mobility is small.

Further information about diffusion was obtained from an experiment, D-20, in which $PbCl_2$ diffused into KCl from the vapor phase. The concentration-distance profile is shown in Figure 5.11. The initial concentration at the surface, C_o, at t = 0 was estimated from an extrapolation of the profile to the line representing the surface of crystal. The diffusion distance observed was about 0.5 mm. This experiment and diffusion experiments on NaCl:Pb performed in our laboratory suggested that diffusion beyond 1.5 mm is not expected under the experimental conditions of diffusion time and temperature used in the author's experiments.

Diffusion and Electolytic Transport from an Extended Source

In studying diffusion and electrolytic transport from an extended source, two different schemes were used. The first involved the use of three separate regions, each composed of a separate crystal section, while the second used the "dual" crystal described in a

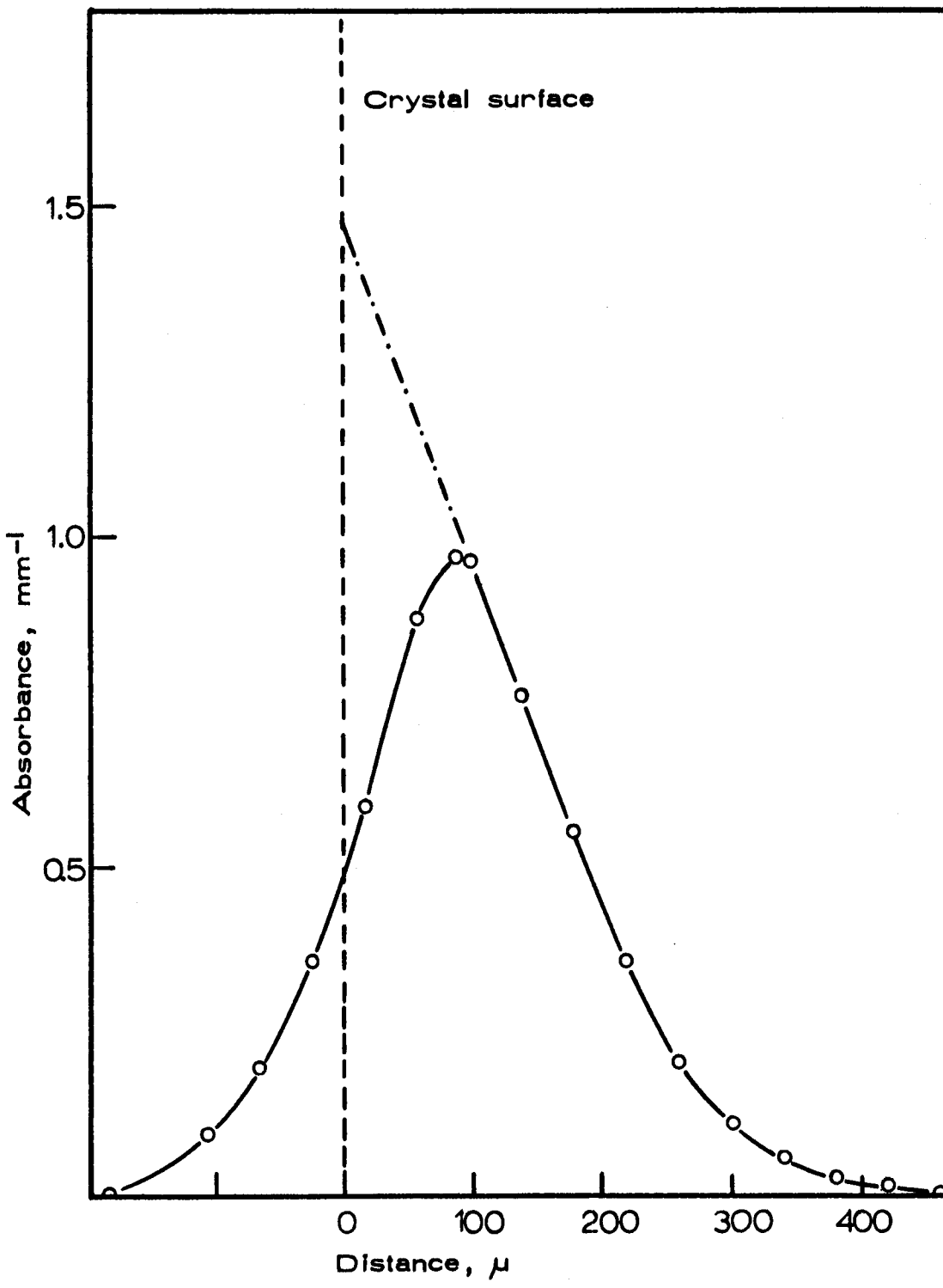

Figure 5.11. Concentration profile of the vapor phase diffusion of $PbCl_2$ into KCl; crystal D-20.

previous section.

The end crystals used in these experiments were single KCl crystals obtained from the Harshaw Chemical Company or high purity KCl crystals grown by the author. The absorption spectra of samples corresponding to these regions were recorded before they were incorporated into the crystal stack. No lead ion and little hydroxide ion was found in these crystals. Region 2, that of KCl: Pb, contained a uniform Pb^{++} concentration. The uniformity of an adjacent slice was checked with the scanning absorption cell and the absorbance taken as representative of the sample. In the early experiments, the junctions between the center region and the end crystals were taken as reference positions. Any diffusion of lead ion was measured with reference to these junctions.

Anomalous scattering and reflection effects at the relatively rough edges of the crystal stack made it difficult to substantiate the position of the crystal edge by absorption measurements. The apparent position of the crystal edge varied with the thickness of the sample, and the flatness and alignment of the plane face directly behind the leading edge. In the later experiments a fiducial line was placed in one of the pure end regions and the distances between the regions were taken with reference to this line. Measurements with a traveling microscope indicated that the distance between the fiducial mark and the junctions remained constant before and after the sample had

been subjected to the conditions of the experiment. The positions of the junctions and the presence of Pb^{++} in the crystals, relative to this mark, indicated any motion of lead in the three regions. The conditions of these experiments are given in Table 5. 3. The entire length of the stack, sum of regions 1, 2, and 3, did not change more than 1% before and after transport. Two samples, T-6 and T-10, did show a 2% decrease in length. Representative transport profiles are given in Figure 5. 12 through 5. 20. Although continuous data was taken by the scanning absorption cell, analysis of each sample required subtraction of absorption curves. The figures are produced from point data. Each figure represents the processed data from four scanning curves. Since most crystals were of the "dual" type, the boundary position in the "dual" crystal is near the center of the sharp rise in absorption. The exact position was relative to the fiducial line before and after transport. The junctions between the electrode and the sample are beyond the borders of the figures. Figure 5. 12 shows the profile of sample D-3 before and after diffusion has taken place. The transport profile shows a change expected for diffusion from a semi-infinite extended source. Figure 5. 13, an analysis of T-5, shows a decrease in lead ion concentration near the cathode junction. This is attributed to the reduction of Pb^{++} to elemental lead and will be discussed shortly. Figure 5. 14 shows the results of sample T-7. Again the shift in

Table 5.3 Experimental conditions for diffusion and electrolytic transport from a semi-infinite extended source.

Crystal	Temp., °C	Time, minutes	Potential, volts	Field, volts/cm*	Current passed, equivalents x 10^{-4}	A band absorbance, mm^{-1} (before transport) Region 2	Length, mm: Anode region	Center region	Cathode region
T-3	580	1400	20	18.8	62.0	2.69	2.73	← 7.89 →	
D-3	588	1770	0	0	0	2.67	3.90	← 9.79 →	
T-4	567	1980	10	1.0	0.20	-	← 6.61 →		3.18
T-5	570	2300	30	20.6	0.53	0.18	3.47	6.21	3.01
T-6	584	2070	100	68.0	6.16	0.43	← 11.53 →		3.15
T-7	503	2475	150	113	0.50	1.83	← 9.84 →		3.48
T-8	452	2800	150	115	0.12	1.00	4.26	← 8.78 →	
T-9	482	2320	150	122	0.21	1.19	2.36	← 9.91 →	
T-10	495	3023	300	273	0.71	2.78	← 7.84 →		3.16
T-11	519	1240	400	403	0.90	0.13	2.48	→ 7.47 →	
T-12	477	1420	297	213	0.24	0.25	← 10.58 →		3.36
T-13	502	2125	200	134	1.42	-	← 11.95 →		3.03
T-14	580	2332	30	33.0	-	20.70	2.48	2.99	3.62
T-15	556	2140	50	44.8	1.08	1.20	3.18	4.73	3.26
T-16	567	2200	30	28.5	1.02	6.60	3.21	4.07	3.24
T-17	547	4210	100	89.6	1.67	-	2.95	3.69	4.52
T-18	573	2350	10	8.40	0.20	-	3.02	5.54	3.40
T-19	478	3200	10	7.95	0.14	-	4.51	3.59	4.48
F-T-6	560	2805	20	17.2	3.27	8.0	3.02	5.55	3.18
D-18	574	2350	0	0	0	-	4.44	3.83	4.35

* Calculated assuming constant conductivity throughout the sample

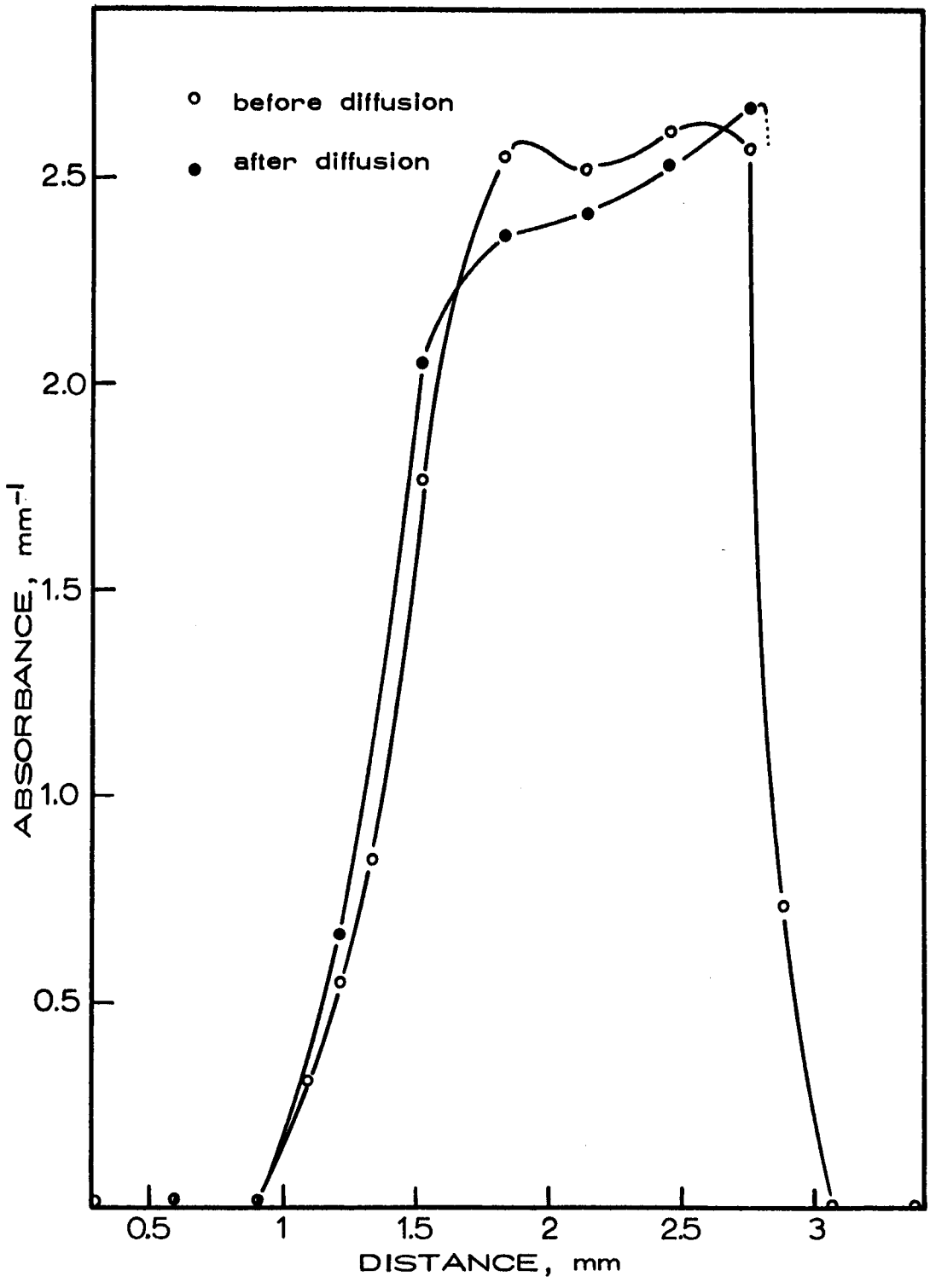

Fig. 5.12. Diffusion profile of crystal sample D-3.

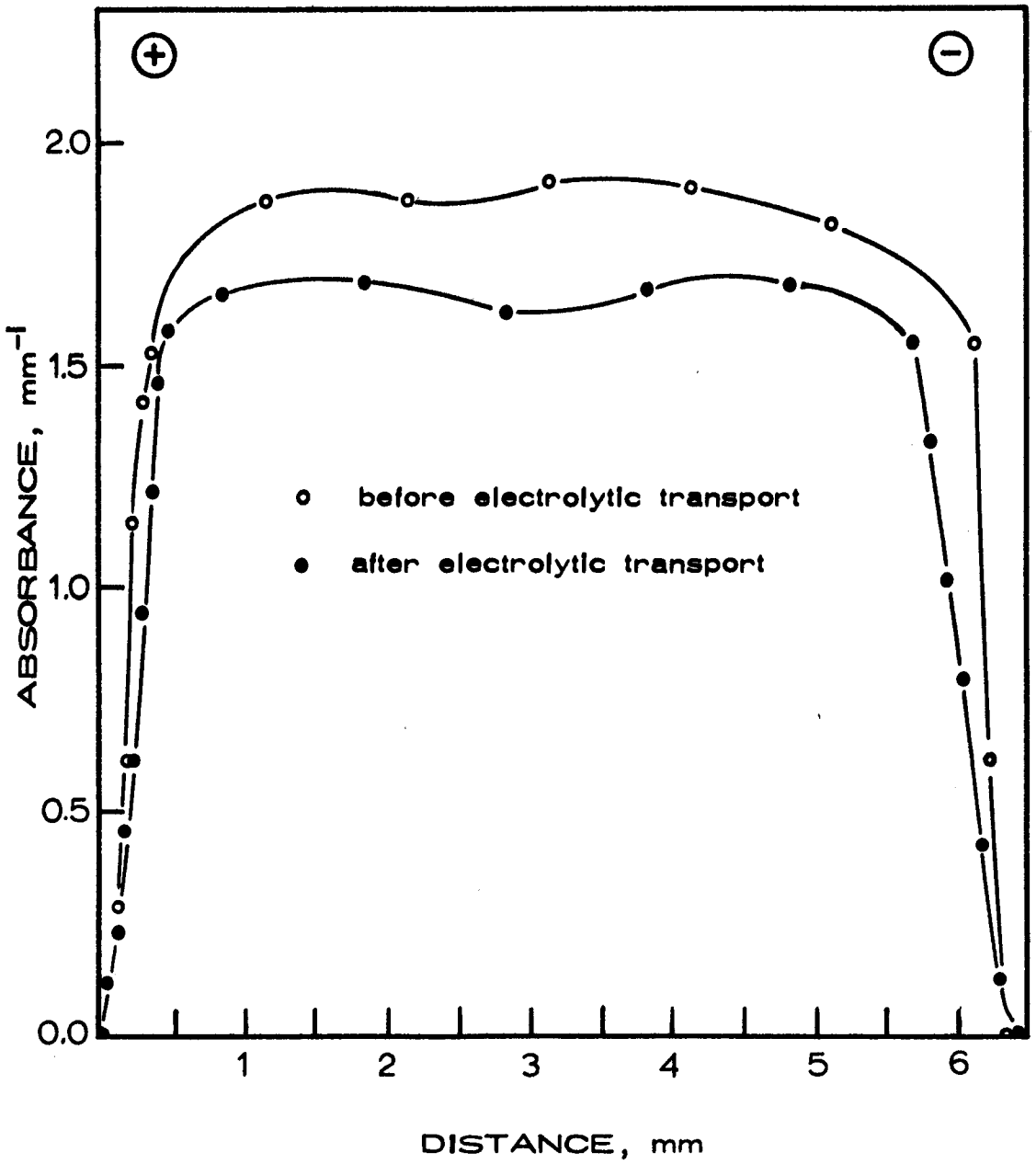

Figure 5.13. Electrolytic transport profile of crystal T-5. Note the decrease in the lead ion concentration near the junction with the cathode crystal.

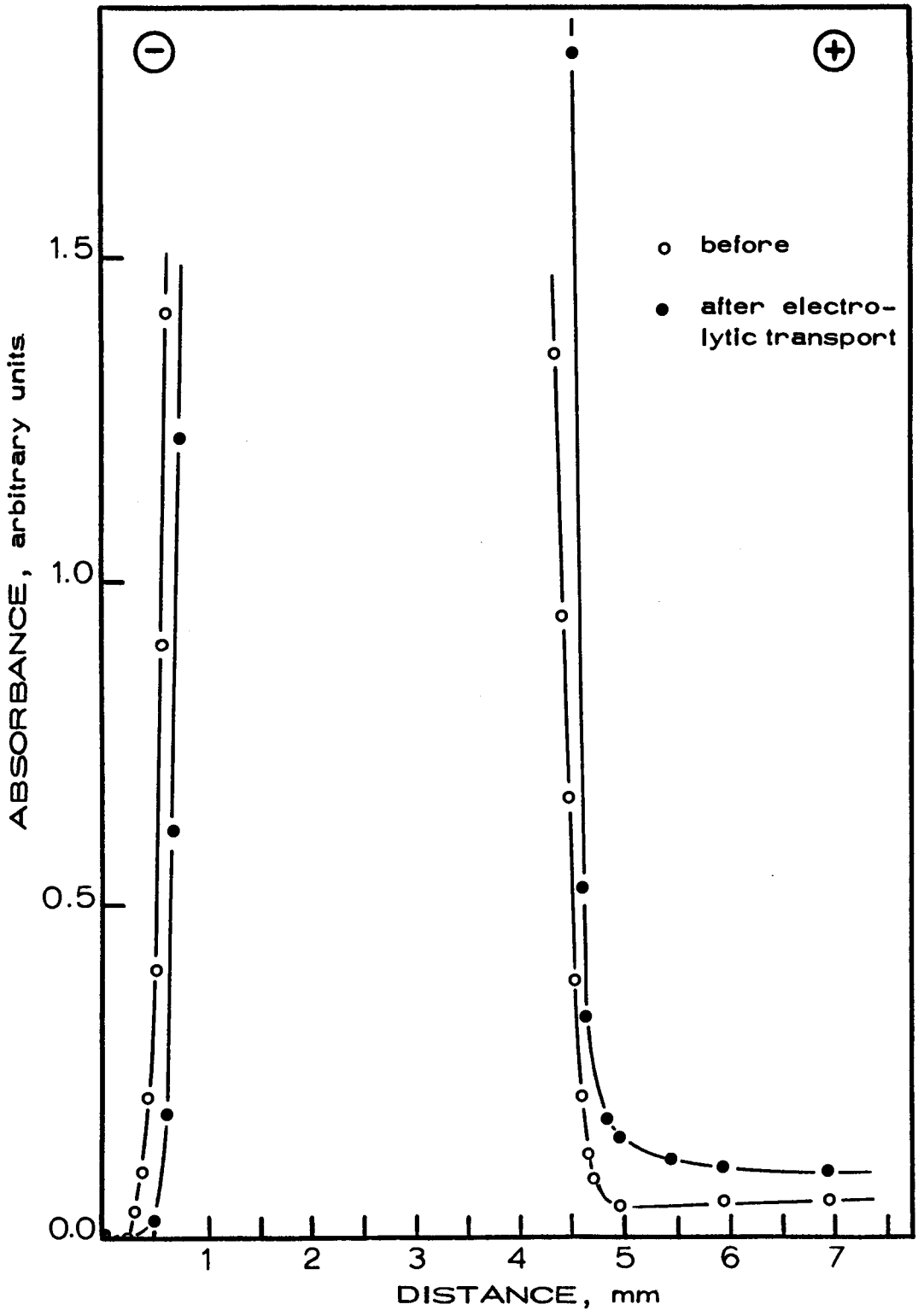

Fig. 5.14. Electrolytic transport profile of crystal T-7.

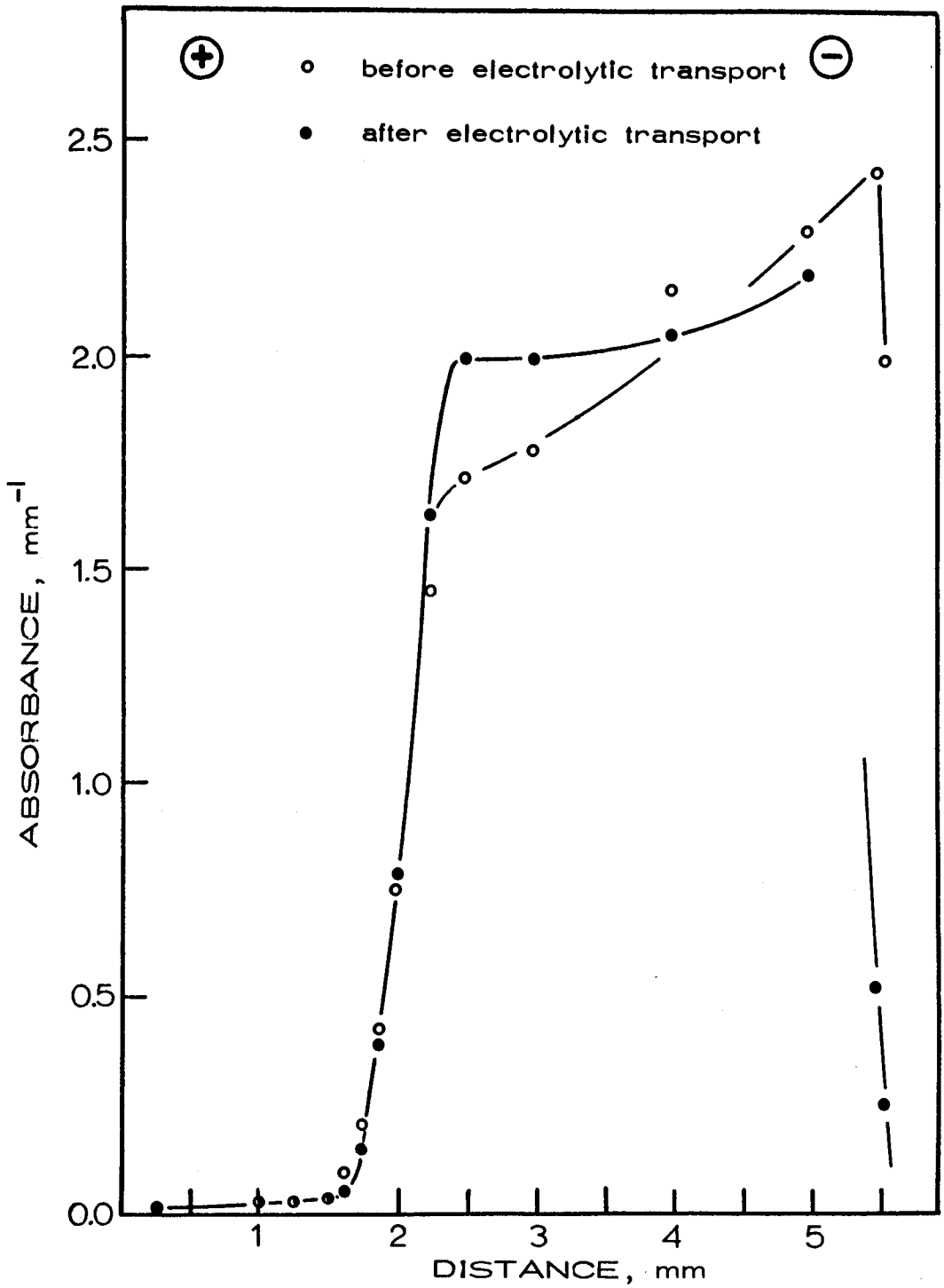

Figure 5.15. Electrolytic transport profile of crystal T-10.

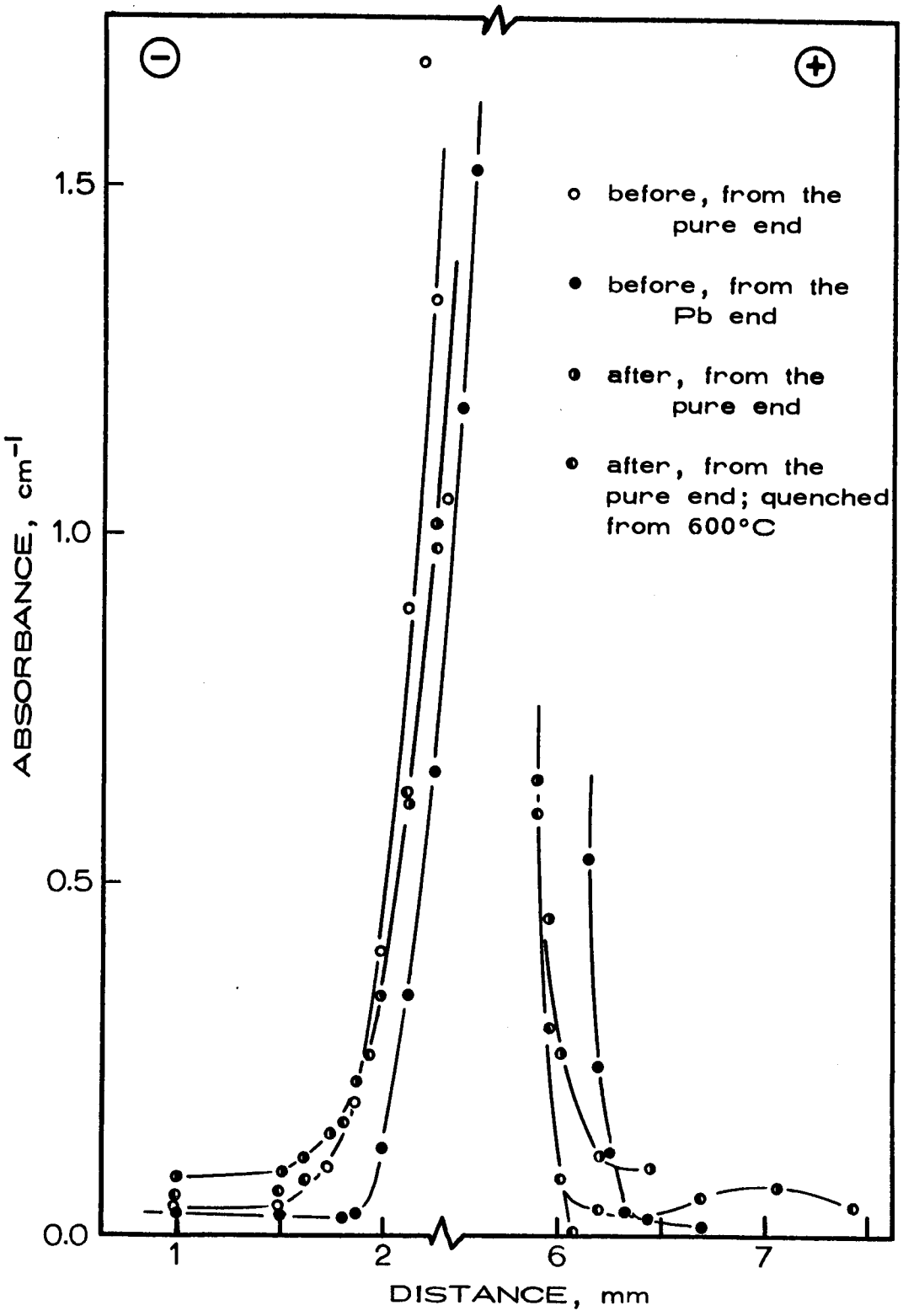

Fig. 5.16. Electrolytic transport profiles of crystal T-II. The scatter indicates that all scanning profiles must be taken in the same direction for consistent data.

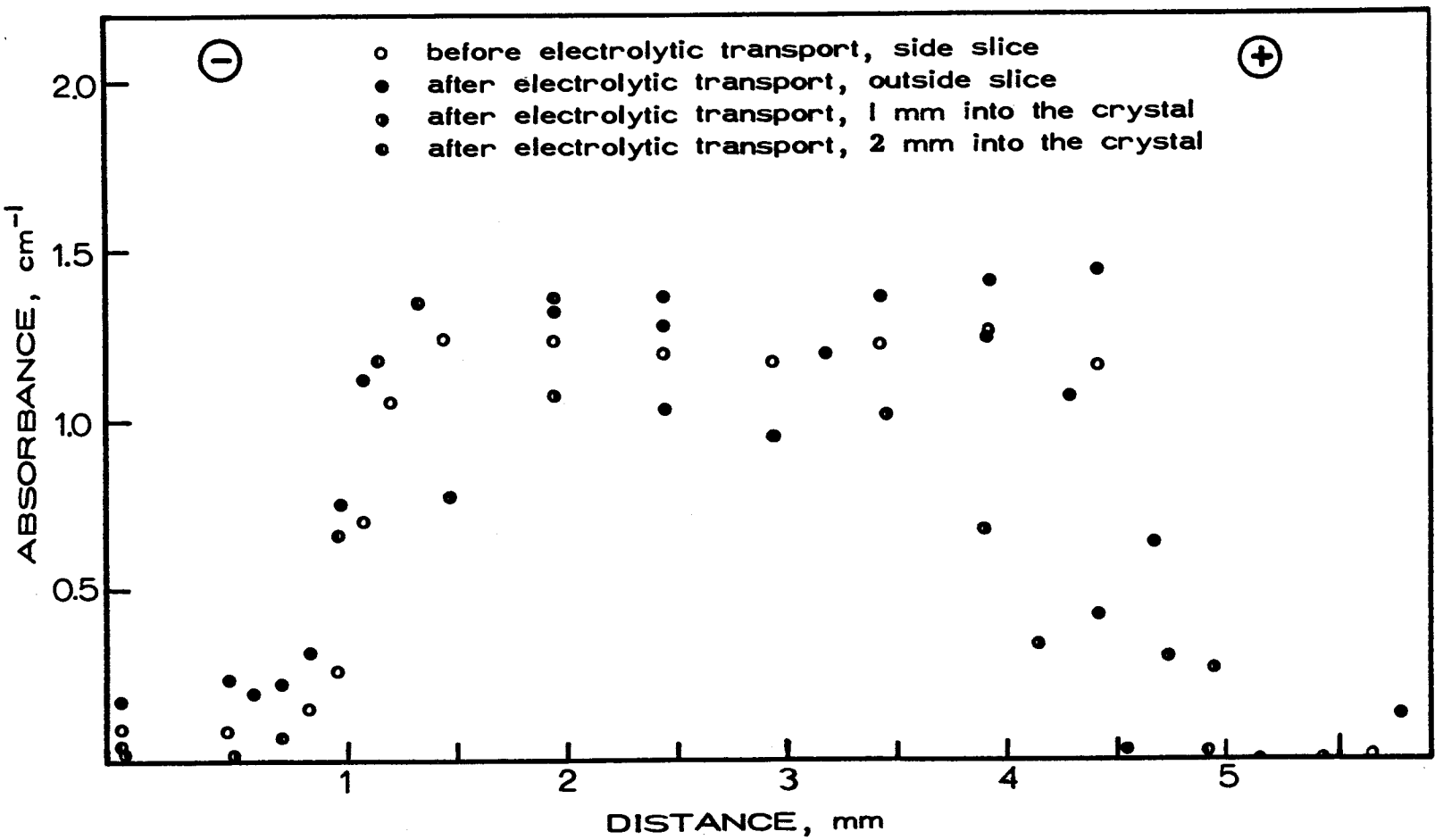

Fig. 5.17. Electrolytic transport profiles of crystal T-II. The variation in the profiles indicates that the current is not being carried across the entire cross-section of the crystal.

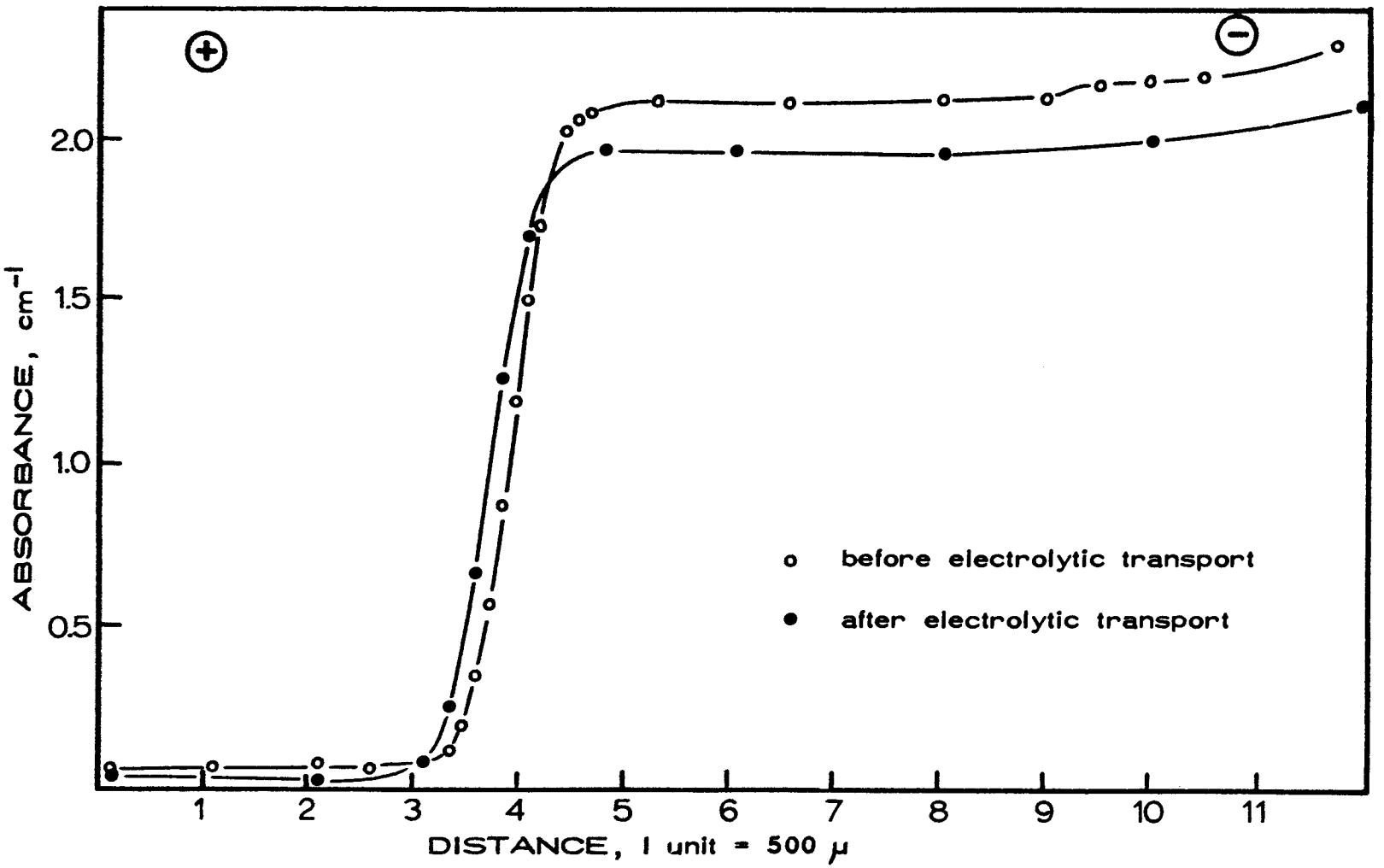

Fig. 5.18. Electrolytic transport profile of crystal T-12, section a. A comparison between figures 5.18, 5.19, and 5.20 indicates that the plane junction in a "dual" crystal was perpendicular to the direction of the electric field.

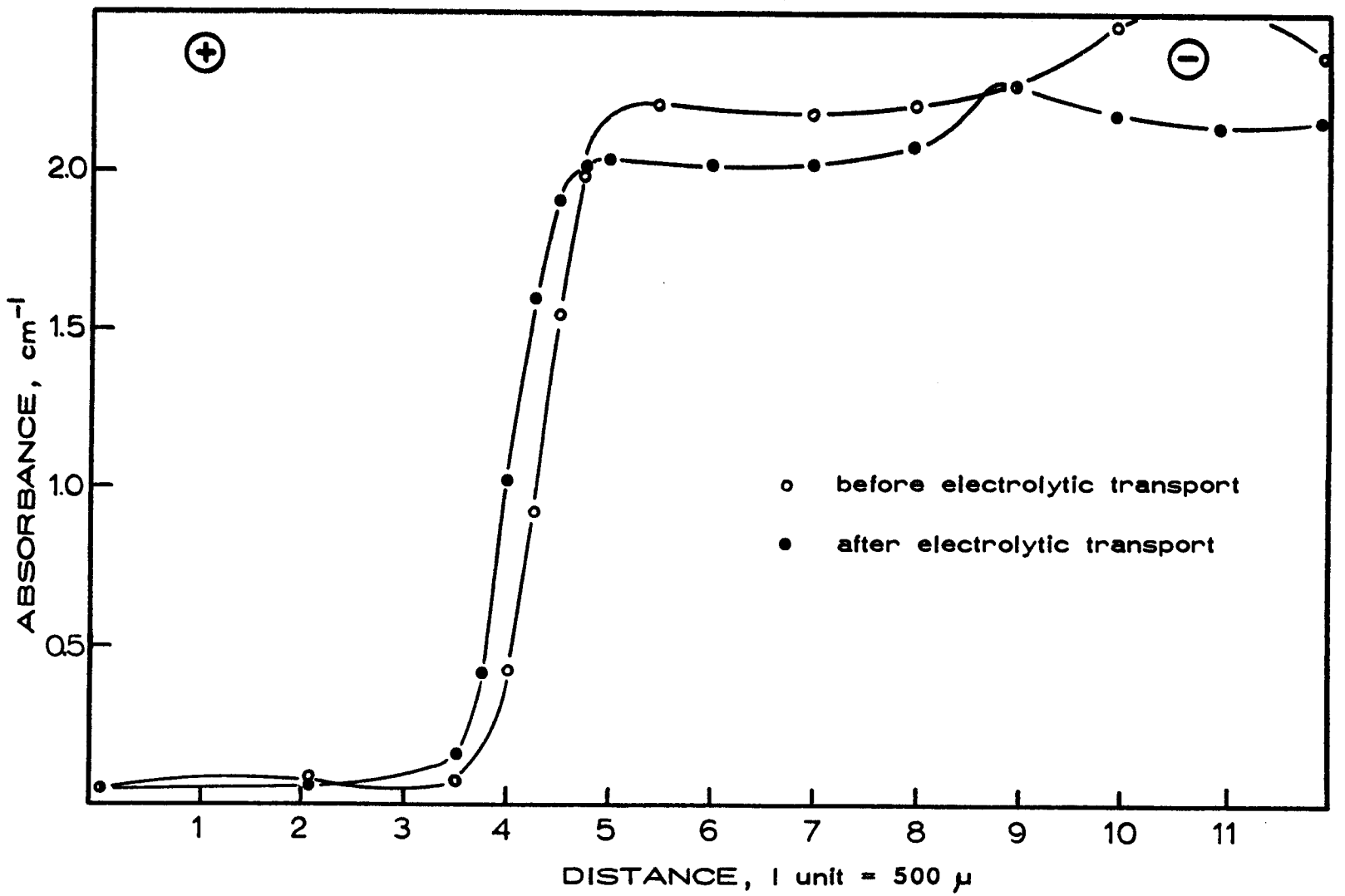

Figure 5.19. Electrolytic transport profile of crystal T-12, section b.

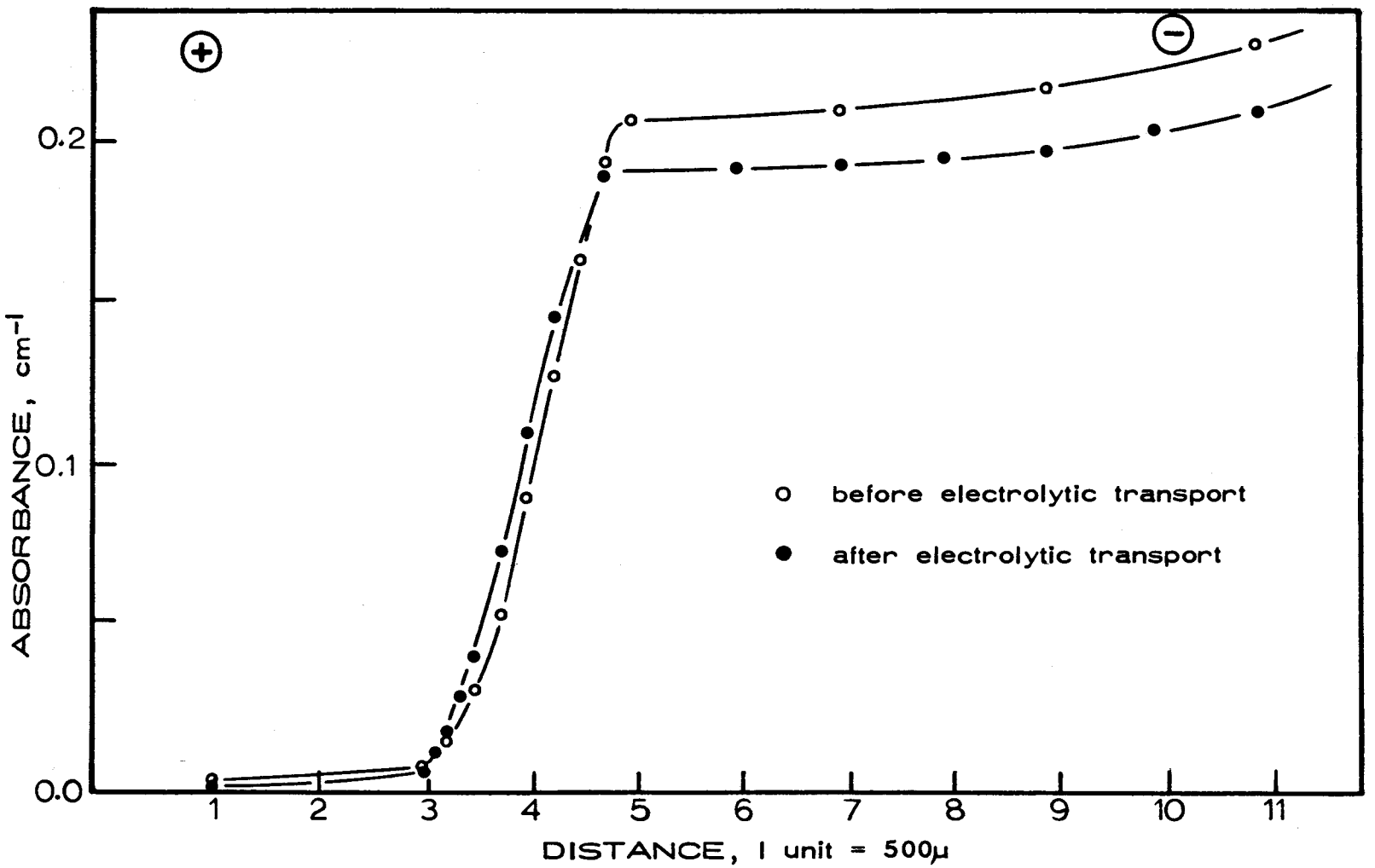

Figure 5.20. Electrolytic transport profile of crystal T-12, section c.

the profile is small, and a reliable measurement of the profile shift was not within the limits of the experimental method. Figure 5. 15 shows similar results derived from sample T-10. Figure 5. 16 demonstrated the scatter of data derived on one sample, T-11. Indexed sections of this crystal, cut parallel to the field direction, were scanned from the anode and the cathode contact surfaces and the results were compared. The data derived from scanning in one direction, say the anode to the cathode, are consistent within themselves before and after diffusion, but not with data derived from scanning in the opposite direction. For this reason, scanning data was taken consistently in one direction. Figure 5. 17 is an analysis of T-11 and shows the transport profiles of a series of slices cut parallel to the field. This figure demonstrates that the current in the crystal is not carried across the entire area of the electrode contacts but travels in definite paths. If transport was taking place across the entire cross section of the sample, these sections should have identical transport profiles. Imperfect contacts between the regions and at the electrode surfaces would produce a variation of this type in the profiles.

Figures 5. 18, 5. 19, and 5. 20 show the results of experiments on sample T-12. The crystal was cut parallel to the field into three sections, indexed and the absorption spectra recorded. The sections were realigned and subjected to transport. After cooling,

the sample was split on the original junctions and the absorption spectra of the sections recorded. Although diffusion distances were small, the results of each section were in accord with the other sections. This demonstrated that the plane of the integral-junction between the KCl and KCl:Pb regions was flat and perpendicular to the axis of the field, and that transport was taking place across the entire cross sectional area. The data from experiments T-3, T-5, T-8, and T-9 support the observation that Pb^{++} did not move significantly under the influence of an electric field. In simple diffusion experiments Pb^{++} definitely crossed the crystal junctions (or the integral junction in the "dual" crystal); in the presence of a field, additional movement was small and not detected within the limits of the experimental method.

Comparison with Results of Fredericks and Scott

Fredericks and Scott (27) observed lead ion to be transported toward the anode under the influence of an electric field. In addition, they did not observe simple diffusion across the junction in experiments without the field. Figure 5. 21 is a reproduction of a typical transport profile reported by these authors. The results were found by sectioning the crystal perpendicular to the field axis. The base of the transport profile in the anode region is about two mm from the original junction. The concentration of Pb^{++} in the KCl:Pb region

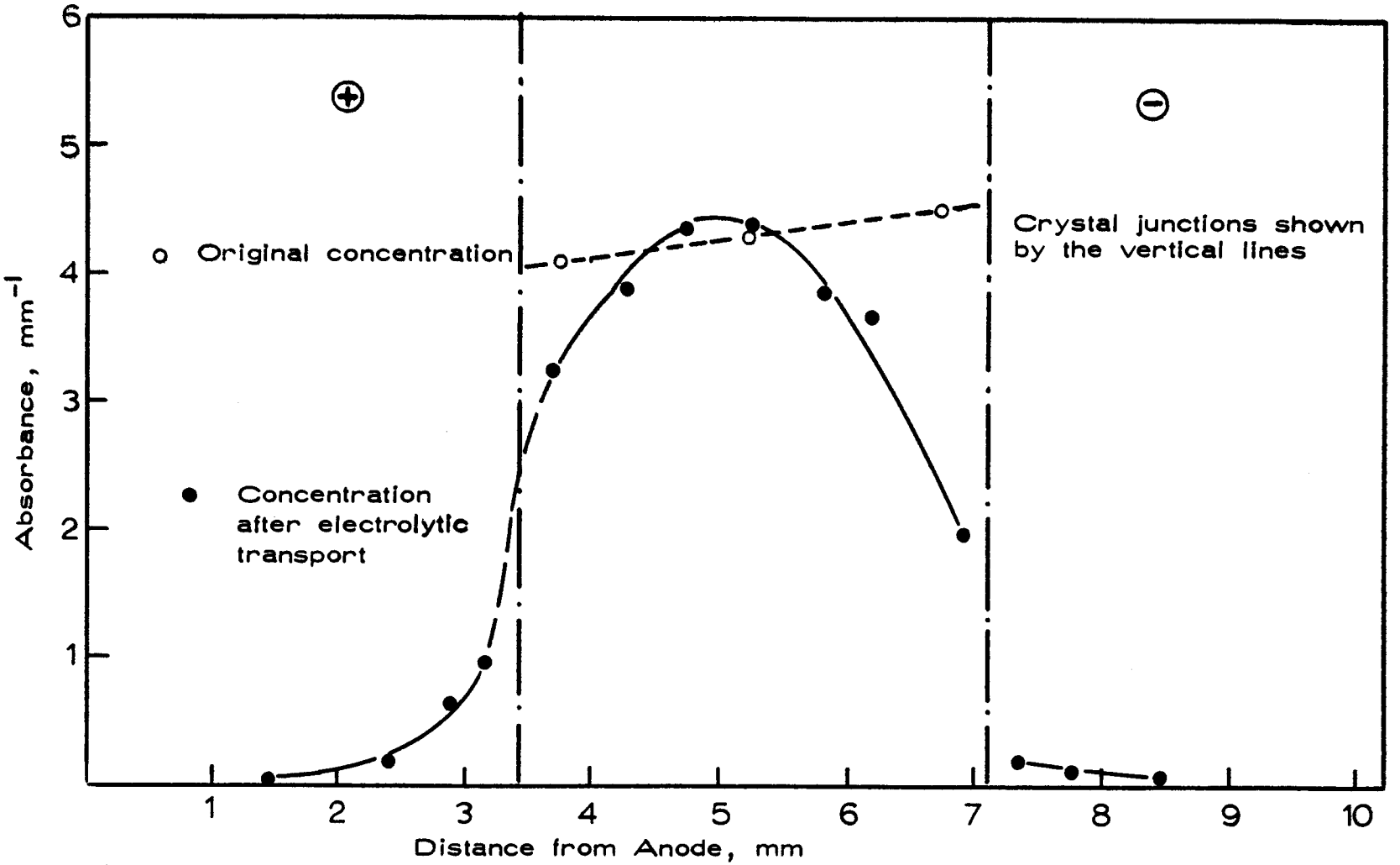

Fig. 5.21. Typical electrolytic transport profile after Fredericks and Scott (27).

near the junction with the cathode region has decreased by a factor of two. The transport distance in these samples were an order of magnitude greater than those found by the author. The distance that the lead ion moved toward the positive electrode in the author's samples were not significantly different from those of diffusion without a field.

The author proposes that some of the differences in the results is resolved by a consideration of the contact surfaces of the junction. Since only one side of the junction contained lead ion on the surface, the diffusing ion was required to cross this junction. If the contact surface was not flat and well aligned, evaporation of $PbCl_2$ was probable Lead ion will evaporate from the initial surfaceas $PbCl_2$, condense on the opposing face, and begin to diffuse into that surface. However, the $PbCl_2$ can condense on the original surface as well and the process of transfer across the junction will be inhibited. The author has studied the contact surfaces in junctions of the type used and found areas of intermittent contact. In addition, the $PbCl_2$ deposited on the surface of the pure region was found present in some cases as a species which did not contribute to the intensity of the A band. Only upon quenching to room temperature, after holding the sample at 600° C for 15 minutes, did the A band appear. In several samples, the A band intensity increased up to 150% of its original value. As suggested in Chapter IV, lead ion could be

entering the lattice at dislocation sites or positioning itself at the surfaces of mosaic boundaries. Clearly, lead ion does diffuse across the junction, but diffusion coefficients determined from this type of experiment would be erroneous, the error being caused by the discontinuity in the lattice. When no physical separation was present at the junction, as was the case with a "dual" crystal, junction effects were absent.

In some cases, the junction between the KCl:Pb and the cathode region was darkened in the author's crystals as well as those of Fredericks and Scott. Microscopic examination of the volume immediately surrounding the junction was undertaken. A black, finely-divided precipitate was present. The material, subjected to chemical investigation, proved to be elemental lead. The distribution of elemental lead was not uniform across the junction plane but showed its greatest intensity at points of complete contact. In areas where elemental lead was not observed, Pb^{++} was noted to have diffused into the cathode region. This is further evidence that the entire contact surface did not carry the observed current flow.

A sample not analyzed in the study by Fredericks and Scott was obtained for direct comparison. The transport profile for the crystal, F-T-6, is shown in Figure 5. 22. Analysis of this crystal confirmed the author's proposal that lead ion was reduced to elemental lead at the cathode junction. Microscopic observations indicated the

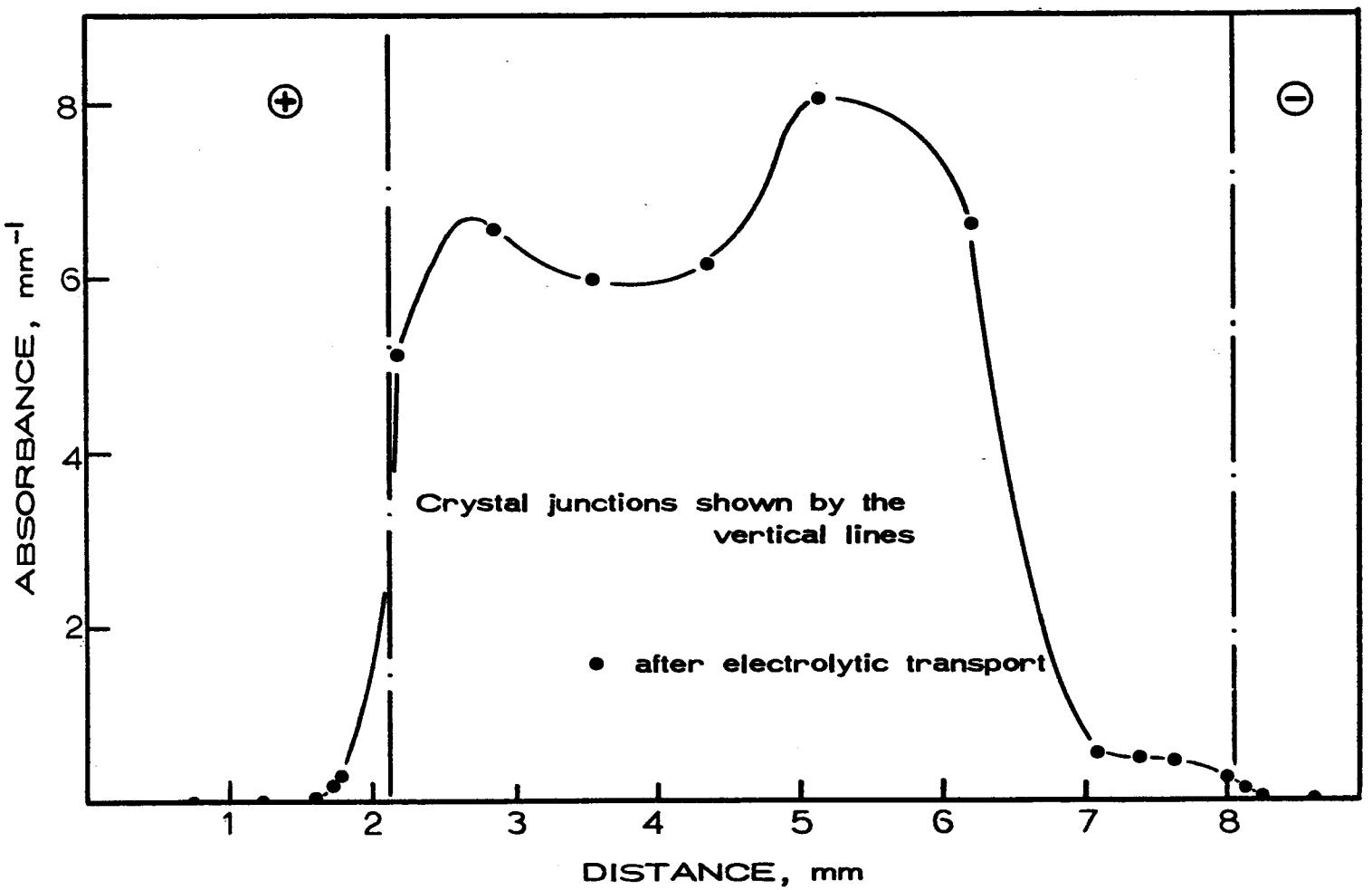

Figure 5.22. Electrolytic transport profile of crystal F-T-6.

presence of a large density of bubbles in the pure region near the anode crystal-KCl:Pb junction. These could be chlorine produced by electronic conduction in the crystal. It is puzzling, however, that they did not appear instead at the junction between the anode crystal and the electrode. The presence of these bubbles would augment diffusion into this region. An anomalous presence of lead ion was observed near the anode. Both Fredericks and Scott, and the author observed $PbCl_2$ evaporation during transport and it is possible that $PbCl_2$ could have condensed near the anode and diffused back into the sample. This phenomenon also occurred in two of the author's samples. For comparison, Figures 5. 23 and 5. 24 show the transport profiles for two of the author's samples T-15 and T-16 treated and analyzed under conditions similar to F-T-6. Limited data was available on the author's samples because of the small transport distances observed. The profiles of T-15, T-16, and F-T-6 are similar, as are the transport distances. Some variation in transport distance was expected since the author's crystals were not identical to those used in F-T-6. In these samples an apparent shift toward the anode was observed because of the reduction of lead ion at the junction between the KCl:Pb and cathode crystal regions.

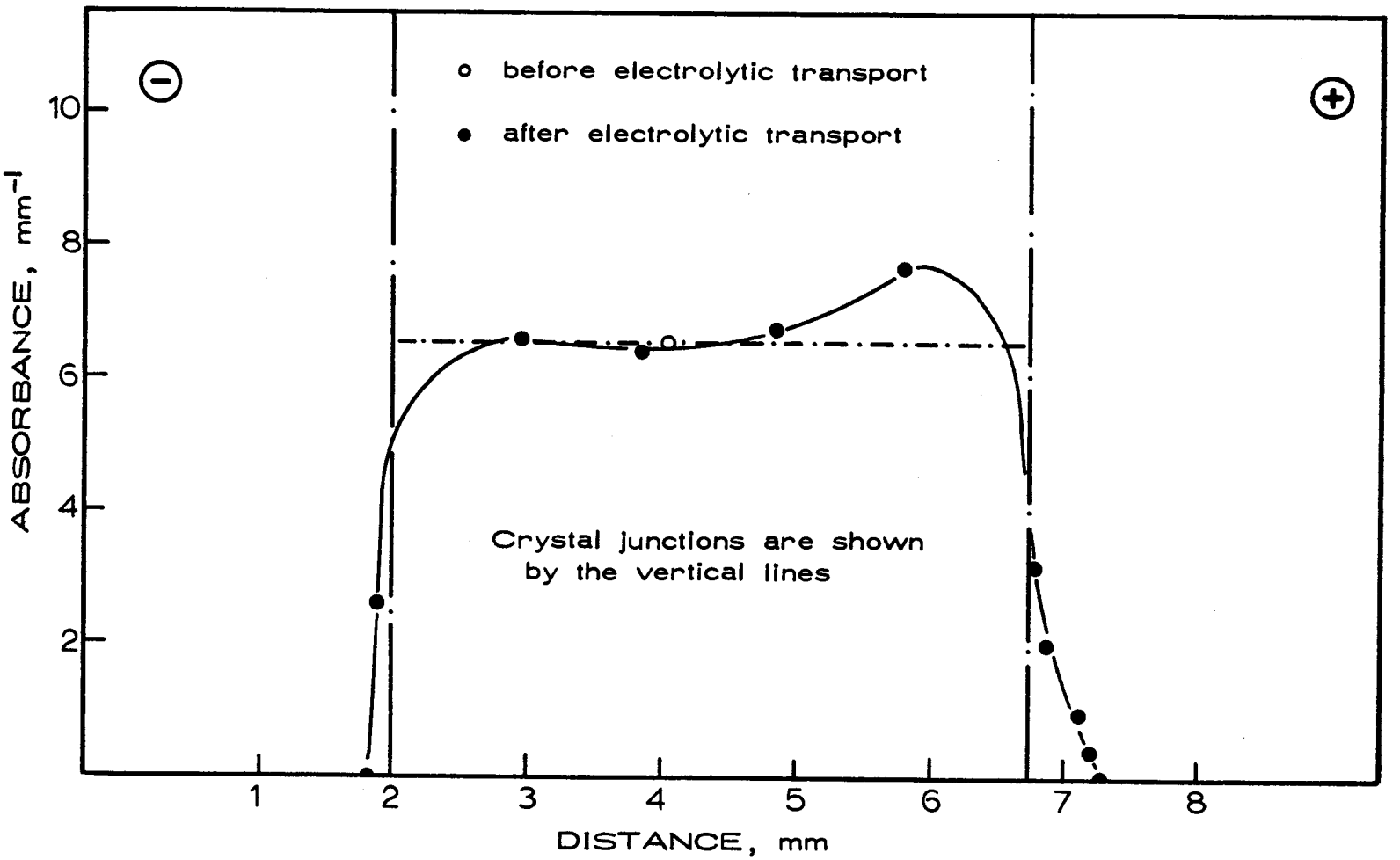

Figure 5.23. Electrolytic transport profile of crystal T-15. The broken horizontal line represents the original concentration of the center (KCl:Pb) region.

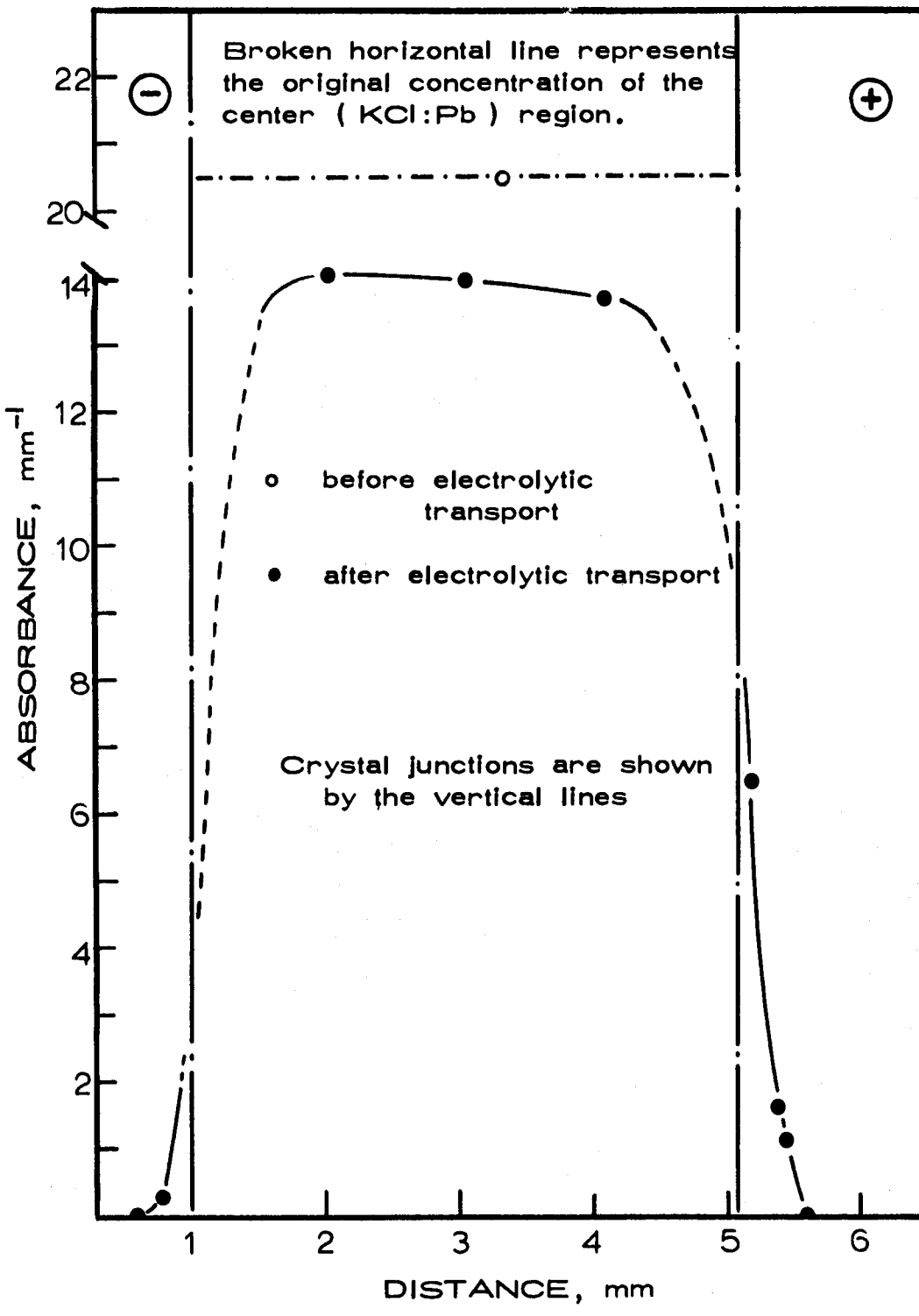

Fig. 5.24. Electrolytic transport profile of crystal T-16.

Migration of Pb^{++} in KCl:Pb, Ca

The author attempted to determine the mobility and effective charge on the migrating species by studying the migration of lead ion in crystals of sufficient impurity that the amount of $PbCl_2$ added to the center region did not significantly change the conductivity of that region nor that of the pure end crystals as the lead ion diffused. This method would establish a linear potential drop across the crystal stack. This condition was established by producing crystals containing Ca^{++} throughout and $PbCl_2$ in the center region. These were crystals T-13 and T-15. Electrolytic transport studies in these crystals failed due to the complete coloration of the crystal stack (red-violet or brown) and reduction of Pb^{++} to elemental lead.

Results paralleling those of the author have been observed in NaCl:Ca. Banasevich, Luré, and Murin (2) determined the effective charge on Ca^{++} at 650° C and 700° C to be close to 4×10^{-2} e, a very small fraction of the charge on a free calcium ion 2e. They studied migration from a plane source and found that in some samples the original boundary between the two sections had shifted as much as 200 μ. At 600° C the total shift in the profile was of the same order of magnitude. The authors gave no reason or reference position for this shift. Severe deformity of the profiles was observed at high temperatures and high fields, as well as coloration of the crystals.

In these experiments the calcium ion has a small effective charge and must be migrating as $Ca^{++}\boxplus\boxplus$, $CaCl_2$, or $Ca^{+}\boxplus Cl^{-}$.

Mobility and Effective Charge of Pb^{++} in KCl

The mobility of the lead ion is calculated from

$$u = \frac{x}{Et}$$

where x is the migration distance under a field E for a time t.

One of the chief problems associated with the calculation of the mobility involves the lack of precise knowledge of the electric field acting upon the migrating ions. It was known (see Chapter VI) that the higher conductivity of the KCl:Pb region produced a lower field there than that in the pure KCl regions. A small increase in the current during the electrolytic transport experiments indicated a decrease in overall stack resistance as lead ion diffused into the pure regions. The potential across the stack remained constant, but the field acting on the lead ions was lower than the value determined from the potential and the stack length. The effective field acting on the lead ions crossing the junctions between the pure and doped regions will be the field determined by the conductivity of the pure crystals, that determined by the conductivity of the KCl:Pb region, or an intermediate value. The initial field in any of the three regions can be calculated from the conductivity of the region.

The conductivity of the KCl:Pb region, however, is not well correlated to the concentration of lead ion present in the crystal. Thus, the field in this region is determined with less precision than that in the pure KCl regions. In migration from a plane source, the KCl:Pb region is infinitely thin and the field is initially determined by the conductivity of the two pure KCl crystal regions. In migration from an extended source the ratio of the conductivities at 560° C of the KCl and KCl:Pb regions is given by

$$\frac{\sigma_{KCl}}{\sigma_{KCl:Pb}} = \frac{6.8 \times 10^{-7} (\text{ohm cm})^{-1}}{3.9 \times 10^{-6} (\text{ohm cm})^{-1}} = 1.7 \times 10^{-1}$$

A ratio of the fields in these regions is given by

$$\frac{E_{KCl}}{E_{KCl:Pb}} = \frac{47 \text{ volts/cm}}{0.1 \text{ volts/cm}} = 4.7 \times 10^{2}$$

The conductivity and field of the KCl:Pb region are concentration (lead concentration) dependent and the values given are for 6×10^{-3} mole percent Pb. Ratios of this type are typical of those observed.

Both migration from a plane source and from an extended source were used to estimate the mobility. The distance of migration was that observed in the anode region. Distances observed in the cathode region were not used because of the reduction of lead that took place near the KCl:Pb-cathode crystal junction. The migration distances observed in the anode region were less than the sensitivity of the experimental method. It is estimated that no consistent shift in the

profile, either +uEt or -uEt, less than 100 μ could be observed. Any profile shift due to electrolytic migration must have been less than 100 μ. Based on the minimum detectable profile shift, 100 μ, an assumed field of 10 volts/cm, and transport time of 2200 minutes, the mobility of lead ion at 560° ± 15° C was found to be 8×10^{-9} cm^2/volt sec.

The effective charge can be estimated from

$$\frac{\mu}{D} = \frac{(ze)_{effective}}{kT} \tag{5.18}$$

if the diffusion constant is known. As pointed out earlier in this chapter, diffusion constants were not determined from the experimental data. The values of the diffusion constants found by Keneshea and Fredericks (44) were used to determine the effective charge on the migrating species. They found that the diffusion of lead ion into KCl was described by

$$D_{c \to o} = 1.02 \times 10^{-3} \exp\left(\frac{23,300}{RT}\right)$$

The diffusion constant is calculated to be 1×10^{-9} cm^2/ sec in the temperature range mentioned. It was assumed that the value for concentration approaching zero, the value used, approximates the experimental conditions. It was known (44) that the diffusion constant increases with lead ion concentration. The value found at high concentrations is about ten times that of $D_{c \to o}$. Use of the high concentration value would decrease the effective charge by a factor of ten.

Using equation (5. 18) the effective charge is found to be 0. 6 e.

There are several factors which can explain the deviation from the value of 2 e, the charge of the Pb^{++} ion. The equation as applied here does not include the necessary corrections for correlation effects which were discussed earlier. These corrections would be within a factor of 1. 5 and were not considered significant for this calculation. The association of the lead ion with vacancies or chloride ions produces the observed effective charge. Since the migration distance was small and the direction of migration was not known, the associated complex could be neutral, positive, or negative in charge. No attempt is made to suggest the particular migration species because of the limitations imposed by the estimates in the calculation of the effective charge. A particular species could be prevalent, its probability of dissociation producing the effective charge. Some likely complexes may be $Pb^{++}\boxplus\boxplus$, $PbCl^{+}$, $PbCl_2$, and $Pb^{++}\boxplus Cl^{-}$, which may exist in some equilibrium. Additional complexes with a net negative effective charge are also possible. These would be complexes like $PbCl_3^{-}$, $Pb^{++}\boxplus\boxplus\boxplus$, $Pb^{++}\boxplus\boxplus Cl^{-}$, and the like.

VI IONIC CONDUCTIVITY

Introduction

As late as 1930, the subject of ionic conductivity in crystals was still in a descriptive stage. Lehfeldt (54) was one of the early investigators in the field and studied the conductivity of various alkali halides. He established the validity of Ohm's Law in several materials for various field strengths and temperatures. Among the materials he studied was KCl containing known amounts of added $PbCl_2$.

The conductivity observed in ionic solids is much smaller than that of metals. However, in both cases it can be described by Ohm's Law. The mechanism of conduction in metals is different from that in ionic conductors. In metals, the electrons are the current carriers, while in ionic solids, the carriers are the ion themselves. Whereas a classical picture of a perfect crystalline lattice does not permit motion of the ions themselves, the presence of point defects in an ionic solid does allow for the movement of ions. Frenkel (28) and Schottky (92) have proposed well known models which carry their names. The model proposed by Schottky is one in which an equal number of positive and negative ions migrate to the surface of the crystal, leaving behind an equal number of positive and negative

ion vacancies. On the basis of the latter model, ionic conductivity involves the migration of vacancies under the influence of an electric field. Mott and Littleton (72) have shown that the majority of point defects in KCl are of the Schottky type.

If the current carriers are the ions themselves, then it is important to know the amount of current carried by each species. Transference numbers give this type of data. We can write

$$t_+ = \frac{\sigma_+}{\sigma} \quad \text{and} \quad t_- = \frac{\sigma_-}{\sigma}$$

where t_+ and t_-, and σ_+ and σ_- are the transference numbers and conductivities of the respective carriers. The total conductivity is then

$$\sigma = n_+ e_+ \mu_+ + n_- e_- \mu_-$$

where n is the concentration of carriers, e their charge, and μ their mobility. The subscripts indicate anionic or cationic character of the carrier.

In KCl it has been observed (103, 45) that the predominant carrier up to about 550°C is the cation. Anion conduction is not significant in dopted KCl crystals until even higher temperatures. KCl:Ca, for example, is primarily a cation conductor until 600°C and KCl:Pb should show the same behavior. If we assume that the cations are the primary carriers in KCl:Pb, then the conductivity is given by

$$\sigma = n_+ e\mu_+$$

The observed conductivity rises rapidly with temperature; a typical curve of log σ versus $\frac{1}{T}$ is given in Figure 6. 1.[5]

Theory

The following expression for the conductivity in KCl is expected if the conductivity depends on the number of carriers and their mobility,

$$\sigma = A \exp\left(\frac{-E}{kT}\right) \exp\left(\frac{-U}{kT}\right)$$

where A is a constant, E the energy of formation of a pair of Schottky defects, U the activation energy for mobility, k the Boltzmann constant, and T the absolute temperature. A plot of log σ versus $\frac{1}{T}$ should give a straight line. However, Figure 6. 1 has shown that two straight lines of different slopes are observed. The upper part of the curve is characteristic of the alkali halide, while the lower depends on the history and purity of the sample.

Smekal (95) suggested that the conductivity in each portion of the curve could be described by a "different" mechanism and proposed the formula

$$\sigma = A_1 \exp\left(\frac{-E_1}{kT}\right) + A_2 \exp\left(\frac{-E_2}{kT}\right) \qquad (6.1)$$

---

[5]The plot generally used. log σT versus $1/T$ is more rigorously correct. See, for example, Lidiard (57).

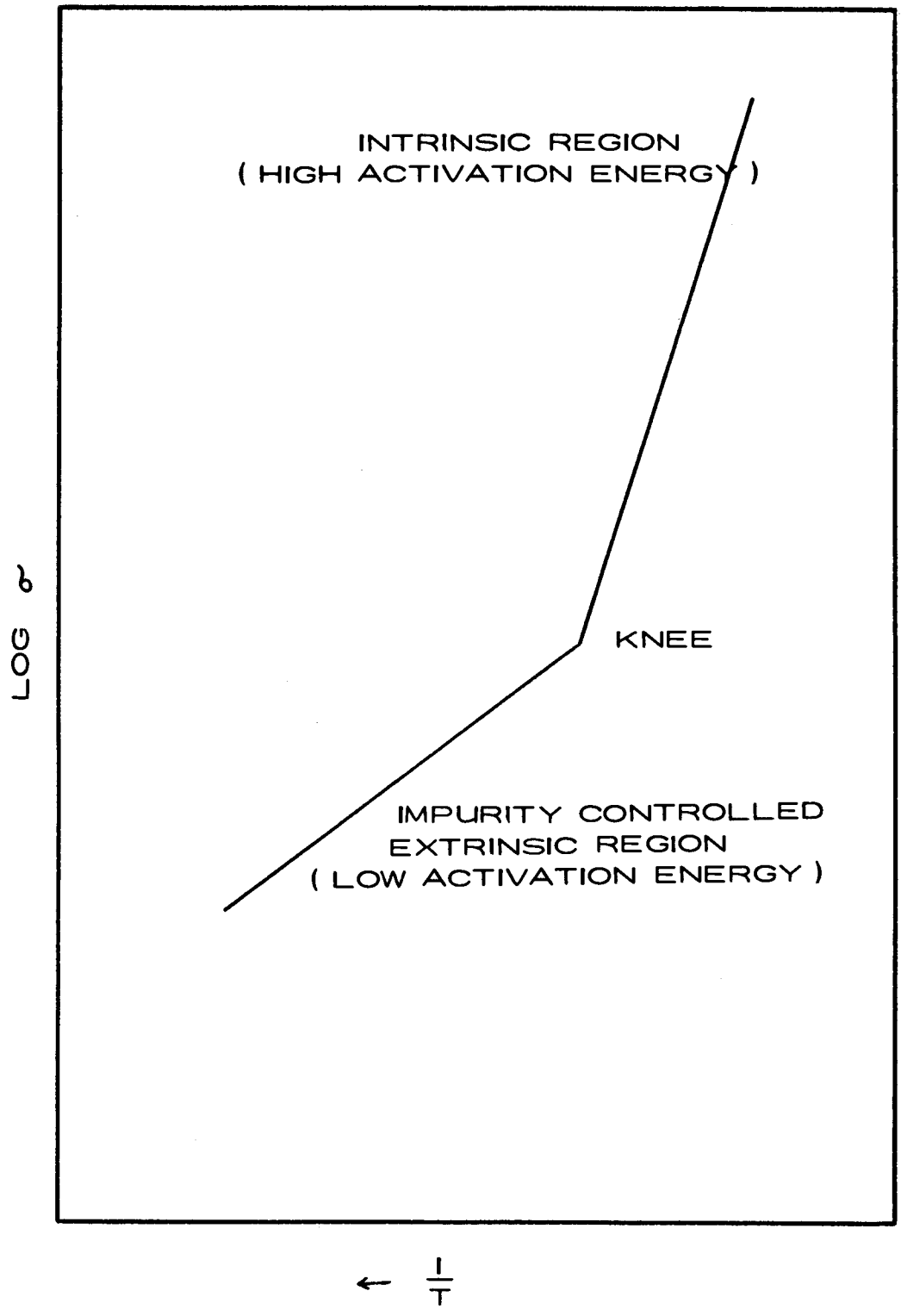

FIGURE 6.1 . TYPICAL CONDUCTIVITY CURVE OF AN IONIC CRYSTAL CONTAINING IMPURITIES.

where A_1 and A_2 are constants and E_1 and E_2 the activation energies for the conduction mechanisms at the high and low temperatures, respectively. Although the mechanisms proposed in Smekal's original interpretation have been modified, equation (6. 1) is still used to describe conductivity. The interpretation followed currently by most investigators is that at high temperatures, the conductivity observed is that characteristic of the pure alkali halide, while at low temperatures impurity effects give rise to the observed curve. Any impurity which can enhance the conductivity mechanism will produce a noticeable effect on the conductivity.

As has been discussed earlier, various mechanisms of diffusion and conduction are possible. Since the primary defects in KCl are of the Schottky type, ionic conductivity in this material can be described by the migration of vacancies. The number of vacancies present in a crystal is a function of the thermal energy and the concentration of aliovalent impurities. At any temperature, the equilibrium concentration of thermally created vacancies is given by the Boltzmann formula. With the addition of small amounts of divalent impurity cations to the crystal, the number of cation vacancies can be increased. If the divalent cation enters the lattice substitutionally, an extra chloride ion must enter and interstitial position or a potassium ion vacancy must be formed, in order to preserve charge neutrality. The latter is found to be energetically more favorable.

The cation vacancies introduced by doping can be less, equal to, or greater than the number of thermally produced vacancies. At high temperatures, sufficient thermal energy is present to produce vacancies in a concentration greater than those created by doping. The observed activation energy is then the energy required to form a vacancy plus that required for the motion of an ion into a vacancy. At low temperatures, the number of cation vacancies created by doping is dominant and the activation energy is that due to the migration of ions into vacancies which are already present in the lattice. This interpretation gives different activation energies for the extrinsic and intrinsic regions. A greater slope is predicted for the intrinsic region, since the energy of activation is a combination of the energy of vacancy formation and the activation energy for motion of the ions into the vacancies. Experimental evidence supports the theories outlined.

This discussion of conductivity has been limited to KCl and at best is but a brief outline. The reader is referred to comprehensive review articles such as the one by Lidiard (57) for a more complete treatment of the subject.

Apparatus

Direct current conductivity measurements were made on KCl and KCl:Pb single crystals with a Keithley Model 610A Electrometer.

A Keithley Model 241 Regulated High Voltage Power Supply provided 1-1000 volts DC for the measurements. The conductivity cell was designed by R. Seevers in our laboratory and is shown in the schematic in Figure 6.2. The spring loaded upper electrode maintained constant contact of the electrodes on the sample, while a guard ring concentric with the electrodes was used to eliminate the effects of surface conductivity and establish a more uniform field across the sample.

Experimental

Single crystal sections were cut to a nominal size of 5/8" by 3/4" by 1/32" and their ultraviolet absorption spectra recorded. The sections were cut so that the major plane surface had been perpendicular to the growth axis of the original crystal. These samples had a uniform concentration of lead ion across their surface and only a small variation in concentration through their thickness. If the lead concentration was high, thin sections immediately adjacent to the sample were used for spectrophotometric data. The concentration of these sections were assumed the same as that of the sample. The sample thickness was measured in three places with a micrometer.

A gold film was evaporated under vacuum onto the surfaces of the sample to provide contact between the crystal and the rhodium-plated rods used as electrodes. A circular-ring mask placed on one

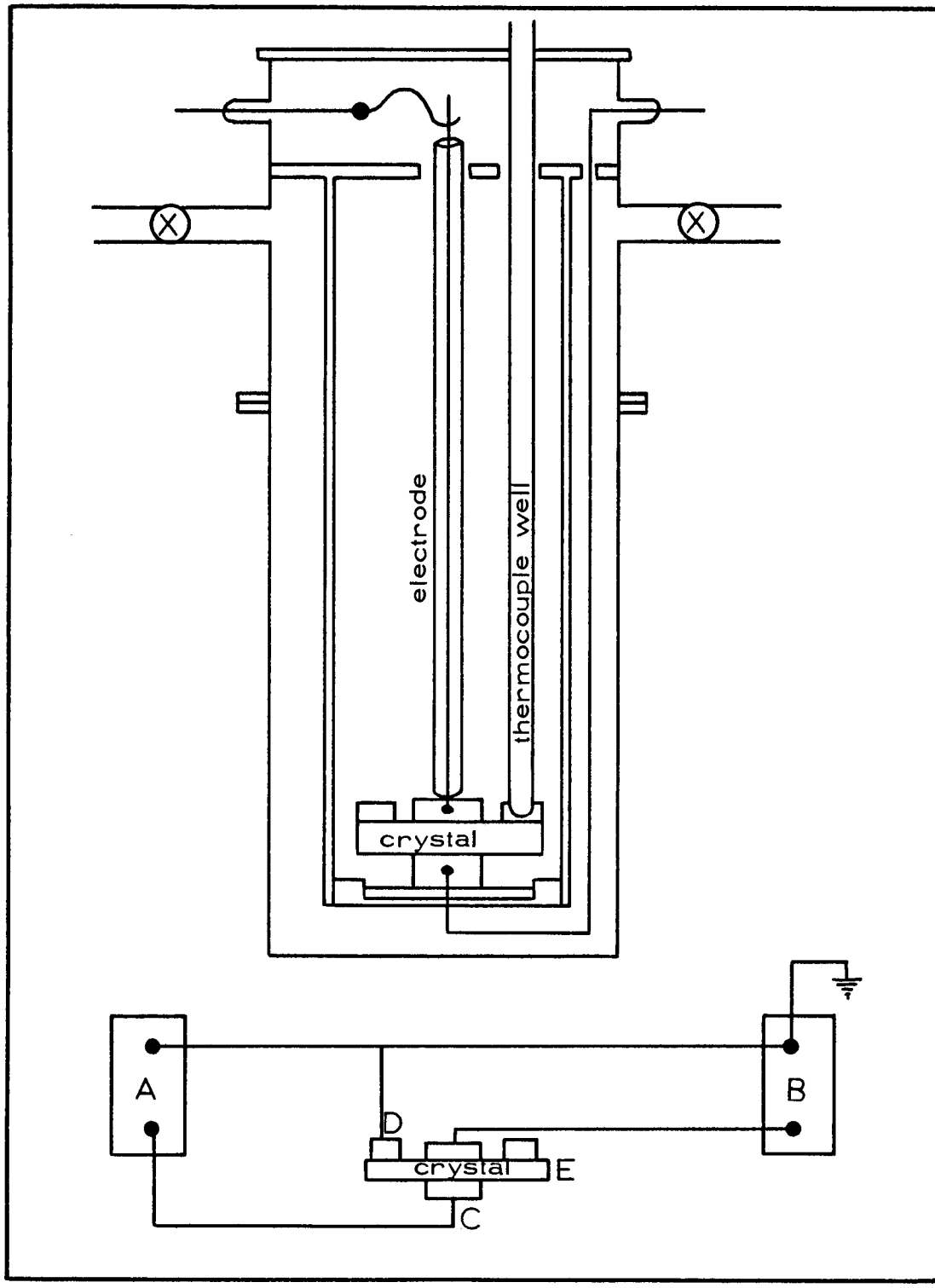

Fig. 6.2. Conductivity cell and electrical circuit. A, power supply; B, electrometer; C, electrodes; D, guard ring; E, crystal sample.

surface of the sample produced two separate plated areas as shown below:

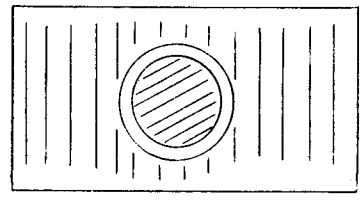

The inner area was an electrode contact; the outer area was the guard ring contact. A value of 0.495 cm^2 for the inner ring area was used to calculate the specific conductivity of the sample. The reverse side of the sample was entirely plated and the edges were cleaved off to remove any plating connecting the two surfaces.

The sample was mounted in the cell and an argon atmosphere established in a manner analogous to that described for transport studies. A potential was placed across the sample and maintained only while the current was being measured. A potential of 1000 volts was required near room temperature, but was decreased to 1 volt at the highest temperatures. At about 100° C the ohmicity of the contacts was checked by varying the potential across the sample. The temperature of the sample to ± 3° C was measured with a thermocouple mounted within the guard ring. The furnace controller was advanced 50° C, the system allowed to establish equilibrium for 50 minutes, and the procedure repeated. Measurements of the conductivity were made from 25° C to 700° C. In some cases,

the current at room temperature was below the sensitivity of the electrometer and conductivity values were not obtained until the temperature became about 150° C.

Results and Discussion

Pure KCl Crystals

The specific conductivities as a function of temperature were determined for four pure KCl crystals. Table 6. 1 gives the background of each sample, the knee temperature and the conductivity at 550° C. A portion of the conductivity curves are given in Figure 6. 3. Although measurements were made over a wider range of temperatures, only the knee region is shown in the figures. An extrapolation of the curves gives a good representation of the data not shown on the graph. For comparison the data of Lehfeldt (54) and Gruzensky (36, p. 86-87) are included with the author's data.

Provided ionic conductivity can be considered as a criterion for the absence of polyvalent cations in these crystals, there is an improvement in purity in the crystals produced in the last few years. Estimates of the polyvalent impurity cation content can be made from conductivity data, but the results can be in error. If polyvalent anions are incorporated into the lattice simultaneously with the cations, compensation takes place and the data is no longer a criterion for

Table 6.1 Conductivity and methods of preparation of pure KCl.

Crystal	Starting material	Growth atmosphere	Growth crucible	σ at 550°C, ohm^{-1} cm^{-1}	"Knee" temperature, °C
1	ion exchange purified	argon	quartz	5.1×10^{-7}	364
2	ion exchange purified*	argon	quartz	5.0×10^{-7}	372
3	Harshaw, 1964	air	platinum	6.0×10^{-7}	401
4	Anderson Physical Laboratories	HCl, argon	quartz	5.9×10^{-7}	400
Gruzensky-1	doubly recrystallized	air	graphite	1.5×10^{-6}	527
Gruzensky-2	Harshaw, 1958	air	platinum	4.4×10^{-7}	512
Gruzensky-3	reagent	air	graphite	4.2×10^{-7}	442
Lehfeldt	reagent	air	porcelain	2×10^{-6}	620

* pure region of a "dual" crystal

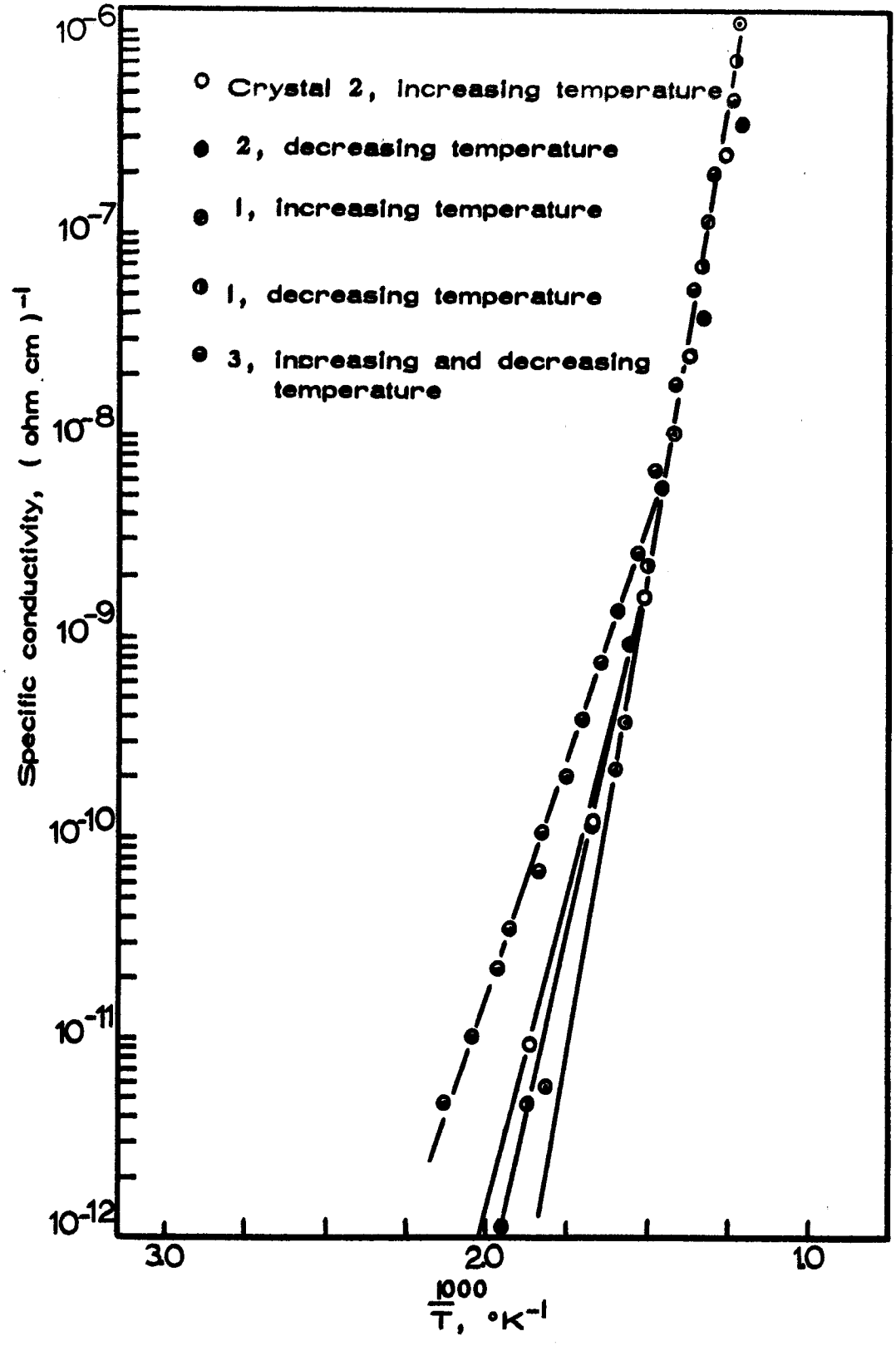

Fig. 6.3. Specific conductivity of KCl crystals.

crystal purity. Moreover, reaction products of divalent cations with O_2 or OH^- can produce species which do not contribute to the conductivity. In any case, the data determined are useful in assessing the conductivity of the pure KCl regions used in the transport studies.

The intrinsic and extrinsic portion of the conductivity plots were linear and the knee well defined. Smekal's equation was used to calculate the activation energies in each region of the curve. The second term in equation (6. 1) was neglected in the intrinsic region and the first in the extrinsic region. Values for E_1 are given in Table 6. 2. For comparison, this table also included the values determined by other authors.

Table 6. 2 Activation energies in the intrinsic region of conductivity.

Sample or Investigator	E_1, eV
1	1. 89
2	1. 62
3	1. 67
4	1. 67
Dreyfus and Nowick (19)	1. 95
Lehfeldt	2. 06
Gruzensky-1	2. 06
Gruzensky-2	1. 68
Gruzensky-3	1. 58
Phipps and Partridge (81)	2. 02

The lowest knee value obtained was for crystal 1. This crystal was grown in an argon atmosphere from salt purified by ion exchange. Crystal 2 demonstrated that a "dual" crystal could be grown without the contamination of the pure region. The conductivity of these pure crystals at temperatures below the knee was comparable to values obtained for ten-pass zone refined material, but higher than that of 10-50 pass zone refined salt (35). It was also comparable to the values found by the originators of the ion exchange purification method (26, p. 12).

Lead Doped Crystals

The specific conductivities as a function of temperature were determined for seven KCl:Pb crystals. Table 6. 3 gives the conductivity, the methods of preparation, and the concentration of each sample. The data of Lehfeldt on KCl:Pb is included for comparison. Figures 6. 4 through 6. 8 are the conductivity curves found. In most figures the increasing and decreasing temperature curves and the extrapolated intrinsic curve are given. Figure 6. 7 presents the data of four different KCl:Pb samples. In a comparison of all samples, no exact relationship between the conductivity or the knee temperature and the actual concentration of the lead in the crystal was found. Figure 6. 8 is a comparison of sample 11 with the curves observed by Lehfeldt. It is interesting to note that Lehfeldt found

Table 6.3 Conductivity, concentration, and methods of preparation of KCl:Pb crystals.

Crystal	Starting material	Concentration of Pb^{++}, mole %: Initial	Concentration of Pb^{++}, mole %: Final	σ at 550°C, $ohm^{-1}\ cm^{-1}$	"Knee" temperature, °C
6 +	doubly recrystallized	4.93×10^{-3}	0	7.0×10^{-7}	560
7 +	reagent grade	2.57×10^{-4}	2.72×10^{-3}	2.9×10^{-6}	620 x
8	ion exchange purified	6.56×10^{-3}	6.92×10^{-3}	4.0×10^{-6}	670
9	"	1.14×10^{-2}	9.54×10^{-3}	1.2×10^{-5}	600 x
10	"	7.26×10^{-3}	7.33×10^{-3}	2.2×10^{-6}	627
11	"	3.06×10^{-3}	5.89×10^{-5}	1.8×10^{-6}	577 x
12	"	3.2×10^{-3}*	3.06×10^{-3}*	1.4×10^{-5}	727
Lehfeldt +	reagent	4×10^{-2} (melt composition)		3×10^{-6}	690
Lehfeldt +	"	7×10^{-2} (melt composition)		8×10^{-6}	690

+ crystals grown from platinum in air; all others grown from quartz in argon or HCl-argon

* contains Ca^{++}

x crossed intrinsic curve

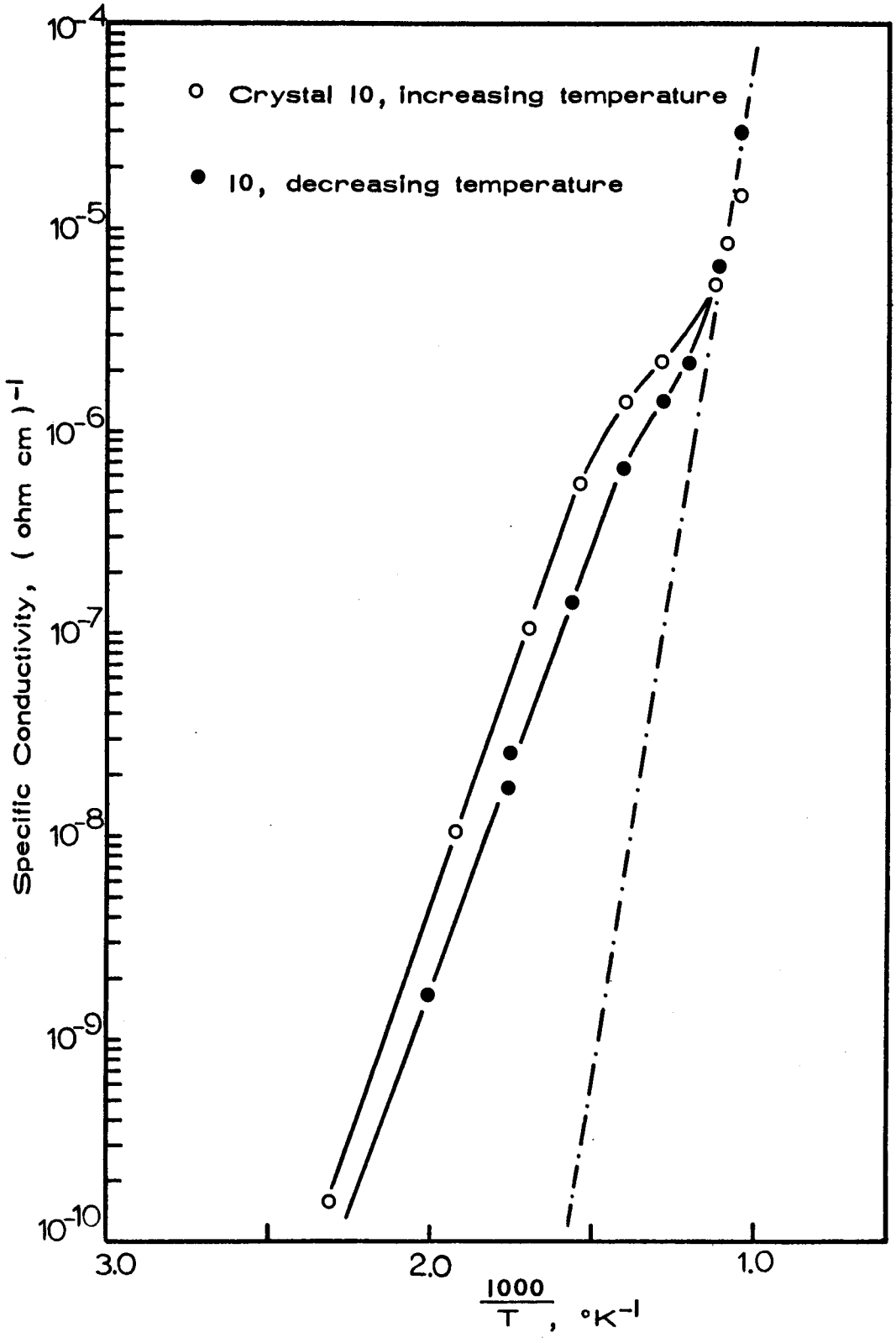

Fig. 6.4. Specific conductivity of KCl:Pb crystal 10.

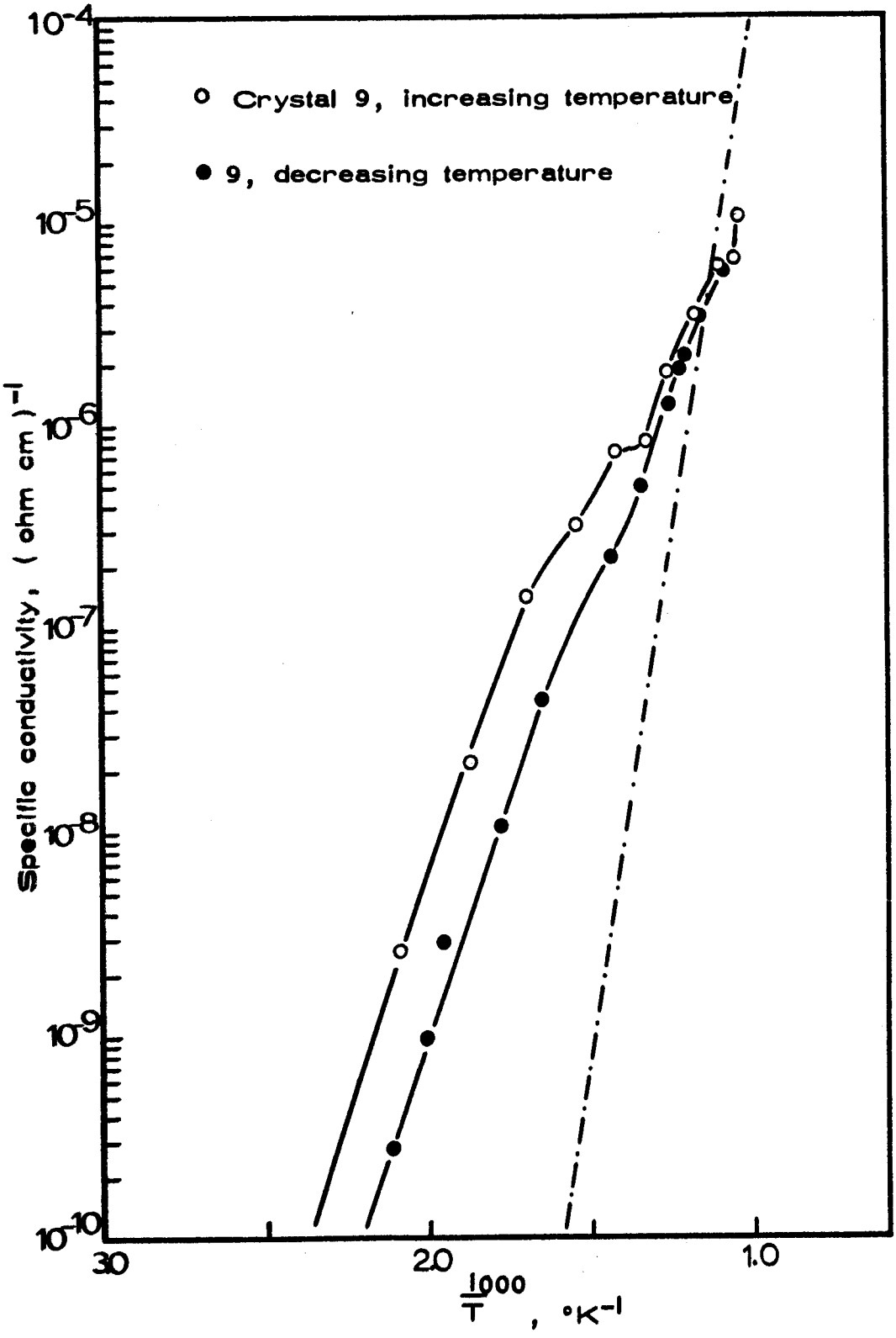

Fig. 6.5. Specific conductivity of KCl:Pb crystal 9.

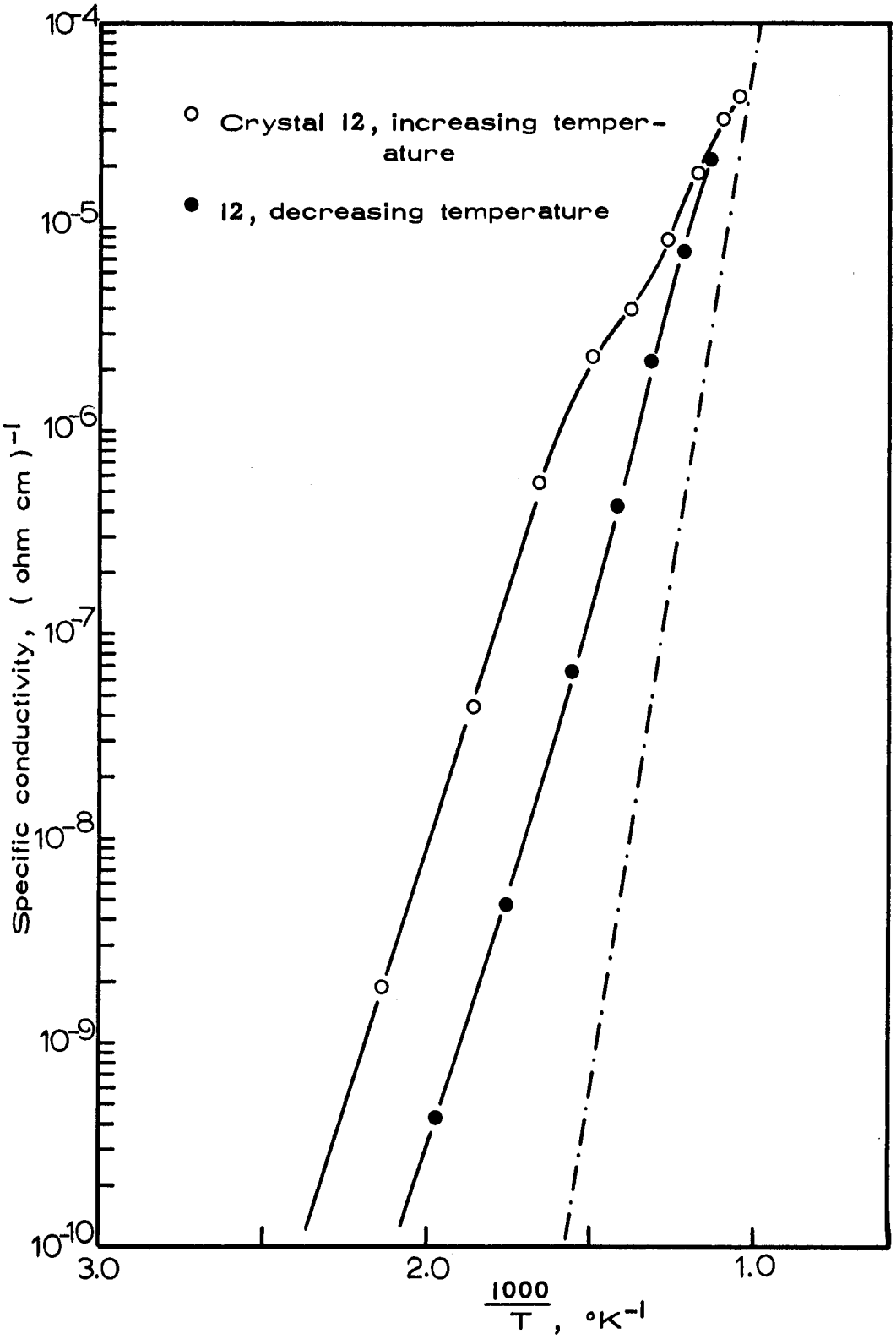

Fig. 6.6. Specific conductivity of KCl:Pb crystal 12.

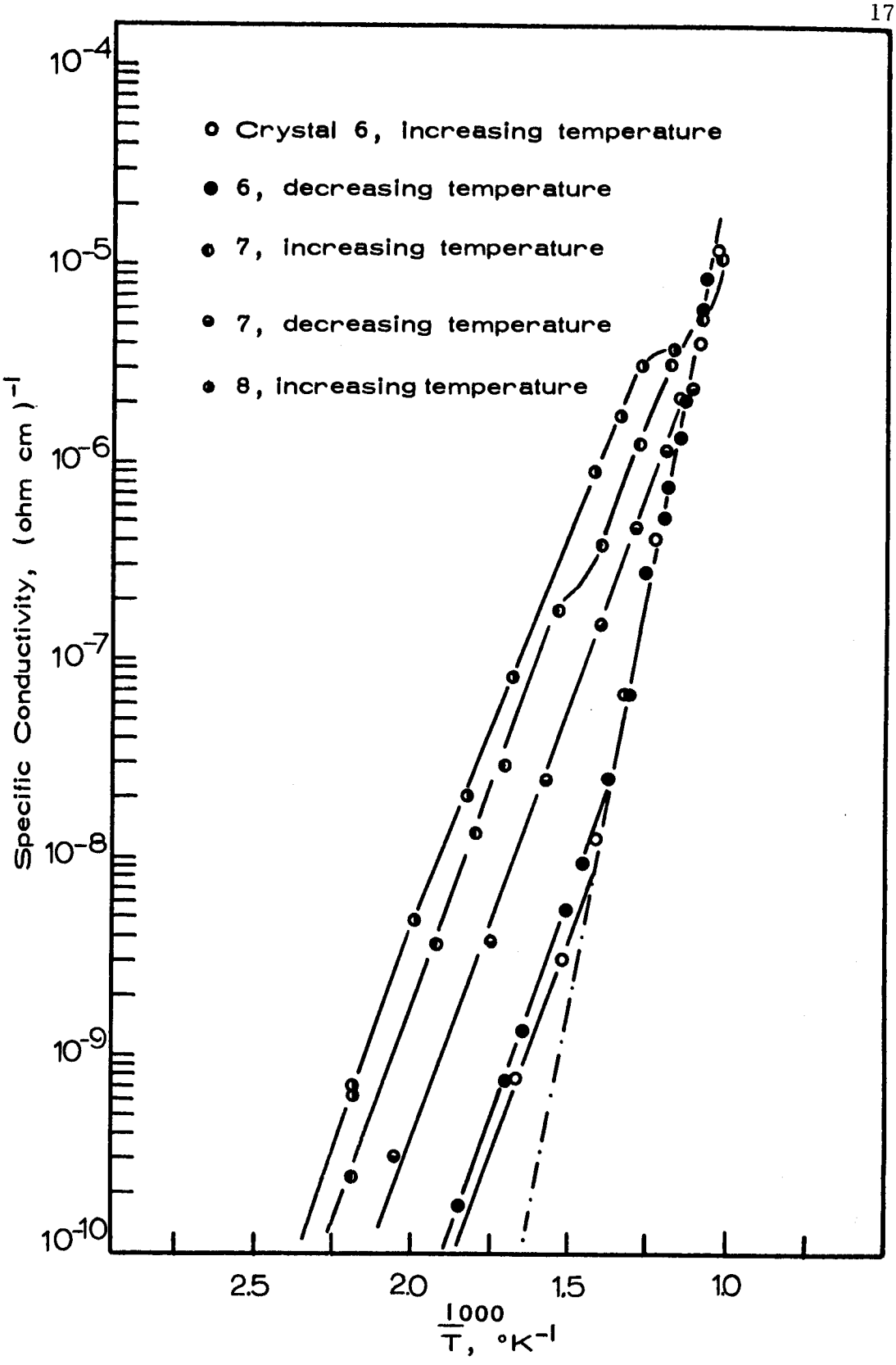

Fig. 6.7. Specific conductivities of KCl:Pb crystals.

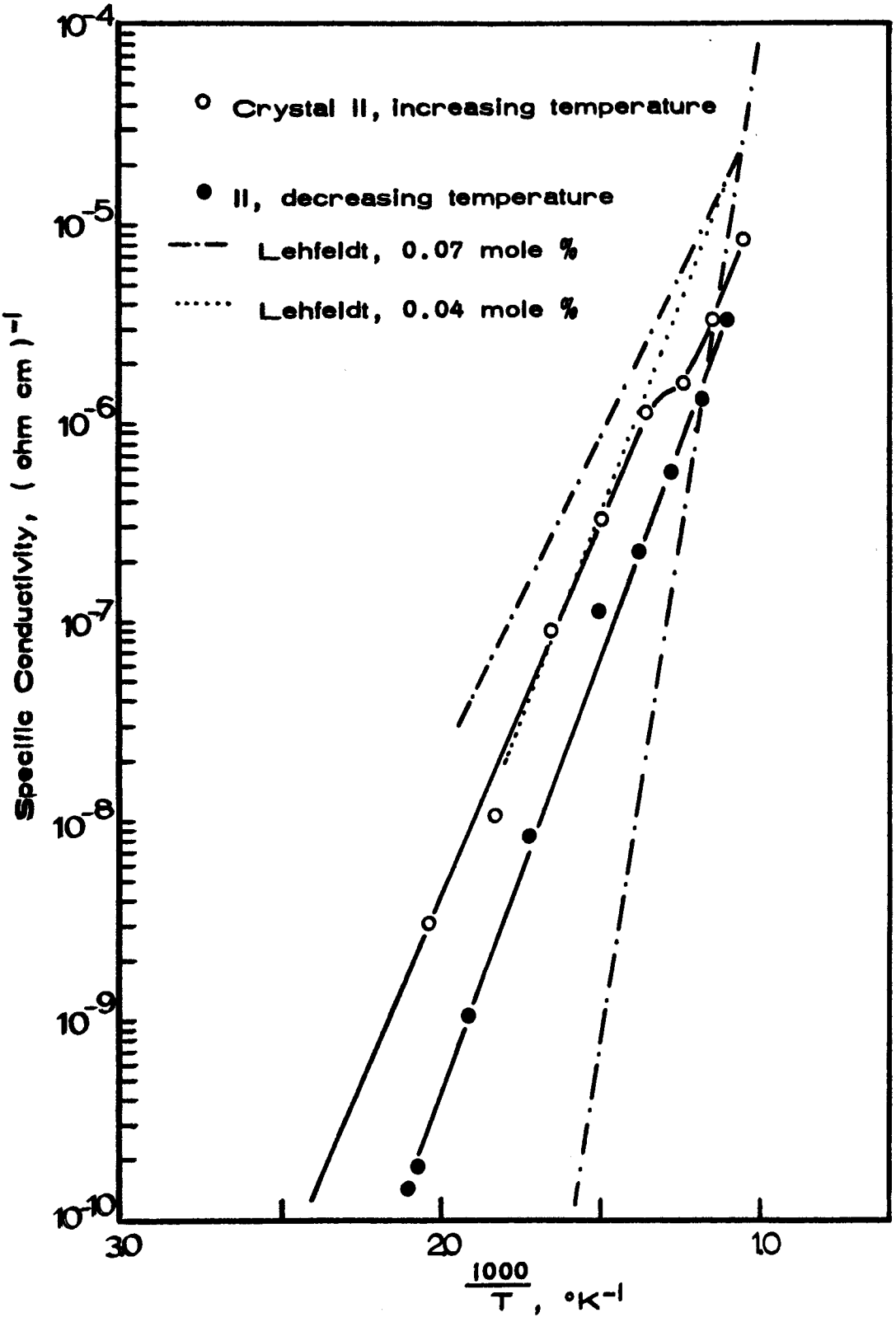

Fig. 6.8. Specific conductivities of KCl:Pb crystals.

the same knee temperature for samples of different lead ion concentration. His values are given as mole-percent lead added to the melt. The actual concentration in these crystals would be one tenth to one hundredth of the reported value, because a segregation coefficient of 0.10-0.01 for the incorporation of lead ion into KCl was observed in this study. (See Chapter III.)

The curves obtained are not well defined in the region about the knee. At temperatures below 300° C little or no polarization was observed. Above this temperature, polarization occurred and the steady-state value of the current was recorded. The extrinsic curve was linear with a slight curvature up to 350° C, at which point it began to bend toward the intrinsic curve. In some crystals the extrinsic curve would return to its original slope leaving a dip in the conductivity curve. It was not uncommon for the extrinsic curve to cross the intrinsic curve, then to coincide with it at higher temperatures.

The departure from linearity can be explained on the basis of association between Pb^{++} and a positive ion vacancy. Curvature in the extrinsic region is predicted by the association theory of Stasiw and Teltow (96). However, difficulty arises in determining the generally small curvature because of experimental errors. A comparison of the values for the activation energy for mobility E_2 given in Table 6.4 suggests that this value is not independent of the

impurity, but depends on the association energy of the positive ion vacancies with the aliovalent impurity cations present. Kelting and Witt (43) and other authors have noticed a variation in this value with different impurities.

Dreyfus and Nowick (19) have studied the DC ionic conductivity of NaCl and KCl doped with divalent impurity cations and propose that the conductivity plot in the region about the knee is really composed of three separate curves. The intrinsic region is as described earlier, but the extrinsic region is two curves with separate slopes, as shown below:

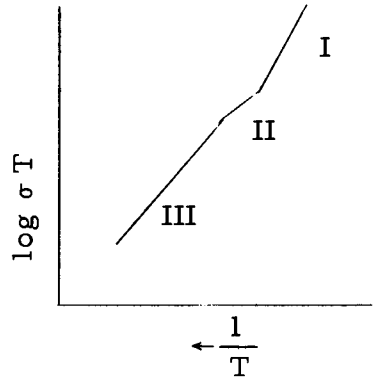

In region II the cation vacancy concentration is equal to the concentration of divalent cations added to the crystal. Although region II is a very small segment of the total curve, determination of the slope has been made by these authors using data compiled from the literature. In region III simple association of a vacancy and an impurity ion is suggested to take place. We can write for this region,

$$E_{III} = E_{II} + \frac{E_A}{2} \qquad (6.2)$$

where E_A is the association energy.

The activation energies found by the author and those found by other investigators are given in Table 6.4. The activation energy for motion of a cation vacancy in KCl, E_{II}, is given by Dreyfus and Nowick as 0.84 ± 0.05 eV. The average value of E_{III} (the author's E_2) was found to be 0.91 ± 0.13 eV. Using equation (6.2) the association energy E_A in KCl:Pb was estimated to be 0.1 eV. Applying the same calculation to the data of Kelting and Witt, a comparison of the degree of association can be made. The degree of association would be approximately the same as that in KCl:Ba, but greater than that in KCl:Sr or KCl:Ca, if it is assumed that the association energies are nearly the same. If the degree of association is not large, an appreciable dip in the conductivity curve would not be expected.

Table 6.4 Activation energies in the extrinsic region of conductivity

Sample or investigator	Type of crystal	E_2, eV
6	KCl:Pb	0.88*
7	"	0.83
8	"	0.82
9	"	1.00
10	"	1.01
11	"	0.81
12	"	1.05
Lehfeldt	"	0.43
Kelting and Witt	KCl:Ca	0.79
"	KCl:Sr	0.86
"	KCl:Ba	0.94

* Values for E_2 for the author's samples are averages of the values determined from the increasing and decreasing conductivity curves of each sample.

The author proposes the following explanation for some of the curvature observed near the knee. It was observed in Chapter V that $PbCl_2$ was lost by evaporation from the crystal. This took place in all the KCl:Pb conductivity samples. Examination of the sample after conductivity measurements had been made, showed that $PbCl_2$ had been evaporating from the sample. The gold plating on the lower electrode surface, the cathode, was gone and the surface was cloudy. The separation between the guard ring contact area and that of the upper electrode was also cloudy. Comparisons of the initial and final concentrations of the samples in Table 6.2 were inconsistent. In one case the concentration of lead ion became zero, in others it stayed the same, and in some it decreased or increased. Here, we must consider the fact that lead was shown (Chapter IV) to be present in more than one site in the crystal. Correspondingly, the concentration of lead ion followed by the A band can fluctuate. There was a distinct blackening at the cathode due to elemental lead and the formation of F-centers near the same electrode. These effects were the same as those observed in the transport studies of Chapter V. The loss of lead ion by this process is due to the reduction of Pb^{++} to elemental lead. The electrolytic purification observed by Lehfeldt can also be explained by the reduction of lead ion in the crystal. He found that the conductivity of a sample decreased by a factor of ten after it had

been electrolyzed for ten ampere-seconds. Further, the conductivity curves determined by the author with increasing and decreasing temperature did not coincide. This factor is additional support for the evaporation or reduction of lead ion. In any case, the behavior in the knee region is complicated and is, no doubt, a combination of the effects discussed.

The conductivity values determined for the KCl:Pb crystals were used in Chapter V to evaluate the field in electrolytic transport experiments.

VII SUGGESTIONS FOR FURTHER WORK

The task of elucidation is a continual challenge in the field of ionic solids. During the course of experimentation and discussion, several new ideas arose and they are suggested here.

1. Further purification of the KCl used for crystal growth is necessary to remove monovalent ions. High temperature heat treatment of the material under vacuum would produce a material more suitable for all methods of crystal growth. Some foreign monovalent halides are removed by this treatment.

2. A quantitative study of the variation in A-band intensity with quenching and temperature should be made. Resolution of the bands in the 250-273 mμ region would allow studies of conversion between the species giving rise to these bands.

3. Growth of crystals containing various ratios of lead to halide ion could produce information regarding the complex structure. Some indication of band splitting suggests that incorporation of lead with various quantities of halides in a neutral lattice (no halide in the host) could determine the nature of incorporation of the lead ion into the lattice.

4. Further study on the transport of lead ion employing the transport of a radioactive lead tracer into a KCl:Pb crystal should give a quantitative value for the effective charge on the lead-vacany

or lead-halogen complex. The reduction of Pb^{++} to elemental lead at the cathode must be prevented. Microtome techniques could be used to produce well defined diffusion and transport profiles. Experiments of this type would insure a linear potential drop across the section and a precisely known field.

5. The conductivity of KCl:Pb crystals should be determined for a greater concentration range and the reproducibility of the dip at the knee investigated.

BIBLIOGRAPHY

1. Anderson, S., J. S. Wiley, and L. J. Hendricks. Zone refining and chemical analysis of KCl and KBr. Journal of Chemical Physics 32:949-950. 1960.

2. Banasevich, S. N., B. G. Luré, and A. N. Murin. Determination of the effective charge of calcium ions in NaCl + $CaCl_2$ solid solutions. Soviet Physics - Solid State 2:72-78. 1960. (Translated from Fizika Tverdogo Tela)

3. Beaumont, F. T. Dithizone as a microchemical reagent. Metallurgia 29:217-220. 1944.

4. Belyaev, L. M., V. A. Perlshtein, and V. P. Panova. Use of radiotracers to study activator distribution in alkali halide crystals. In: Growth of crystals, ed. by A. V. Shubnikov and N. N. Sheftal'. Vol. 1. New York, Consultants Bureau, 1959. p. 267-269. (Translated from Russian)

5. Brauer, P. Über Störstellen, die in Erdalkalichalkogeniden durch Einbau Seltener Erden hervorgerufen werden. Zeitschrift für Naturforschung, ser. A 6:562-563. 1951.

6. Bridgman, P. W. Change of phase under pressure. I. The phase diagram of eleven substances with especial reference to the melting curve. Physical Review, ser. 2, 3:153-203. 1914.

7. Burstein, E. et al. A note on the distribution of impurities in alkali halides. Physical Review 81:459-460. 1951.

8. Burton, J. A. et al. Distribution of solute in crystals grown from the melt. Part II. Experimental. Journal of Chemical Physics 21:1991-1996. 1953.

9. Carus, Titus Lucretius. Of the nature of things. London, Dent and Sons, 1938. 301 p.

10. Chemla, Marius. Diffusion et migration de $^{137}Cs^{+}$ dans des mono cristaux de ClNa. Comptes Rendus de L'Académie des Sciences 236:484-486. 1953.

11. Coker, Earl Howard, Jr. Interactions of sulfate ions in potassium chloride crystals. Ph. D. thesis. Corvallis, Oregon State University, 1963. 144 numb. leaves.

12. Cook, Gerhard A. (ed.) Argon, He and the rare gases- elements of the He group. Vol. 1. New York, Interscience, 1961. 394 p.

13. Crank, J. The mathematics of diffusion. Oxford, Clarendon Press, 1956. 339 p.

14. Czochralski, J. Ein neues Verfahren zur Messung der Kristallisationsgeschwindigkeit der Metalle. Zeitschrift für physikalische Chemie 92:219-221. 1918.

15. Dexter, D. L. Theory of the optical properties of imperfections in non-metals. Solid State Physics 6:353-410. 1958.

16. _____. Absorption of light by atoms in solids. Physical Review 101:48-55. 1956.

17. _____. On Smakula's equation in insulating solids. Physical Review 98:1533-1534. 1955.

18. Dow Chemical Company, Dowex: ion exchange. Midland, Mich., Dow Chemical Company, 1964. 80 p.

19. Dreyfus, R. W. and A. S. Nowick. Energy and entropy of formation and motion of vacancies in NaCl and KCl crystals. Journal of Applied Physics 33 (supp):473-477. 1962.

20. Dryden, J. S. The aggregation of divalent impurities and their associated cation vacancies in alkali halides. Journal of the Physical Society of Japan 18(supp. 3):129-133. 1963.

21. Duerig, W. H. and J. J. Markham. Color centers in alkali halides at 5°K. Physical Review 88:1043-1049. 1952.

22. Etzel, H. W. and D. A. Patterson. Optical properties of alkali halides containing OH^- ions. Physical Review 112: 1112-1116. 1958.

23. Fisher, H. W. and Woldemar Weyl. The absorption spectra of the metal complexes of dithizone and their analytical significance. Wissenschaftliche veröffentlichungen aus den Siemens-Werken 14:41-53. 1935.

24. Fredenhagen, K. and G. Caderbach. Bindung von Kalium durch Kohlenstoff. Zeitschrift für anorganische und allgemeine Chemie 158:249-263. 1926.

25. Fredericks, William John. An investigation of solid alkali halide phosphors. Ph. D. thesis. Corvallis, Oregon State University, 1956. 132 numb. leaves.

26. Fredericks, W. J., F. E. Rosztoczy, and J. Hatchett. Investigation of crystal growth processes. Palo Alto, 1963. 24 numb. leaves. (Stanford Research Institute. Final Report. SRI Project #PAU-3523. Results presented at 1962 International Color Center Symposium, Stuttgart, Germany.)

27. Fredericks, W. J. and Allen B. Scott. Transference experiments on lead and thallous ions in potassium chloride crystals. Journal of Chemical Physics 28:249-252. 1958.

28. Frenkel, J. Über die Wärmebewegung in festen und flüssigen Körpern. Zeitschrift für Physik 35:652-669. 1926.

29. Friauf, Robert J. Correlation effects for diffusion in ionic crystals. Journal of Applied Physics 33 (supp):494-505. 1962.

30. Fritz, B. F., F. Lüty, and J. Anger. Der Einfluss von OH^--Ionen auf absorptionsspektrum und Ionenleitfähigkeit von KCl-Einkristallen. Zeitschrift für Physik 174:240-256. 1963.

31. Girifalco, L. A. Atomic migration in crystals. New York, Blaisdell, 1964. 162 p.

32. Gomes, W. Distribution of silver ions in melt-grown alkali halides. Journal of Chemical Physics 34:2191-2192. 1961.

33. Grigoruk, L. V. and I. Ya. Melik-Gaikazyan. Impurity distribution and formation of color centers under the action of x-rays in NaCl-Mn, NaCl-Cd, and NaCl-Pb. Optics and Spectroscopy 15:210-213. 1963. (Translated from Optica i Spektroskopiya)

34. _____. The effect of thermal treatment and x-raying on the activator absorption spectrum of NaCl-Pb. Optics and Spectroscopy 12:285-6. 1962. (Translated from Optica i Spektroskopiya)

35. Grundig, Hellmut. Ionenleitfähigkeit von zonengereiningten Alkalihalogeniden. Zeitschrift für Physik 158:577-594. 1960.

36. Gruzensky, Paul Milnore. Electrical conductivity and ultraviolet absorption spectra of high-purity potassium chloride single crystals. Ph. D. thesis. Corvallis, Oregon State University, 1960. 100 numb. leaves.

37. Hiscox, Gardner D. (ed.) Henley's twentieth century book of recipes, formulas and processes. New York, Henley Publishing Co., 1907. 787 p.

38. Ikonnikova, G. M. and A. P. Izergin. On the entry of lead impurities into KCl crystals under the influence of vibration. Soviet Physics-Crystallography 9:110-112. 1964. (Translated from Kristallografiya)

39. Ivanova, N. I., and A. P. Zhukovskii. The luminescence centers of alkali halides phosphors doped with divalent metals. Optics and Spectroscopy 12:56-57. 1962. (Translated from Optika i Spektroskopiya)

40. Jones, R. Norman. The absorption of radiation by inhomogeneously dispersed systems. Journal of the American Chemical Society 74:2681-2683. 1952.

41. Kaifu, Yozo. Some optical properties of lead activated potassium halide phosphors. Journal of the Physical Society of Japan 16:1605-1616. 1961.

42. Kanzaki, Hiroshi and Keishiro Kido. Purification of alkali halide crystals through fractional distillation and normal freezing. Journal of the Physical Society of Japan 15:529-530. 1960.

43. Kelting, Heinke and Horst Witt. Über KCl-Kristalle mit Zusätzen von Erdalkalichloriden. Zeitschrift für Physik 126:697-710. 1949.

44. Keneshea, F. J., Jr. and W. J. Fredericks. Diffusion of lead ions in potassium chloride. Journal of Chemical Physics 38: 1952-1958. 1963.

45. Kerkhoff, F. Überfuhrungszahlen fur KCl-Kristalle. Zeitschrift für Physik 130-449-456. 1951.

46. Kobayashi, Koichi and Tetsuhiko Tomiki. Studies on the preparation of pure alkali chlorides. Journal of the Physical Society of Japan 15:1982-1990. 1960.

47. Koch, Werner. Über den Fremdionen gehat einiger Alkalihalogenidphosphore. Zeitschrift für Physik 57:638-647. 1929.

48. Konitzer, John D. and Jordan J. Markham. Experimental study of the shape of the F-band absorption in KCl. Journal of Chemical Physics 32:843-856. 1960.

49. Kozelka, F. L. and E. F. Kluchesky. Photoelectric colorimetric technique for the dithizone system. Industrial and Engineering Chemistry, Analytical Edition 13:484-487. 1941.

50. Kroll, W. J., A. W. Schlechten and L. A. Yerkes. A new carbon resistor furnace. Transactions of the Electrochemical Society 89:317-329. 1946.

51. Kyropoulos, S. Dielektrizitäls Konstanten regülarer Kristalle. Zeitschrift für Physik 63:849-854. 1930.

52. _____. Ein Verfahren zur Herstellung grosser Kristalle. Zeitschrift für anorganische und allgemeine Chemie 156:308-313. 1926.

53. Lawson, W. D. and S. Nielsen. Preparation of single crystals. London, Butterworths, 1958. 255 p.

54. Lehfeldt, Von Wilhelm. Uber die elektrische Leitfahigkeit von Einkristallen. Zeitschrift für Physik 85:717-726. 1933.

55. Lehovec, K. et al. Apparatus for crystal pulling in vacuum using a graphite resistance furnace. Review of Scientific Instruments 24:652-655. 1953.

56. Lidiard, A. B. Correlation effects in diffusion in solids. Del Nuovo Cimento 7(supp):620-631. 1958.

57. _____. Ionic conductivity. In: Handbuch der Physik, ed. by von H. Geiger and Karl Scheel. Berlin, Springer, 1957. p. 246-349.

58. Lukirsky, P., S. Scukareff and O. Trapensnikoff. Die Elektrolyse der Kristalle. Zeitschrift für Physik 31:524-533. 1925.

59. Malkovich, R. Sh. Methods for calculating the mobility of impurity ions in a solid. Soviet Physics-Solid State 2:2479-2488. 1961. (Translated from Fizika Tverdogo Tela)

60. Manning, J. R. Correlation factors for impurity diffusion in B. C. C. and F. C. C. structures. Physical Review, ser. A, 136:A1758-A1766. 1964.

61. _____. Correlation factors for impurity diffusion-F. C. C. lattice. Physical Review 128:2169-2174. 1962.

62. _____. Drift mobility of an ionic impurity in an electric field. Physical Review 125:103-108. 1962.

63. _____. Correlation effects in impurity diffusion. Physical Review 116:819-827. 1959.

64. Marshall, K. H. J. C. and R. Wickham. An improved Czochralski crystal-pulling furnace. Journal of Scientific Instruments 35:121-125. 1958.

65. Mathre, Owen B. Lead-dithizone equilibria in water-carbon tetrachloride systems. Ph. D. thesis. Minneapolis, University of Minnesota, 1956. 92 numb. leaves. (microfilm)

66. Melik-Gaikazyan, I. Ya., E. K. Zavadovskaya, and M. N. Treskina. Effect of annealing on the absorbion spectra and electrical conductivity of crystalline NaCl:Pb and KCl:Pb phosphors. Optics and Spectroscopy 9:43-44. 1960. (Translated from Optica i Spektroskopiya)

67. _____. Concerning the distribution of impurities in alkali-halide crystals. Soviet Physics-Crystallography 5:456-458. 1960. (Translated from Kristallografiya)

68. Menzies, A. C. and J. Skinner. The growing of crystals. Discussions of the Faraday Society 5:306-312. 1949.

69. Miller, C. F. Dithizone, an excellent reagent for lead. Chemist Analyst 26:55. 1937.

70. Mil'vidskii, M. G. The crystallization front and the distribution across the transverse section of monocrystals grown from the melt by the Czochralski method. Soviet Physics- Crystallography 6:647-648. 1962. (Translated from Kristallografiya)

71. Mott, N. F. and R. W. Gurney. Electronic processes in ionic crystals. 2d ed. London, Oxford, 1950. 275 p.

72. Mott, N. F. and M. J. Littleton. Conduction in polar crystals. Transactions of the Faraday Society 34:485-499. 1938.

73. Murin, A. N., S. N. Banasevich, and Yu. S. Grushko. Diffusion of calcium ions in NaCl + $CaCl_2$ mixed crystals. Soviet Physics-Solid State 3:1762-1766. 1962. (Translated from Fizika Tverdogo Tela)

74. Nacken, R. Über das Wachen von Krystallpolyedern in ihrem Schmelzfluss. Neues Jahrbuch für Mineralogie Geologie und Palaeontologie 2:133-164. 1915.

75. Neubert, T. J. and John A. Reffner. Thermal bleaching of Cl_2^- centers. Journal of Chemical Physics 36:2780-2782. 1962.

76. Noble, G. A. and J. J Markham. Effect of impurities on the F band in KCl. Journal of Chemical Physics 41:1880-1881. 1964.

77. Otterson, Dumas A. Neutralization of hydroxide ion in melt-grown NaCl crystals. Journal of Chemical Physics 34:1849. 1961.

78. _____. On presence of NaOH in crystalline NaCl. Journal of Chemical Physics 33:227-229. 1960.

79. Patterson, D. A. Effects of oxygen and water vapor on the "OH" absorption in melt-grown alkali halides. Physical Review 127:1564-1566. 1962.

80. Petrov, D. A. and A. A. Bukhanova. The determinative part played by super cooling of the melt in the formation of helical macroinhomogeneities in crystals grown by the Czochralski method. Soviet Physics-Crystallography 7:349-353. 1962. (Translated from Kristallografiya)

81. Phipps, T. E. and E. G. Partridge. Temperature-conductance curves of solid salts. II. Halides of potassium and thallium. Journal of the American Chemical Society 51:1331-1345. 1929.

82. Pohl, R. W. Electron conductivity and photochemical processes in alkali halide crystals. Proceedings of the Physical Society 49:3-31. 1937.

83. Pringsheim, Peter. Fluorescence and phosphorescence of thallium-activated potassium-halide phosphors. Review of Modern Physics 14:132-138. 1942.

84. Quincy, R. B., Jr., and D. E. La Valle. High purity potassium chloride. Oakridge, Tenn., 1965. 14 numb. leaves. (Oakridge National Laboratory. Report ORNL-1071)

85. Rauch, C. J., and C. V. Herr. f_F by static magnetic susceptibility. Physical Review 105:914-920. 1957.

86. Reisfeld, Renata, Abraham Glasner, and Alexander Honigbaum. Diffusion of thallous chloride in single crystals of KCl by a novel spectrophotometric method. Journal of Chemical Physics 42:1892-1895. 1965.

87. Rolfe, J. Infrared and ultraviolet absorption bands in KBr crystals containing hydroxide ion impurity. Canadian Journal of Physics 41:1525-1527. 1963.

88. _____. Hydroxide absorption band in alkali halide crystals. Physical Review Letters 1:56-58. 1958.

89. Rolfe, J., F. R. Lipsett, and W. J. King. Optical absorption and fluorescence of oxygen in alkali halide crystals. Physical Review 123:447-454. 1961.

90. Rosa, E. B. and G. W. Vinal. Summary of experiments on the silver voltameter at the Bureau of Standards and proposed specifications. Washington, 1916. p. 479-514. (U. S. National Bureau of Standards, Scientific Paper. 285)

91. Sandell, E. B. Colorimetric determination of traces of metals. New York, Interscience, 1959. 1032 p. (Chemical analysis. Vol. 3)

92. Schottky, W. Über den Mechanismus der Ionenbewegung in festen Elektrolyten. Zeitschrift für physikalische Chemie B29:335-355. 1935.

93. Sibley, W. A., E. Sonder and C. T. Butler. Effect of lead on the room-temperature colorability of KCl. Physical Review 136:A537-541. 1964.

94. Smakula, A. Über Erregung und Entfärbung lichtelektrisch leitender Alkalihalogenide. Zeitschrift für Physik 59:603-614. 1930.

95. Smekal, A. Elektrizitatsleitung und diffusion in Kristallisierten Verbindungen. Zeitschrift für Elektrochemie 34:472-483. 1928.

96. Stasiw, O. and J. Tetlow. Über Fehlordnungserscheinungen in Silberhalogeniden mit Zusätzen. Annalen der Physik 1:261-272. 1947.

97. Stockbarger, Donald C. The production of large artificial fluorite crystals. Discussions of the Faraday Society 5:294-299. 1949.

98. _____. Improved crystallization of lithium fluoride of optical quality. Discussions of the Faraday Society 5:299-306. 1949.

99. _____. The production of large single crystals of lithium fluoride. Review of Scientific Instruments 7:133-136. 1936.

100. Strong, John. A method for growing large crystals of the alkali halides. Physical Review 36:1663-1666. 1930.

101. Tammann, G. and G. Veszil. Die electrisch Leitfahigkeit von Salzen in Einkristallen und Kristallitenkonglomeraten. Zeitschrift für anorganische und allgemeine Chemie 150:355-380. 1925.

102. Tubant, C. and Fritz Lorenz. Das electrische Leituermogen als Methode zur Bestimmung des Zustandsdiagramms binarer Salzgemische. Zeitschrift für physikalisch Chemie. 87:543-561. 1914.

103. Tubant, C., H. Reinhold and George Liebold. Bipolare Leitung in festen Electrolyten. Zeitschrift für anorganische und allgemeine Chemie 197:225-253. 1931.

104. Turovskii, B. M. and M. G. Milvidskii. Modelling the mixing of a melt during the growing of crystals according to the Czochralski method. Soviet Physics-Crystallography 6:606-608. 1962. (Translated from Kristallografiya)

105. Verma, Adjit Ram. Crystal growth and dislocations, New York, Academic Press, 1953. 182 p.

106. Voronov, B. K., M. Ya. Dashevskii, E. M. Titova and V. D. Khovostikova. Growing homogeneous semiconducting monocrystals by the Czochralski method. In: Proceedings of the Fourth All-union Conference on Semi-Conductor Materials, ed. by N. Kh. Abrikosov. New York, Consultants Bureau, 1963. p. 40-43.

107. Wagner, Carl and Paul Hantelmann. Determination of the concentrations of cation and anion vacancies in solid potassium chloride. Journal of Chemical Physics 18:72-74. 1950.

108. Warburg, E. and F. Tegetmeier. Über die electrolytische Leitung des Bergkrystalls. Annalen der Physik und Chemie 35:455-467. 1888.

109. Watkins, George D. Electron spin resonance of Mn^{++} in alkali chlorides; association with vacancies and impurities. Physical Review 113:79-90. 1959.

110. White, W. E. Dithizone as an analytical reagent. Journal of Chemical Education 13:369-373. 1936.